

CWP-186  
July 1995



Residual Statics Estimation for Data  
from Structurally Complex Areas  
Using Prestack Depth Migration

Timo Tjan

— Master's Thesis —  
Geophysics

---

Center for Wave Phenomena  
Colorado School of Mines  
Golden, Colorado 80401  
303/273-3557



eration between estimation of velocity and estimation of static time shifts can produce accurate estimates for both, provided that one uses a migration-based method for both estimation efforts. For the Marmousi data example the iterative migration-based statics and velocity estimation yields a good statics solution after just three iterations even though the velocity model after these three iterations is still far from accurate. Further iterations, however, can concentrate solely on improving the velocity model.

## ACKNOWLEDGMENTS

I am grateful to my advisor, Dr. Ken Lerner, who helped and encouraged me with his enthusiasm for this work and his always enlightening advise. He also initiated some of the demonstrations shown in the thesis.

I would like to thank, Jean-Paul Diet, who initiated this project, and François Audebert, who helped me throughout the work with comments and advise. Also thanks to everyone in the research and development group of CGG in Massy, France, for helping me with many practical problems at the beginning of this work during my summerjob with CGG.

Thanks also go to the members of my committee, Dr. Ilya Tsvankin and Dr. John Scales, for critiquing this thesis.

I am in debt to Fabiola Williams for her support during my most difficult moments as well as to Shirley Miller who put up with me for all this time, to Elisabeth Ong who was always there to fall back on for help and to my parents who taught me always to look for new challenges and who have been encouraging and providing me with all necessary to make this challenge a success.

Special thanks are due to my friends: Raoul Diederer, thanks for reminding me over and over again that there is more to life than geophysics. To Lydia Deng, Wences Gouveia, Tagir Galikeev and Andreas Rüger, for making my time at the Colorado School of Mines so rewarding and for standing by me in the difficult times.

I would like to thank the sponsors of the Consortium Project at the Center for Wave Phenomena for their financial support. Likewise, I am grateful to Verenigde Spaarbanken in the Netherlands, who honored me with their VSB scholarship during my first year of studies at the Colorado School of Mines. I wish to express thanks to Jean-Paul Jeannot, Jim Burcham and Ivan Beringer of GX Technology for providing me with their excellent prestack migration and modeling software and their helpful tips.



## Chapter 1

### INTRODUCTION

Irregularities in the near-surface are a major source of structural distortion and deterioration of signal quality in land seismic data. The deterioration, attributable to surface topography and to lateral variations in the thickness and velocity of weathering layers, introduces trace-to-trace time distortions, thus causing non-alignment of reflections prior to stacking. Given difficulties in modeling the near-surface sufficiently well to correct deterministically for these distortions, the practical solution has been to consider the resulting trace-to-trace time distortions as static (i.e., time-invariant) shifts associated with vertical travel paths near the sources and receivers (i.e., the so-called surface-consistency assumption). With this assumption, the reflection data themselves could be used in statistical procedures (Hileman et al., 1968; Taner et al., 1974; and Wiggins et al., 1976) that have become a mainstay in residual statics estimation and correction, in practice.

Practical methods developed to correct for near-surface-induced distortions have generally worked well in obtaining short-wavelength components of statics corrections where the subsurface structure is layered and relatively uncomplicated, and where the data are not too severely contaminated by noise. Such methods typically involve generating reference (or model) traces, presumed to be free of the influence of the time distortions, against which to compare the statics-contaminated data traces. Most frequently, the comparison is done through cross-correlation between selected windows of the data traces and the reference traces, which yields trace-to-trace time shifts from which are estimated the static corrections. These static corrections are then applied to the contaminated data to correct for the near-surface-induced time distortions.

The reference trace for the traces in a common-midpoint (CMP) gather is typically constructed as the CMP stack of the normal-moveout (NMO) corrected data traces in the gather. Sometimes, in addition, some form of running average of the CMP-stacked traces is used to build the reference traces. The underlying idea is that the reference trace for the gather emulates each of the data traces, but without the statics contamination and with much-reduced additive noise. If the data and reference traces are also sufficiently broad-band, then the time lags of the strongest peak in the cross-correlation traces would give a good estimate of the required time shifts.

Even for simple subsurface structure, however, any error in the NMO correction will cause the reference trace to not be adequately representative of the individual data traces in the CMP gather. In such a situation, the strongest peak of the cross-correlation function might not stand out so prominently among other oscillations in the function. When the data are further contaminated by additive noise and large time distortions caused by variations in the near-surface, the chances for error in the measured time shifts, in particular cycle skips, are increased. Moreover, when the subsurface structure

is complicated the likelihood of error in the NMO correction is measurably worsened (Miller, 1974). The stacking velocity can vary rapidly from one location to another; nearby reflectors with differing dip will give rise to crossing reflections with differing moveout on CMP gathers; and reflectors beneath complex overburden can give rise to reflections with distinctly non-hyperbolic moveout.

Clearly, no hyperbolic correction can adequately compensate for either dip-dependent moveout or moveout that is not hyperbolic. In this thesis, NMO correction is taken to mean hyperbolic correction, with no extra effort, such as dip-moveout, to correct for dip-dependence of moveout. Where subsurface structure is not complex, longer-offset data will have non-hyperbolic moveout, and one can conceive of taking a fourth-order term in the moveout correction into account (e.g., Taner and Koehler, 1969). Here, however, I consider the highly non-hyperbolic moveout, including reverse moveout (i.e. an event has earlier arrival time at a larger offset than at a shorter offset) that can arise where subsurface structure is complex. Even the more sophisticated, fourth-order moveout correction will leave large residual moveout for such data. Therefore, again, when I refer to NMO, I am speaking of hyperbolic moveout correction as is routinely done in practice.

One means of avoiding this problem of poor NMO correction is to sidestep use of reflection-based statics corrections entirely, and settle for obtaining the statics corrections entirely from shallow refraction data (Lawton, 1989). Common practice, however, favors use of both approaches — the reflection-based approach for obtaining the best short-wavelength corrections (i.e., variations whose lateral wavelength is less than the length of the recording spread), and the refraction-based approach for treating long-wavelength near-surface problems, as well as helping to improve on the short-wavelength solution. Where the reflection-based statics corrections are less than desired, they are usually still accepted, along with some resignation that the statics problems in the particular data set happened to be too difficult.

The data-processing steps that are designed to overcome NMO problems are dip-moveout (DMO) or prestack time migration for the problem of crossing events from reflectors with conflicting dip, and prestack depth migration for those same problems, as well as for non-hyperbolic moveout attributable to lateral velocity variation in the overburden. Typically, such processes are applied to data that already have had statics corrections applied. Here, following an idea of J.P. Diet (personal communication, 1993) and Tjan et al. (1994), I suggest that the prestack migration be brought into the statics-estimation effort in order to improve on the all-important moveout corrections used in building the reference traces.

Specifically, I propose the following sequence of steps to build the reference traces. First, perform prestack depth migration using the statics-contaminated data. Next, using the resulting migrated depth section as input, do a multi-offset modeling to generate a separate reference trace for each original data trace. Cross-correlations of the reference and data traces give time shifts that can then be input to the usual linear equations (Taner et al., 1974), which are then solved for estimates of the source and receiver statics corrections. Contingent on having an accurate velocity model for the migration and modeling steps, this process should overcome the problems of poor moveout correction

where subsurface structure is complex.

Of course, at the outset of the imaging process, no accurate velocity model is available, and when data of a complex subsurface are also contaminated with static time shifts, velocity analysis is not at all a trivial process. Superimposed on problems due to non-hyperbolic moveout and crossing events, static time shifts also add to the mis-alignment of events in CMP gathers in conventional velocity analysis, or similarly in common reflection point (CRP) gathers in migration velocity analysis, and thus complicate the velocity analysis. If, however, we wished to remove the static time shifts before doing velocity analysis, we still would need an acceptable estimate of the velocities to obtain reasonable statics estimates. Clearly the treatment of statics- and noise-contaminated data from structurally complex areas presents a chicken-and-egg problem: statics correction, velocity estimation, suppression of noise, and imaging are all intertwined.

It is therefore important to treat the statics and velocity problems as one when we deal with statics-contaminated data from a complex subsurface. Already, in conventional statics-estimation methods, it is common practice to iterate between the statics estimation and velocity analysis. When we are dealing with data of a complex subsurface, however, the only chance to obtain accurate estimates for both the velocity and static time shifts is to introduce prestack-migration-based methods for both efforts. Here, I show that iteration between prestack-migration-based velocity estimation and prestack-migration-based statics estimation can produce accurate estimates for both.

The second chapter deals with conventional statics-estimation methods, and how they perform on data that suffer from different combinations of problems due to noise, static time shifts and complicated moveout. In the third chapter, I show the performance of a conventional statics-estimation method applied to synthetic traces from a complex structural model — the Marmousi model (Versteeg and Grau, 1991) — demonstrating the need for doing something beyond the conventional when addressing statics corrections for subsurface of this complexity.

Then I introduce the proposed prestack-migration-based, statics-estimation procedure, and show with examples of the Marmousi data that this method yields an excellent solution when the subsurface velocity is known and that it works well, even where the velocity model is not perfectly known, or when the data have low signal-to-noise ratio.

Finally, I discuss the importance of treating the velocity- and statics problem as one, again with examples of the Marmousi data. I show that after only a few iterations of statics and velocity estimation using a prestack-migration-based approach, the statics problem has largely been corrected so that subsequent iterations can be directed solely towards improvement of the velocity model.





## Chapter 2

### CONVENTIONAL METHODS FOR ESTIMATING STATIC CORRECTIONS

Over the years, several methods have been developed for residual statics estimation. All conventional methods are based on the assumption that reflections exhibit normal hyperbolic moveout within CMP gathers. The most common statics-estimation method derives statics corrections from time shifts obtained from cross-correlations between model traces, i.e., traces with reduced influence of the statics, and the statics-contaminated traces they represent. A second approach, the stacking-power method, is based on maximization of the power of the stack after NMO correction and trial statics corrections have been applied. Often, refraction-based statics are applied prior to one of these reflection-based residual-statics approaches. Refraction-based methods use first arrivals in the data to model the near-surface (velocity and depth) and then estimate time shifts related to this near-surface.

#### 2.1 Correlation method

The model underlying the assumption of surface-consistency in the residual-statics-estimation problem is that the reflection time for a reflection on an NMO-corrected data trace is given by (Taner et al., 1974; Wiggins et al., 1976)

$$T_{ij} = r_j + s_i + g_k + m_k X_{ij}^2 + \epsilon_{ij}, \quad (2.1)$$

where

- $T_{ij}$  is the time delay for the trace associated with the  $i$ th source and the  $j$ th receiver;
- $r_j$  is the static time shift associated with the  $j$ th receiver;
- $s_i$  is the static time shift associated with the  $i$ th source;
- $g_k$  the structural term, is the normal-incidence reflection time from the datum plane to a subsurface reflector at the  $k$ th CMP position;
- $m_k$  is the time-averaged residual-moveout coefficient at the  $k$ th CMP position;
- $X_{ij}$  is the offset of the  $j$ th receiver and from the  $i$ th source;
- $i$  is the source location index;
- $j$  is the receiver location index;
- $k$  is the CMP position index, equal to  $\frac{(i+j)}{2}$ ; and
- $\epsilon_{ij}$  contains all the errors that arise in modeling  $T_{ij}$  by the first four terms (e.g., random noise, and in particular here, use of erroneous moveout correction.)

Equations (2.1) constitute a system of linear equations in the source and receiver statics,  $s_i$  and  $r_j$ . Given measurements of  $T_{ij}$  for all the traces on a seismic line, this system of equations is usually solved by a straightforward iterative method (Wiggins et al., 1976) for estimates of the source and receiver statics corrections, which are then applied to the data traces to correct them for the near-surface distortions.

In practice, rather than picking actual reflection times on the individual data traces, one often estimates time deviations  $\delta T_{ij}$  associated with each data trace. These deviations, which can be used in a variation of equations (2.1), are obtained by cross-correlating a window of each of the traces within a CMP gather with the corresponding window on a specified reference (or model) trace. The value of  $\delta T_{ij}$  estimated for a trace is the time associated with the time lag at which the computed cross-correlation function is a maximum.

If all the traces in a CMP gather were identical except for trace-dependent time shifts, and if the reference trace were identical to one of the traces (e.g., if one of the traces was selected to define the reference trace), then the time lags associated with the peak cross-correlation values would be guaranteed to give the correct values of  $\delta T_{ij}$  for use in equations (2.1). A practical problem with using just one of the selected traces as the reference trace is that the data are usually contaminated by noise, both random and coherent. Therefore, no single trace is considered to be sufficiently representative of all the other traces in the CMP gather to serve as a reference trace. Shortcomings in the reference trace will translate into errors in the lags associated with observed peaks in the cross-correlation functions.

To make the reference trace more representative of the data traces in the CMP gather, the reference trace is often constructed as an average of the data traces, i.e., a stack of the data. Clearly, if the NMO-corrected reflections are well aligned within the gather, the stack will yield a trace that reproduces the signal, with random noise reduced, suggesting that it should serve well as a model. Unfortunately, in practice, the reflections cannot be expected to be so well aligned since they suffer from the very time distortions that the statics-estimation procedure aims to correct. Moreover, interpretation of stacking velocity for noise-contaminated, land-seismic data invariably yields imperfect estimates of the stacking velocity. These problems will cause the brute-stack to model the signal less faithfully than desired.

## 2.2 Problems that can arise in less-than-ideal situations

Figures 2.1 through 2.9 show degradation of the cross-correlation process for various types of contamination of the data. Figure 2.1 shows the trivial, ideal situation: all traces have identical signal, no noise, no statics, and perfect NMO correction. The top portion (a) shows the 12 traces of a simulated NMO-corrected, 12-fold CMP gather (data stretching is ignored), with the CMP-stacked trace shown as trace 14. The traces have been generated by convolving a random sequence of random-amplitude spikes, having Poisson arrival distribution, with a Ricker wavelet having 27-Hz dominant frequency. Because the traces in the gather are identical, the stacked trace is, of course, the same as

the others. Consequently the cross-correlations between the data traces and the stacked trace are all identical, and have their peak at zero lag. For this situation, the cross-correlations are actually auto-correlations of the traces. Most important for what is ahead, the peak at zero lag has relatively good standout above the subsidiary peaks on either side of it. That is, not only are the peaks at the correct positions, *they are easy to identify correctly.*

Consider next, Figure 2.2, which differs from Figure 2.1 only in that static timing errors have been added. (Figures 2.2 through 2.9 all have the same display format as that in Figure 2.1.) The time shifts are drawn from a random population with uniform distribution between -20 ms and +20 ms. Because the signal is not aligned, the stacked trace is weaker and distorted relative to the data traces. To an approximation, it is a high-cut-filtered version of the data traces, with cutoff frequency governed by the range of time shifts (Marsden, 1993a). Although the stacked trace is an imperfect model, peaks in the resulting cross-correlations still faithfully reflect the true time shifts. The cross-correlation functions are no longer symmetric, but the standout of the main peak remains strong.

Figure 2.3, which simulates data that have been imperfectly NMO corrected, but with no other time shifts, likewise shows a degraded stacked trace. Nevertheless, again the cross-correlation traces have a strong main peak that accurately yields the time shifts related to the residual moveout in the data. This residual moveout is a complication for the estimation of the residual statics; however, we will assume that it can be properly accommodated by the  $m_k X_{ij}^2$  term in equations (2.1) as long as the proper correlation peaks are picked. For the simulation in Figure 2.3, the NMO correction was done with a stacking velocity of 3300 m/s, whereas the correct moveout velocity is 3000 m/s. The residual moveout error is estimated on the basis of an assumed reflection time of 2 s, and the simulated source-to-receiver offsets range from 0 to 2750 m, in 250-m increments.

It might seem that a 10-percent error in stacking velocity, as used here, is unduly large. For noise- and statics-contaminated land seismic data over a complex subsurface, however, such an error may be not at all excessive.

Now, let's add noise to the data. It is with this added complication that problems become more interesting. Figure 2.4 shows the same data as in Figure 2.1, but with bandlimited random noise added. The noise was generated by convolving a Ricker wavelet with a random spike series having random spike amplitudes that are uniformly distributed over a specified range. The root-mean-square amplitude of the noise is 1/2 the peak signal amplitude, multiplied by .707. For this noise level, we shall say that the signal-to-noise (SNR) ratio is 2. The stacked trace here compares favorably with that for the noiseless case, Figure 2.1. This is no surprise: the 12-fold stack has given the expected  $\sqrt{12}$  improvement in SNR since the signal was aligned on the traces. Despite the variations in the cross-correlation functions, and the reduced standout of the main peaks, the peaks still yield the correct (i.e., zero-lag) time shifts.

So, none of the problems — static time shifts, poor NMO correction, or additive random noise — acting alone causes any problem for the cross-correlation process. Let us now see what happens when they occur in combination. Figure 2.5 shows data with

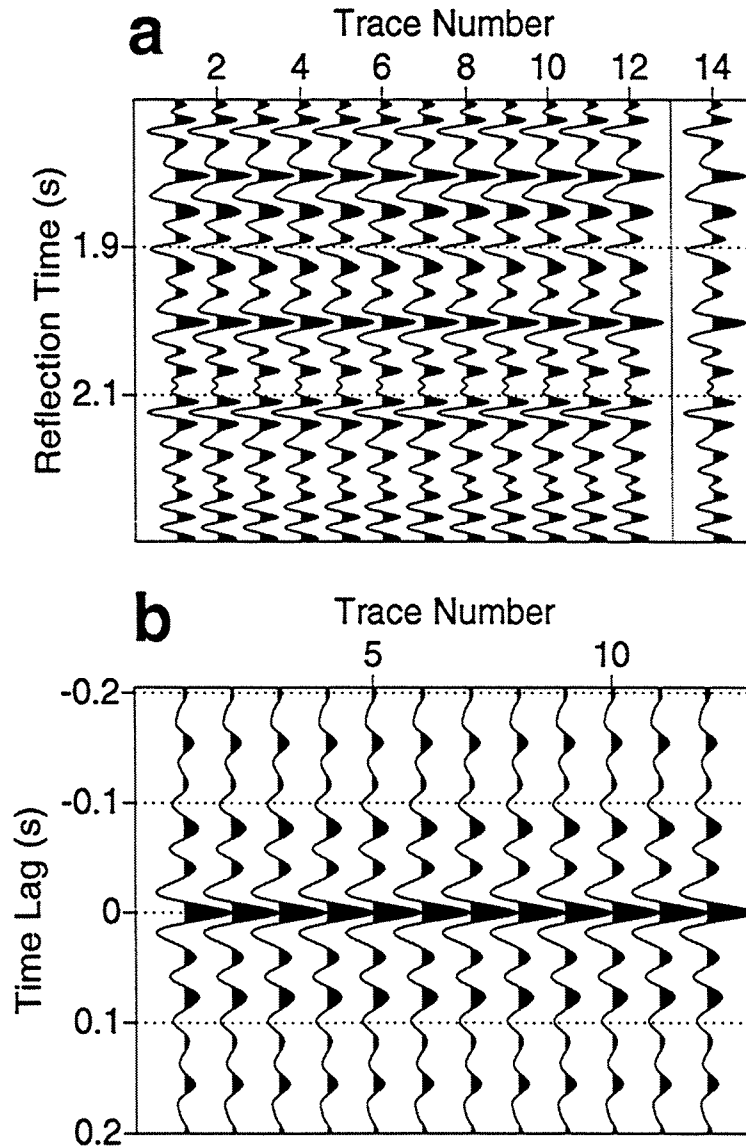


FIG. 2.1. (a) Simulated 12-fold CMP gather and its CMP-stacked trace (trace 14), and (b) cross-correlations between the traces in the gather and the stacked trace (reference trace). Here, the traces have been perfectly NMO corrected, and they are uncontaminated by either statics shifts or additive noise. For the cross-correlations, a 1-s data window was used. Only 0.6 s of the window is shown in the figure.

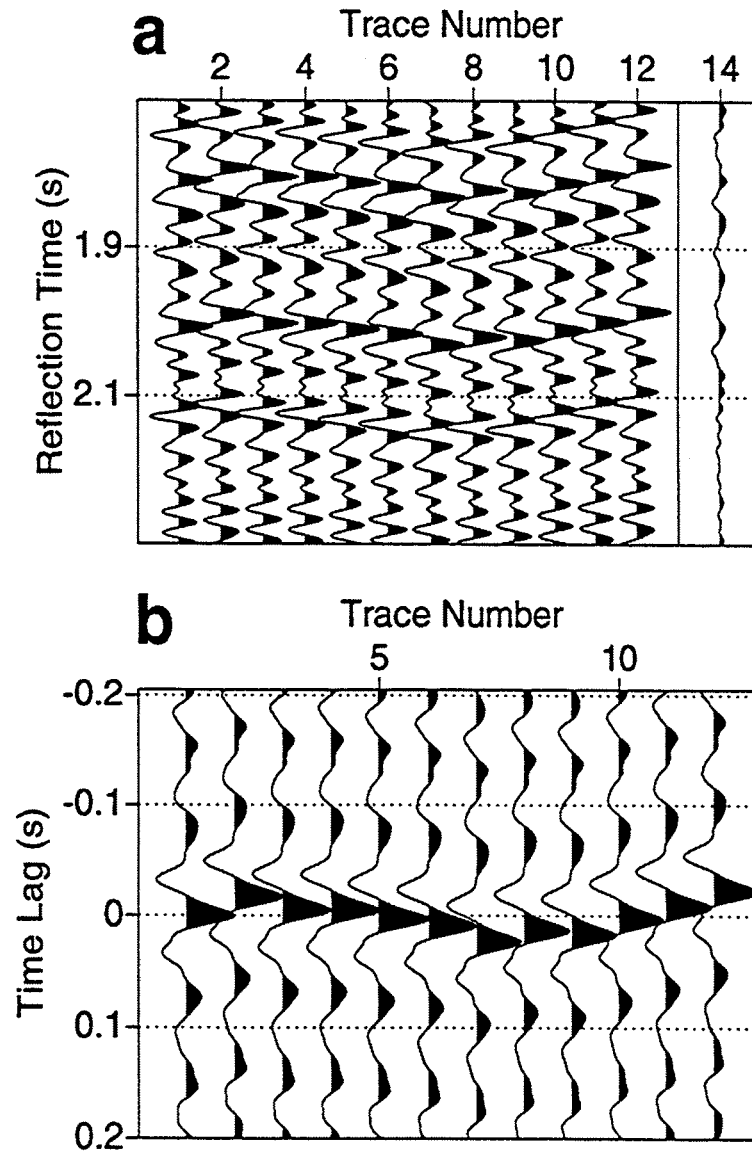


FIG. 2.2. Same as Figure 2.1, but here the data are contaminated by random static time shifts with uniform probability distribution over the range (-20 ms, +20 ms).

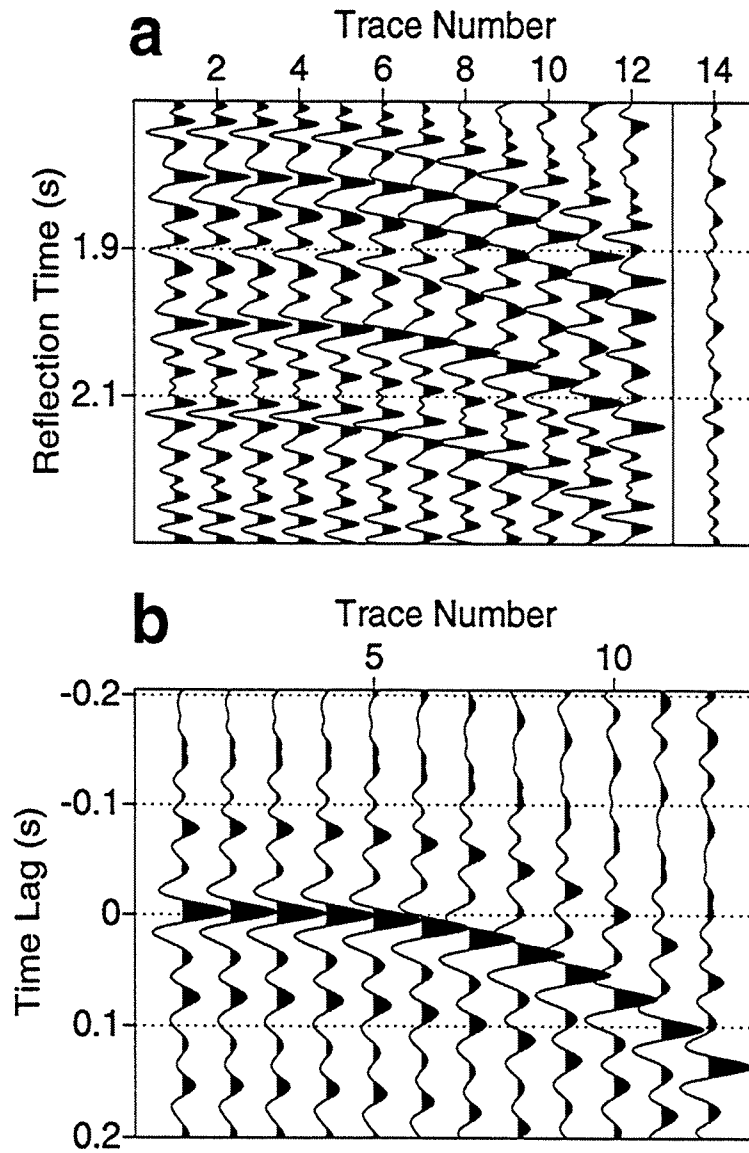


FIG. 2.3. Same as Figure 2.1, but here the data have imperfectly corrected moveout. The NMO-correction velocity is 10 percent too high.

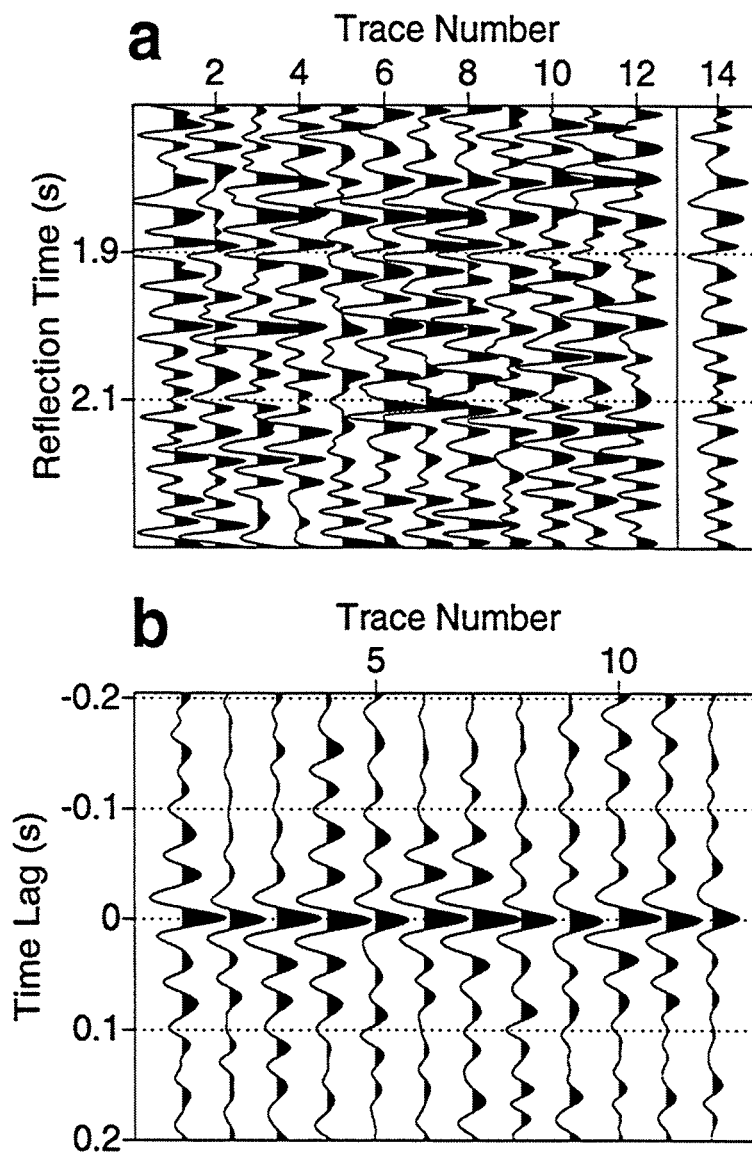


FIG. 2.4. Same as Figure 2.1, but here the data are contaminated by additive bandlimited random noise. The signal-to-noise ratio is 2.



the same static time shifts as in Figure 2.2, but with additive noise, such that  $\text{SNR} = 2$ . Now, not only is the continuity of reflections on the data traces poor, the stacked trace is poorly representative of the individual traces. Signal-to-noise ratio is not so effectively improved by the stack here because the signal is suppressed, actually distorted by the high-cut filter action of the stacking process caused by the static time shifts. As a result, the cross-correlation functions have lost the all-important standout of the main peak. The largest peaks in the cross-correlation functions do somewhat follow the correct time shifts (as seen in Figure 2.2), but sizable errors arise in interpreted peak times. Moreover, on correlation-trace 12 the false peak at a lag of about .03 s has amplitude close to that of the peak at the more nearly correct lag of -.02 s. Interpretation of the wrong peak is the undesirable phenomenon of cycle-skipping.

The next figure, Figure 2.6, simulates data that have  $\text{SNR} = 2$  and have been stacked with a velocity that is 10 percent too high. The cross-correlation functions are more easily interpreted than are those in Figure 2.5, but again, the standout of the peaks is reduced and some timing errors would arise in the interpretation.

Now, let's put all of the problems into a single data set. Figure 2.7 is noisy ( $\text{SNR} = 2$ ), is imperfectly NMO-corrected, and has static time shifts. The cross-correlation functions have now lost all their interpretive character, and cycle-skipping would be rampant. The combination of large time shifts and imperfect moveout correction has made the stacked trace not at all representative of the data. That, combined with the noise in the data, has led to correlation functions that exhibit little correlation between data and reference traces.

The problems imposed on the simulated data are large, for sure, but not extreme for many land seismic situations. (A less severe combination of simulated problems may not have led to the total loss of correlation, as here. This series of demonstrations shows, nevertheless, how cycle skips and timing errors could readily develop.) One could well argue that for such noisy data, higher-fold data should be used. We should point out, however, that while use of higher fold would improve the signal-to-noise ratio on the stacked data in many situations, the improvement is compromised if large-amplitude noise is present where the statics and NMO problems are also large. The  $\sqrt{n}$  improvement expected for  $n$ -fold data occurs only when the signal is aligned on all traces. Moreover, the high-cut filtering action of the stack in the presence of statics variations is not reduced by increase in fold. Similarly, efforts to improve the reference trace by averaging stacked traces from a number of adjacent CMP locations may help with the noise problem, but the improvement again is compromised when large statics and residual NMO are also present.

Yet one more pair of simulations further exemplifies problems of picking time shifts where the subsurface is complex. Figure 2.8 shows noiseless data with no statics imposed. Here, the data consist entirely of signal, but with reflections having two sets of residual moveout — in one set, reflections have been over-corrected because their true NMO velocity was 5 percent higher than the NMO-correction velocity used; in the other set, reflections have been under-corrected because their true NMO velocity was 5 percent lower than the NMO-correction velocity. Such a situation might arise where reflections

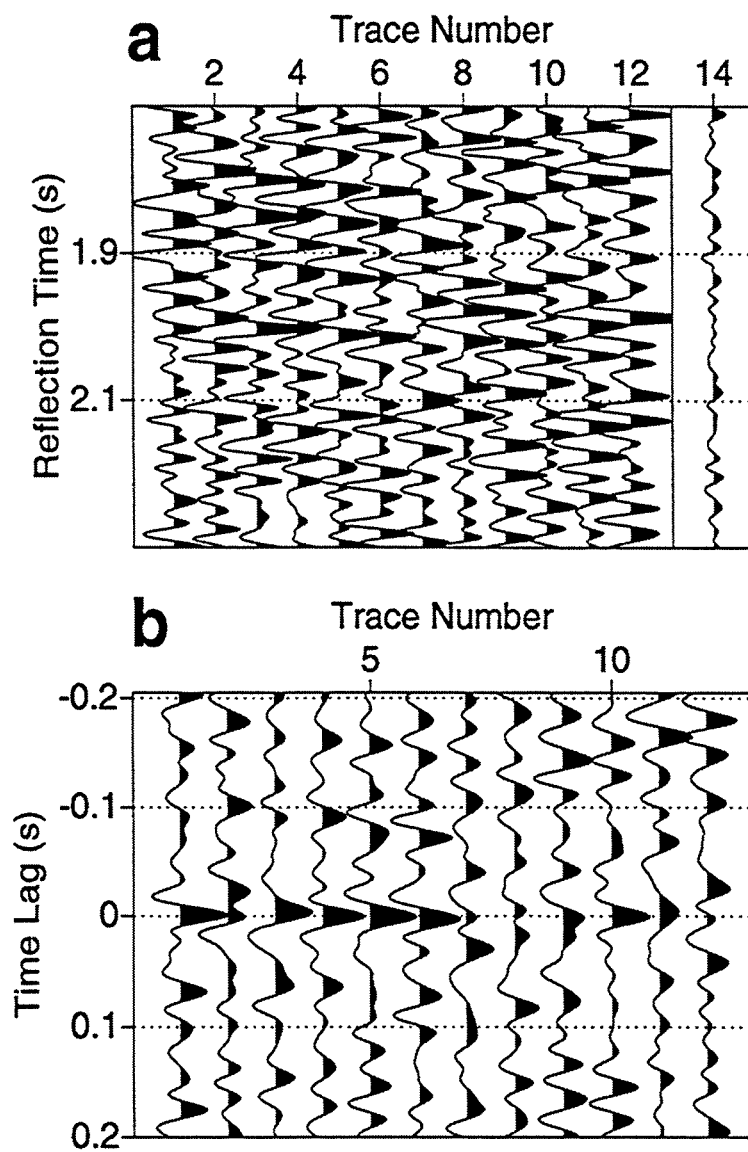


FIG. 2.5. Same as Figure 2.1, but here the data have the same static time shifts as in Figure 2.2 and are contaminated by the same additive bandlimited random noise as in Figure 2.4.

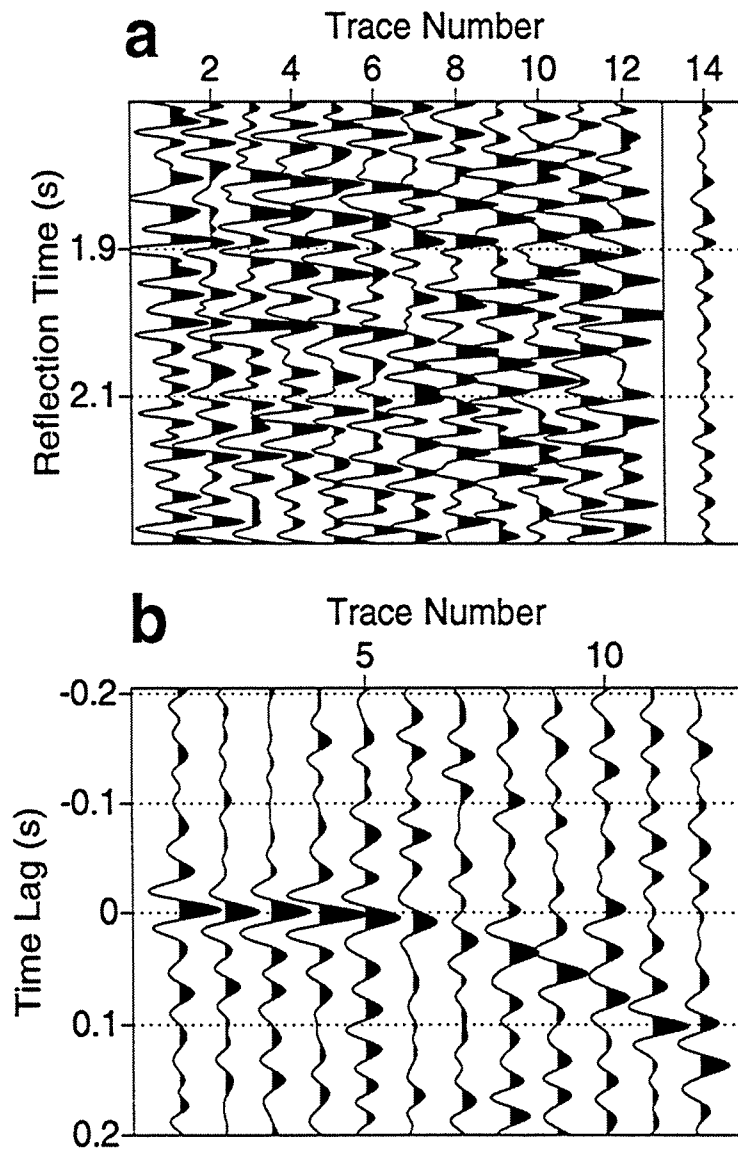


FIG. 2.6. Same as Figure 2.1, but here the data have the same imperfectly corrected moveout as in Figure 2.3 and are contaminated by the same bandlimited additive random noise as in Figure 2.4.

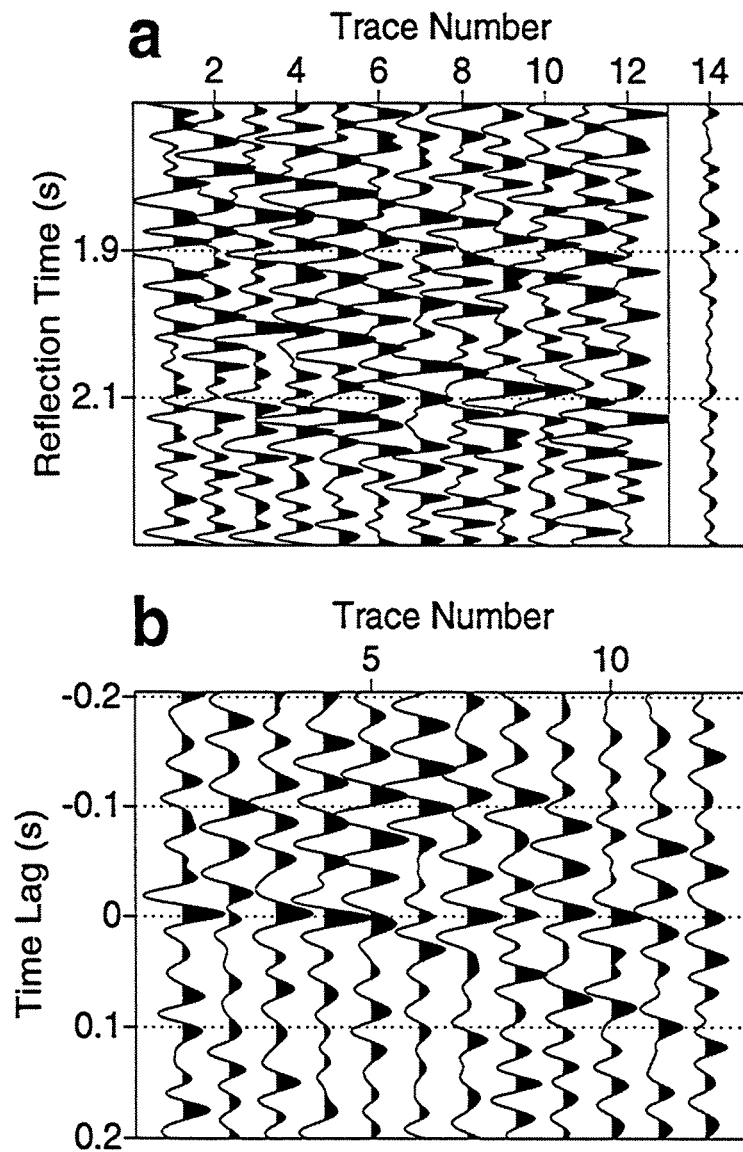


FIG. 2.7. Same as Figure 2.1, but here the data have the same imperfectly corrected moveout as in Figure 2.3, have the same static time shifts as in Figure 2.2, and are contaminated by the same bandlimited additive random noise as in Figure 2.4.

from interfaces having different dips cross one another, and, as happens too often in such situations, the stacking velocity is correct for neither of the sets of reflections. For this simulated CMP gather, the stacked trace is again representative of neither of the sets of reflections, but the cross-correlations exhibit the expected double set of peaks for the longer-offset traces, governed by the time shifts for the two sets of reflections. In this noiseless case, ambiguity would thus arise, since both sets of peaks might have comparable amplitude.

The problem again is compounded by the presence of noise, as seen in Figure 2.9. The traces here differ from those in Figure 2.8 only in that SNR is now 2. Noise again reduces the standout of the signal peaks. Moreover, the largest peak from one correlation trace to another readily flips between peaks related to the events with the two different residual moveouts. This is but another source of cycle skipping.

It could be argued that, in practice, to avoid mistakes of picking the wrong peaks one would likely restrict the range of time lags over which peaks are searched for, in the belief that the statics time shifts are not expected to be too large. The difficulty in so restricting the range of time lags searched, however, is that any problems of residual moveout require that the range of lags be increased beyond that encompassing the statics-related time shifts alone. As seen in the examples, such problems of residual moveout can be expected to be more severe for the traces from longer offsets.

Here I have highlighted problems encountered by a correlation method when NMO correction suffers from erroneous stacking velocities. Additionally, in data from a complex subsurface, moveout may be non-hyperbolic, and crossing events may make the stacking velocity multi-valued. In such situations, NMO correction introduces error not only because stacking velocities are incorrect, but also because NMO never can correct for non-hyperbolic moveout, or for the multi-valued moveout of crossing events. The source of the error due to an erroneous moveout correction in complex structures is thus three-fold:

- stacking velocities can be inaccurate, yielding residual moveout,
- rapid velocity variations in the overburden can cause non-hyperbolic moveout, and
- crossing events can exhibit conflicting moveout within a CMP gather.

Clearly, when complex subsurface structures are involved, the moveout error is likely to be more severe than that seen in the examples above, and special treatment will be necessary.

### 2.3 Stacking power methods

A different conventional approach, described by Ronen and Claerbout (1985), also utilizes cross-correlations to obtain shot and receiver time shifts. In this approach, a "super-reference trace" for each shot or receiver point is built by stacking all NMO-corrected CMP gathers containing a trace from that specific shot or receiver. Then, this super-reference trace is cross-correlated with a stack of all the traces related to that

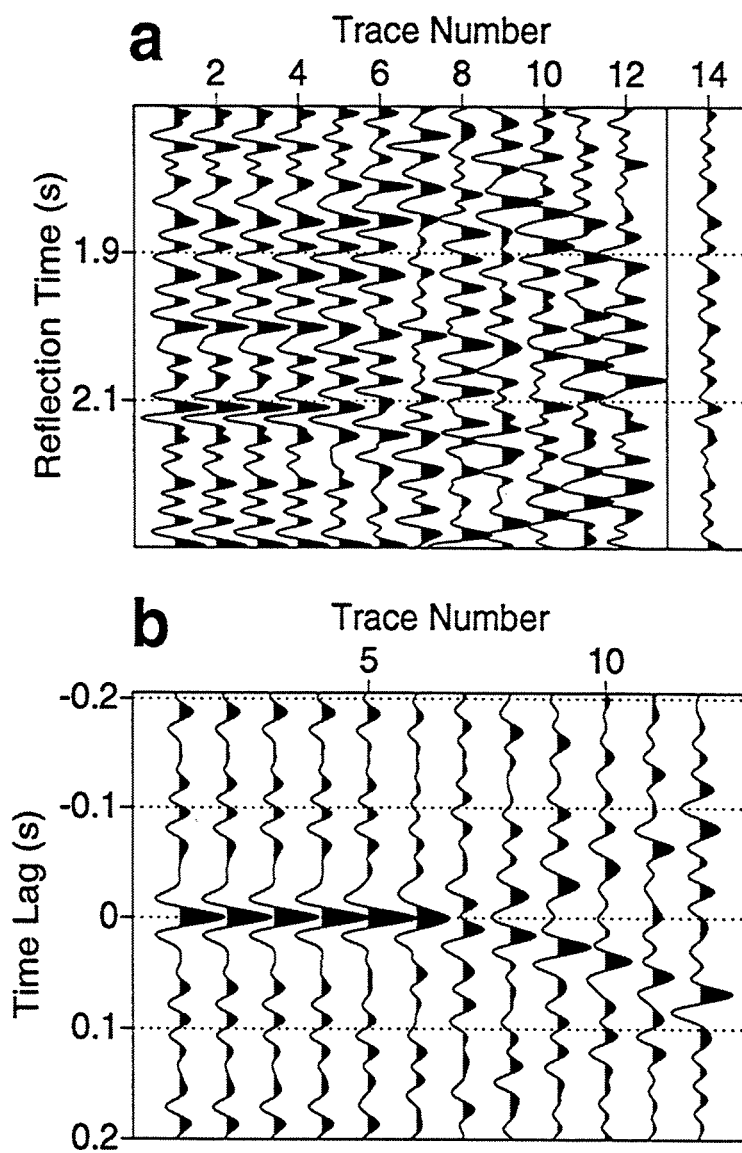


FIG. 2.8. Data containing two sets of interfering reflections. One set has been NMO corrected with a velocity that is 5 percent too high and the other with a velocity that is 5 percent too low.

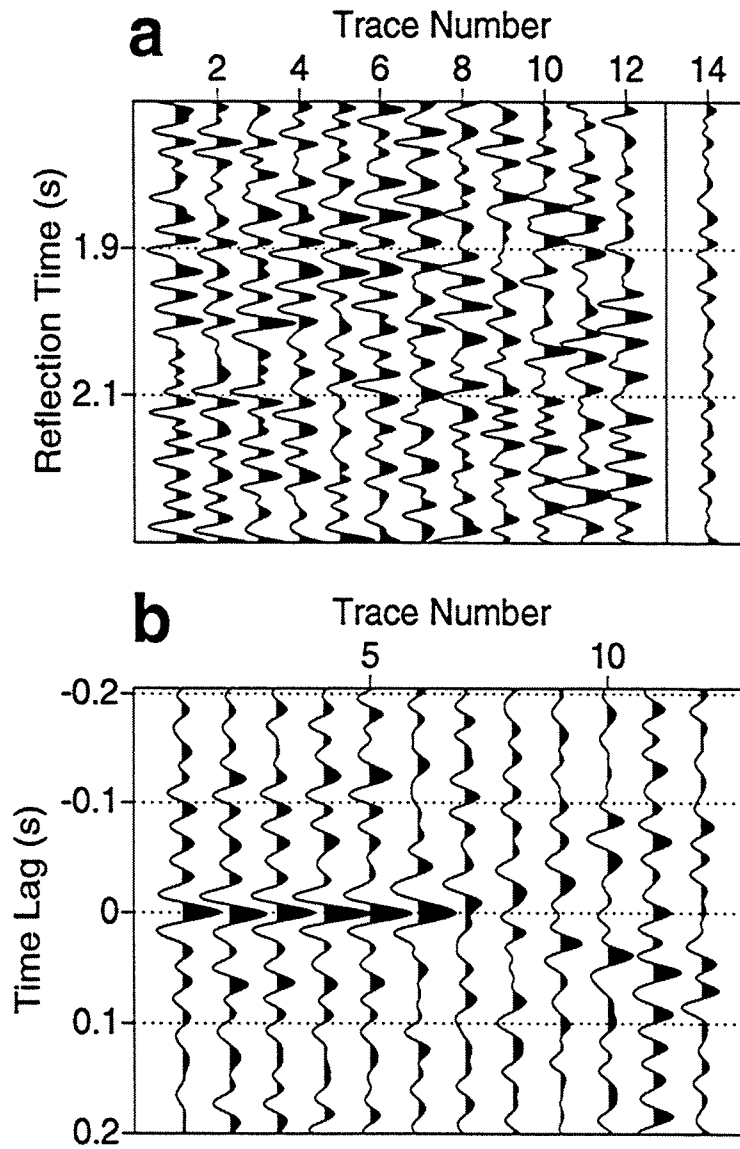


FIG. 2.9. Same as Figure 2.8, but here the data are contaminated with bandlimited random noise, such that  $\text{SNR}=2$ .

specific shot or receiver. Picking of the time lag of the main peak in this cross-correlation yields an estimate of the static time shift associated with that specific shot or receiver. Ronen and Claerbout show that maximizing the main peak in this cross-correlation is equivalent to maximizing the power of a CMP stack as a function of that particular shot (or receiver) static shift. This is done for all the shots to estimate the shot statics and for all the receivers to obtain the receiver statics.

The method is more robust for data with low signal-to-noise ratio than are the correlation methods described above and involves comparable computational cost when few iterations are needed. The method, however, does not have an option to compensate for NMO-correction errors and is therefore more sensitive to RNMO than the correlation method. Ronen and Claerbout suggested reducing the problem of the RNMO by iterating between conventional stacking velocity analysis and the stacking-power statics estimation, making the method more costly. Furthermore, because it is based on the same assumption of hyperbolic moveout, the method also suffers from the same problems as the correlation method when dealing with data of complex subsurface structures. The iterative approach cannot reduce the residual moveout when the moveout is non-hyperbolic or the data contain crossing events. Where the subsurface structure is complex, NMO correction will not suffice.

Rothman (1985 and 1986) introduced an approach that circumvents the cross-correlation with reference traces. Rather than building a reference trace, this method runs through a Monte Carlo search wherein (1) trial random combinations of source and receiver statics corrections are applied to all the NMO-corrected traces in a line, (2) CMP stacks are formed for a selected time window of the data, (3) the stacking power (actually, sum of squared amplitudes) for the window of the stacked section is computed, and (4) some form of global search is done to obtain the stacked section with maximum stacking power. As with any Monte Carlo-type approach, the search can involve an enormous number of trials, and yet is not exhaustive. Nevertheless, it has shown dramatic success (Rothman, 1986; Stork and Kusuma, 1992) where residual statics are large. Residual moveout and crossing events, as in our simulations, however, would introduce complication for the Monte Carlo approaches as well as for correlation-based approaches. Primarily, such complications would require searching over a larger range of trial static corrections than otherwise. Secondly they would cause the objective-function surface (i.e., stacking power as a function of statics corrections) to be more complex, with many more local minima, than otherwise.

## 2.4 Refraction-based statics estimation

The methods discussed above generally yield good solutions for short-wavelength static contamination (variations in the statics with a wavelength smaller than a spread length) in areas with simple subsurface structure. However, longer-wavelength components are poorly estimated by such methods. Methods based on first-break arrival times, so-called refraction methods (Lawton, 1989; Marsden, 1993b), can address both short- and long-wavelength statics. For our purpose, here, a more important advantage of these



methods is that they are not influenced by complications introduced by complex subsurface structure. In particular, refraction-based methods model the velocity and depth of the weathering layer using first-arrival events in the data and derive time shifts associated with this weathering layer. Refraction methods, therefore, should perform equally well for data from complex subsurface structures as for those from simple subsurface structures.

However, typically the model of the weathering layer is a simplification of the geology that can introduce residual errors in the statics solution. General practice, therefore, is to apply a refraction-based method to estimate and correct for the long-wavelength components of the static contamination followed by application of a residual statics-estimation method for the short-wavelength components. We will see that for data from a complex subsurface containing non-hyperbolic moveout, dipping and crossing events, residual statics estimation based on NMO correction can introduce erroneous static time shifts even where none exist in the data. Therefore, even though refraction methods may solve a large part of the static contaminations in data from complex structures, we stand the chance of re-contaminating the data when we apply a residual statics-estimation method based on the erroneous assumption that moveout is hyperbolic.

### Chapter 3

## APPLICATION OF A CONVENTIONAL METHOD TO THE MARMOUSI DATA

The simple examples in the previous chapter showed the problems that conventional statics-estimation methods can encounter when data suffer from statics time shifts, noise and complicated moveout. Let us now test a conventional method on data from a complex subsurface: the Marmousi data set.

The Marmousi data set (Versteeg and Grau, 1991) consists of a line of multi-fold synthetic traces generated for a two-dimensional (2D) structural model of considerable complexity. The model (Figure 3.1) exhibits large folding and faulting, and, although the layers are homogeneous, velocity across the model varies considerably due to structure. The noiseless 96-channel data (sampled at 4-ms interval) consist of 240 shot records, starting at surface location 3 km and ending at surface location 9 km in Figure 3.1. The shotpoint spacing is 25 m, and the receiver group interval is 25 m, yielding a maximum CMP multiplicity of 48. Offsets range from 200 m to 2575 m. Although the data are intended to simulate an off-end marine geometry, and hence ostensibly contain no near-surface-caused time distortions, we shall treat the data as though they were from a land survey by adding statics-related time shifts for some of the simulations.

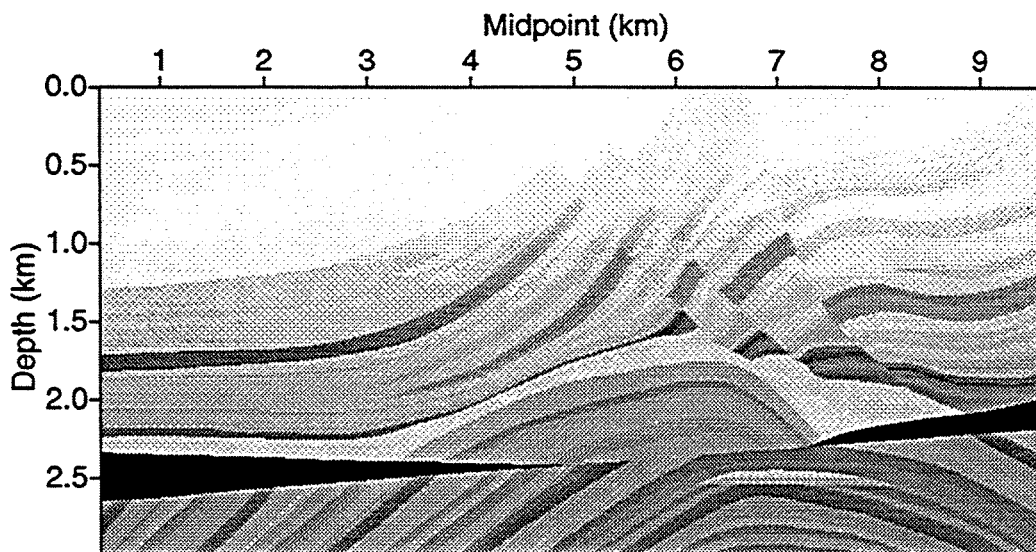


FIG. 3.1. The Marmousi structural model. The shading represents medium velocity, the darker the shade, the higher the velocity.

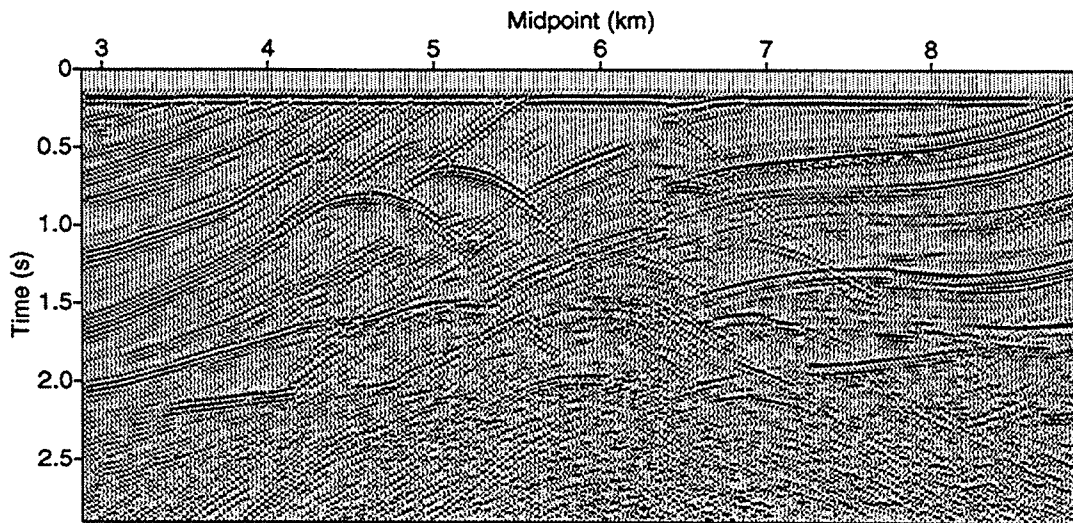


FIG. 3.2. Shortest-offset (200 m) time section from the original Marmousi data.

Although the original data contain no statics problem as such, in fact the lateral structural variation extends all the way to the surface. Certainly these data are replete with distortions in reflection time, from the surface down (Figure 3.2 shows the short-offset traces). The structural model, however, does not exhibit short-wavelength lateral variations in a low-velocity weathered layer as often exist in land seismic data. What the model data do exhibit, however, are rapid changes in stacking velocity across the section, non-hyperbolic moveout within CMP gathers, and crossing events having different moveouts within any given gather.

### 3.1 Application of a conventional statics estimation method to statics contaminated Marmousi data

To illustrate the problem of statics estimation with a conventional statics-estimation procedure where the subsurface is complex, let us contaminate the Marmousi data with random, zero-mean, surface-consistent source and receiver static time shifts uniformly distributed between  $-20$  ms and  $+20$  ms (Figure 3.3). With no loss in generality, I have made the source statics and receiver statics identical. Furthermore, statics shifts varying along the line with wavelengths longer than the cable length (i.e., 2.575 km) have been filtered. The migration-based method proposed here can no better solve for such long-wavelength statics than can conventional methods; therefore we will concentrate on the wavelength components for which residual statics methods are supposed to be well suited. Figure 3.4 shows the statics-contaminated short-offset traces. We can expect a stack of many offsets to suffer from the usual high-cut filtering action when such statics variations have not been resolved.

Prior to the conventional statics-estimation process, we apply NMO corrections using laterally varying stacking velocity functions interpreted from conventional velocity

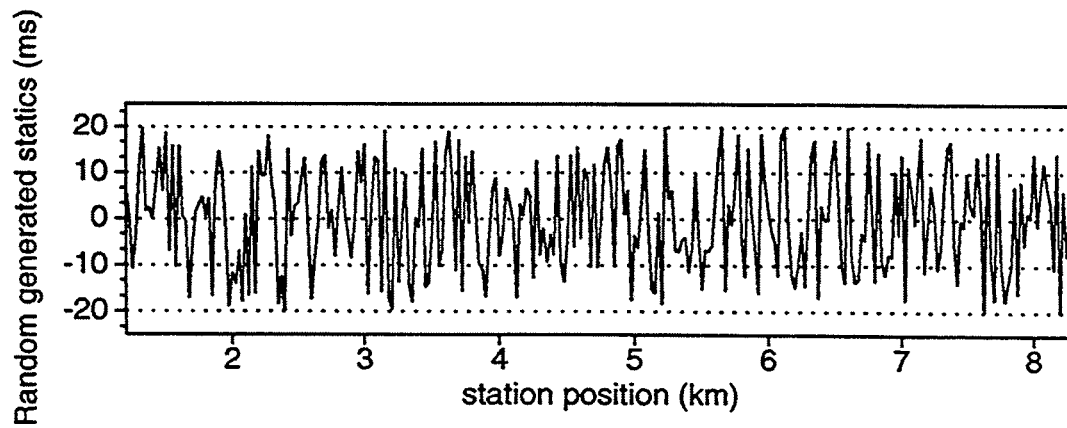


FIG. 3.3. Generated source and receiver static time shifts as a function of station position. The random time shifts are uniformly distributed between  $-20$  ms and  $+20$  ms.

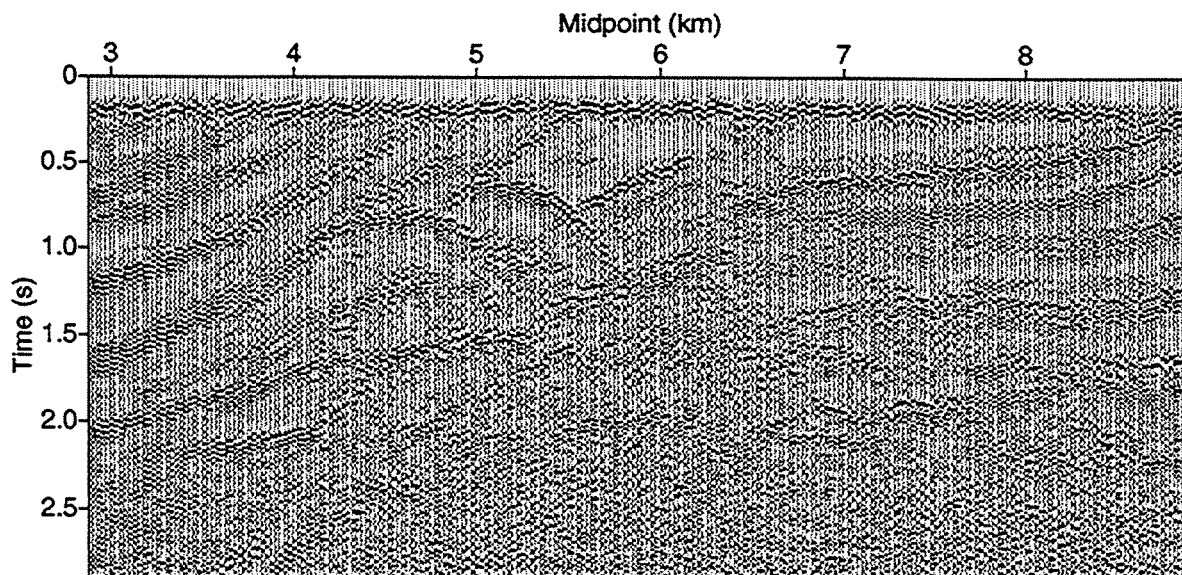
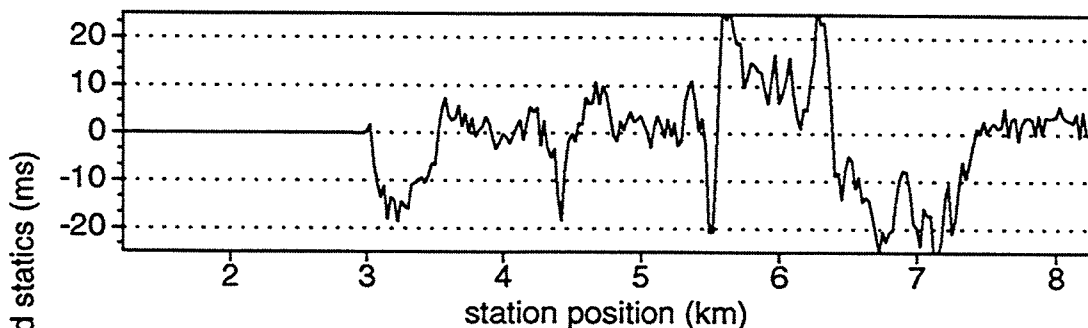


FIG. 3.4. Shortest-offset time section from the Marmousi data contaminated by the imposed source and receiver statics. Compare with Figure 3.2

analysis in the statics-contaminated data, as might be done in practice. Note that, even for events with hyperbolic moveout, this velocity analysis is being complicated by the erratic static time distortions which cause the true moveout to be distorted (Marsden, 1993c). Velocity analysis was done at 28 equally-spaced positions across the section.

The time windows that were used for the cross-correlation analysis in the correlation statics-estimation method extended from approximately 0.5 to 1.7 s, and in these cross-correlation functions the algorithm searched between  $-80$  ms and  $+80$  ms for the largest peak despite the fact that the maximum imposed trace-to-trace shifts were between  $-40$  ms and  $+40$  ms. Where residual moveout is large (typically on the larger-offset traces, but also on the shorter-offset traces when velocity varies rapidly across the seismic section), the correct peaks could otherwise fall outside the search range, thus ensuring cycle skipping.

### Error in source statics



### Error in receiver statics

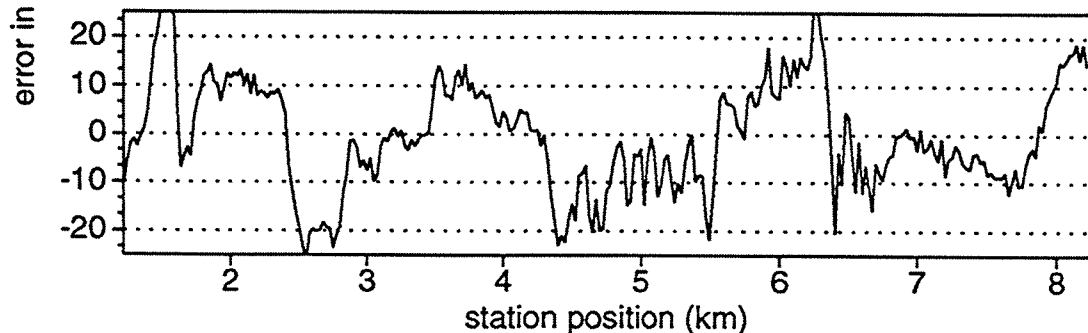


FIG. 3.5. Difference between the imposed random static time shifts (see Figure 3.3) and the conventionally estimated source and receiver corrections. The first shot location is at surface position 3 km (Figure 3.1).

Figure 3.5 shows the difference between the estimated and applied statics for both sources and receivers. Especially for shots and receivers between positions 4.5 km and

7.5 km (i.e., the complex portion of the Marmousi model), errors in computed receiver and source statics are large — sometimes approaching the size of the imposed static shifts themselves. Sizable errors exist over a range of wavelengths, but much of the short-wavelength statics problem has been corrected.

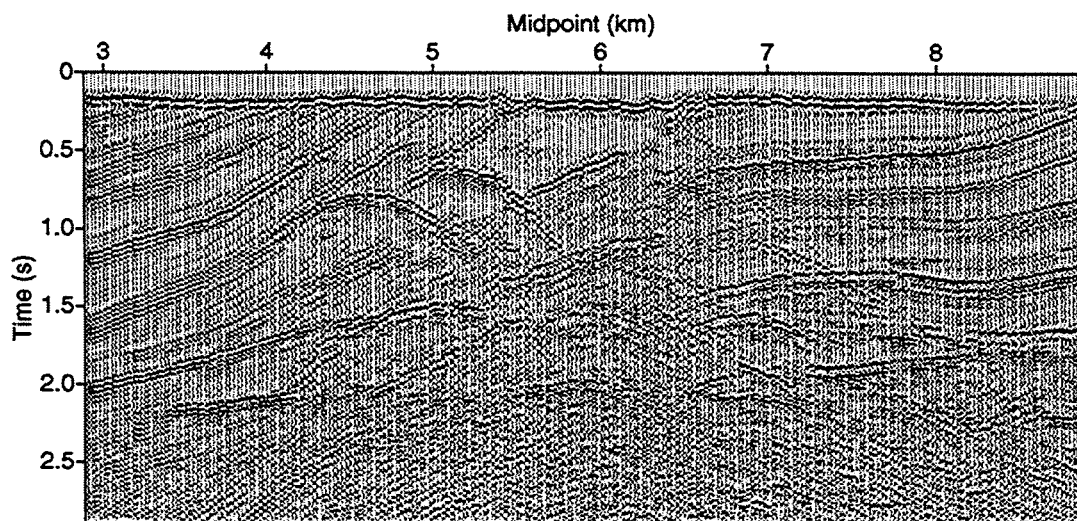


FIG. 3.6. Shortest-offset time section from the statics-contaminated Marmousi data after correction with statics estimates obtained in a conventional manner.

Figure 3.6 shows the the short-offset traces, corrected with the statics estimates given in Figure 3.5. The signal has improved on the sides of the model (compare with the statics-contaminated data shown in Figure 3.4) but in the complex part of the model between midpoints 4.5 km and 7 km, large residual timing errors can be seen in the reflections (compare with the original data in Figure 3.2). Thus application of a conventional statics-estimation method (based on these NMO correction and stacking to build reference traces against which the data traces are cross-correlated) yields estimates of source and receiver statics that differ significantly from the imposed statics.

Certainly, one source of error can be attributed to problems in moveout correction since hyperbolic moveout was assumed for the conventional approach, whereas the moveout is truly not hyperbolic for a subsurface with such structural complexity. However, we should have expected the statics estimation to have been better in the less complex areas of the model. We can sense the source of the problem in Figure 3.7, which shows a window of the NMO-corrected CMP gather taken from the statics-distorted data at surface location 3.475 km in Figure 3.1. Also shown at the far right is the stacked trace, i.e., the reference trace. This CMP gather is off to the side of the more complex part of the model, so we might expect that the moveout of the reflections is primarily hyperbolic. Indeed, the NMO correction for the reflections in this CMP gather is acceptable.

Nevertheless, cross-correlation of the reference trace with the traces in the gather results in the almost featureless cross-correlation functions shown in Figure 3.8. For many

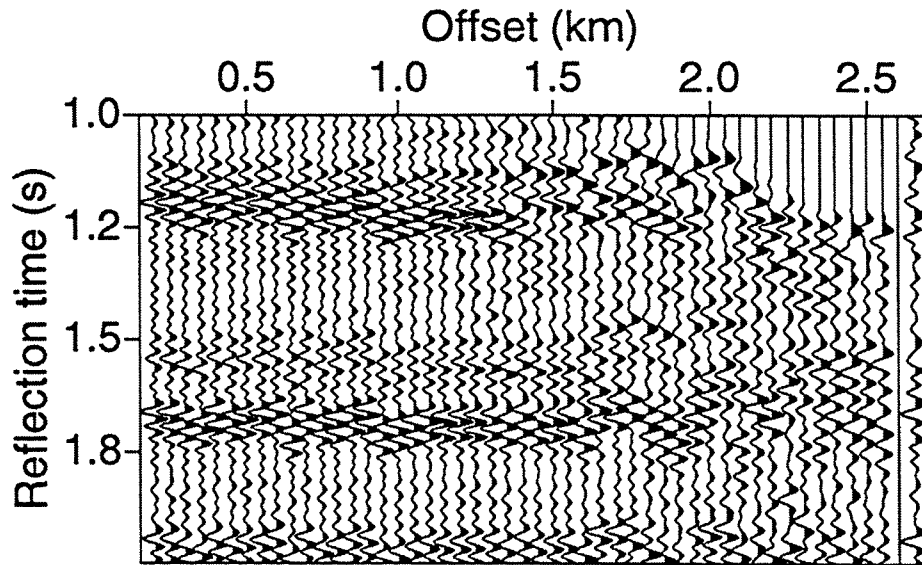


FIG. 3.7. NMO-corrected CMP gather at surface location 3.475 km from the statics-distorted Marmousi data set, and its stacked trace (the reference trace) at the far right. The stacked trace has been gained to boost trace excursions for viewing.

offsets, no consistent, identifiable main peak dominates the cross-correlations. Consequently, time shifts picked for the traces will be incorrect; specifically, cycle skipping, will be rampant. This result is puzzling since the moveout correction for this gather seemed to have generally aligned the signal, except for the static shifts. Since the influence of the statics shifts should be reduced after stacking, we should expect the reference trace to be a good representation of statics-free traces in the gather.

A close look at the cross-correlation functions in Figure 3.8 shows their oscillatory character, which causes the main peak not to stand out over the side-lobes. A similar repetitiveness is present in the reflections in the CMP gather (Figure 3.7). Perhaps deconvolution, which can suppress such an oscillatory character in the data, might aid in enhancing the standout of the main peak in the computed cross-correlations.

Figure 3.9 shows the equivalent of the CMP gather in Figure 3.7, spiking deconvolved with an operator length of 90 ms. Again the far right trace is the reference trace, which now shows distinctive reflections compared with the one in Figure 3.7. Cross-correlation of this reference trace with the deconvolved traces in the gather yields the much improved cross-correlation functions in Figure 3.10. Now the main peaks, for traces up to an offset of 1.5 km, have good stand out relative to the side-lobes; moreover, for these offsets the peaks are at, or close to, their correct positions, as supported by the cross-correlation functions in Figure 3.11 and the picking errors shown in Figure 3.12. Figure 3.11 shows cross-correlations of the original, non-statics-contaminated deconvolved traces of the CMP gather at surface location 3.475 km and their statics-contaminated counterparts. The shifts associated with the main peaks in these cross-correlation func-

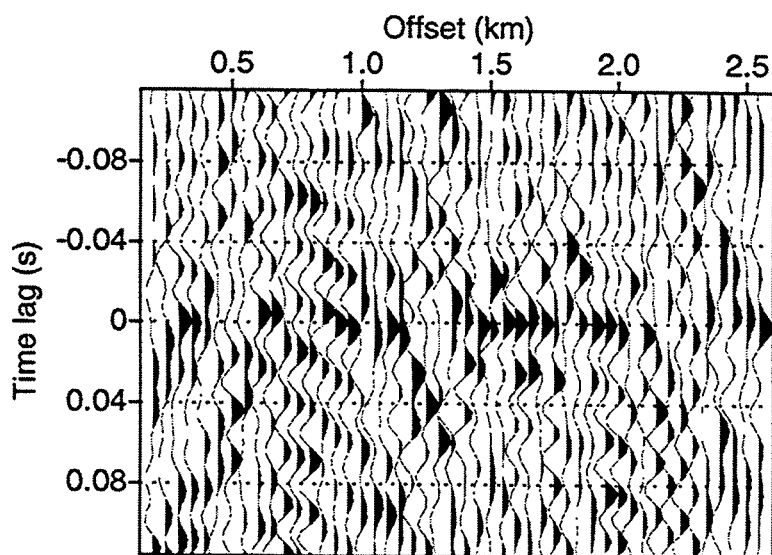


FIG. 3.14. Cross-correlations between the statics-contaminated, deconvolved Marmousi traces in Figure 3.13 and the stacked trace in that figure.

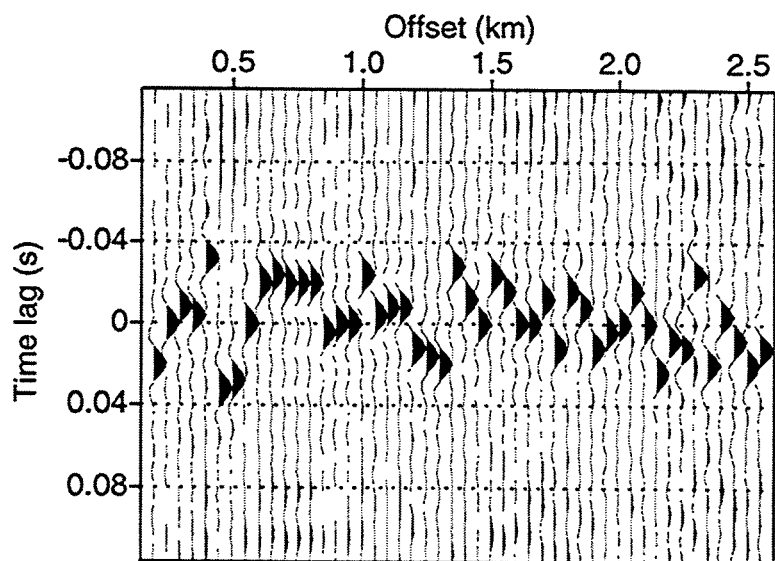


FIG. 3.15. Cross-correlations between the deconvolved statics-contaminated Marmousi data and the deconvolved original Marmousi data, for the CMP gather at surface location 5.9 km. The trace-to-trace time shifts associated with the peak value of the cross-correlation functions are the result of the imposed statics.



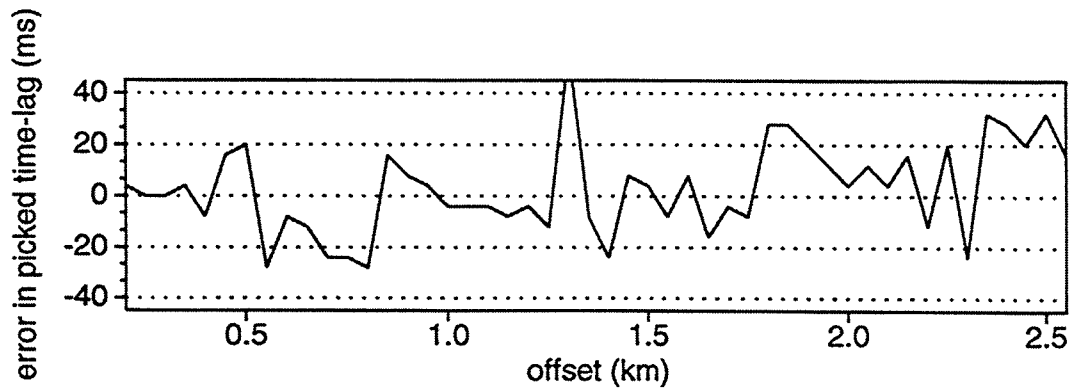
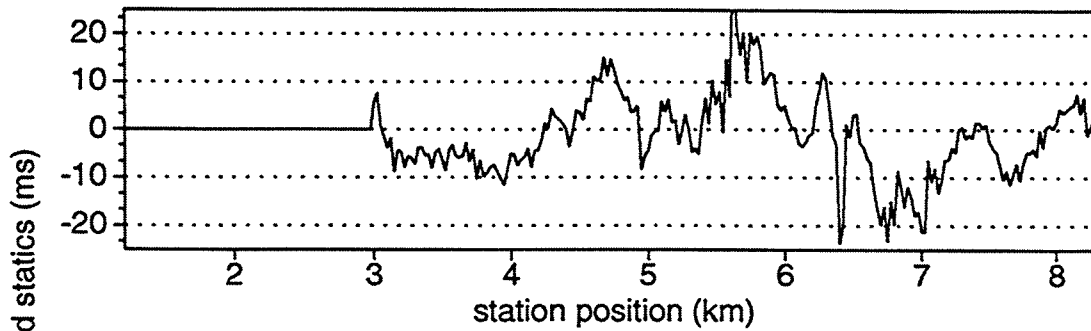


FIG. 3.16. Error introduced by picking peaks in correlations for the CMP gather at 5.9 km after conventional NMO correction.

### Error in source statics



### Error in receiver statics

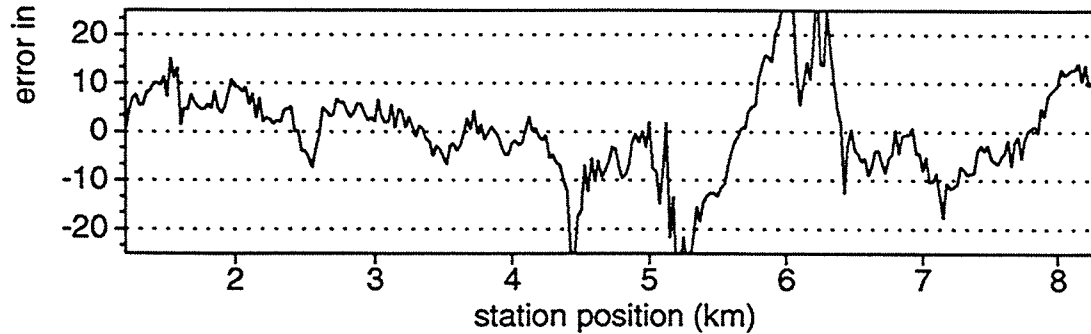


FIG. 3.17. Difference between the imposed random static time shifts and the conventionally estimated source and receiver corrections for the statics-contaminated, deconvolved Marmoussi data.

after applying deconvolution to the data. Especially around midpoint positions 5.5 and 6.5 km time distortions remain in the data (compare with the original data in Figure 3.2). Around these midpoint positions, faults cut through the subsurface and velocity varies rapidly (see Figure 3.1). Unfortunately, just at these positions we would hope to obtain accurate imaging since the section below 2.2 s at these positions is considered of the most interest for exploration.

General practice in conventional processing is to iterate the statics-estimation process. After this first iteration of statics estimation, the velocity model is updated. A second and subsequent iterations of statics estimation and velocity-model updating is done, with the goal of obtaining a more accurate statics solution. I will discuss results of such an iterative approach in Chapter 5.

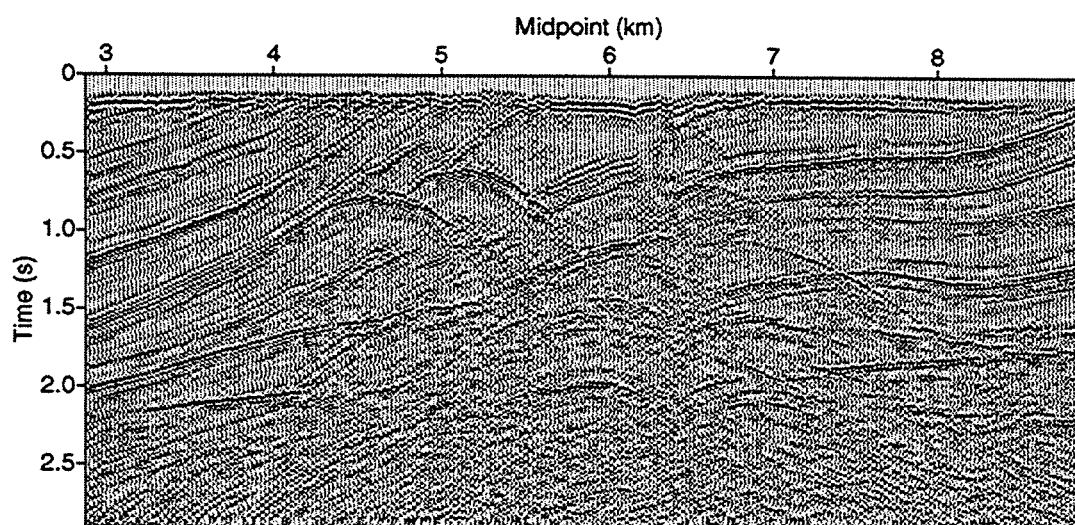


FIG. 3.18. Shortest-offset time section from the statics-contaminated, deconvolved Marmousi data after correction with statics estimates obtained with a conventional method. Compare with the sections shown in Figures 3.2 and 3.6.

### 3.2 Application of a conventional statics-estimation method to the original, uncontaminated Marmousi data

One source of the errors in the derived statics estimates here was the presence of the statics time shifts themselves. The static time shifts cause the events on the CMP gathers to be misaligned, thus deteriorating the stack (i.e. the reference trace). Therefore, not all the errors in Figure 3.17 may be attributed to errors in the moveout correction. Given that enough complication exists from the moveout complexity alone, we might wonder what would be the result of applying a conventional statics-estimation procedure to the deconvolved Marmousi data, with no statics shifts imposed. Ideally, in this test the estimated statics should be zero since the data have not been contaminated with noise

and statics time distortions. The complex moveout, however, remains a source of error. This test would therefore tell us the influence of the error introduced by only the residual moveout in the statics estimation.

For this test, NMO corrections are applied with stacking velocities that are interpreted from conventional velocity analysis done on the deconvolved Marmousi data that are uncontaminated with statics problems. With no statics distortions in the data, accurate stacking velocity estimates are not difficult to obtain off to the sides of the model. In the more complex part of the model, however, it is not possible to flatten reflections across the entire CMP gather and considerable RNMO remains in the data. As a result, Figure 3.19 shows significant computed source and receiver static corrections, even though *no static time shifts are present in this data test*. When applied to the data, these “corrections” introduce distortions into the prestack-migrated data (see Figure 3.20). Compare this with the migrated result of the original Marmousi data shown in Figure 3.21. In the complex part of the model the structure is distorted due to the introduced time shifts. Therefore, applying a conventional statics-estimation method based on just NMO correction to data from structurally complex areas can distort the data. It would be better not to attempt the conventional statics estimation and correction.

Note that the errors in Figure 3.17 show larger-amplitude short-wavelength components compared with the errors in Figure 3.19. This result suggests that the short-wavelength errors in statics seen in Figure 3.17 arise because of the presence of the statics that were imposed on the data for that test. The longer-wavelength errors appear to be caused by the residual moveout that results from shortcomings of the hyperbolic moveout assumption in the conventional statics estimation. We shall see that while iterative use of conventional methods can reduce the short-wavelength errors, longer-wavelength errors remain in the data. Clearly, statics estimation is closely related to velocity estimation.

The source of the errors introduced by the residual moveout becomes clear by examining the CMP gathers of the NMO-corrected data. Figure 3.22 again shows the NMO-corrected CMP gather at surface location 3.475 km and its reference trace, but now for the deconvolved original data—free of any imposed statics shifts. The reflections in this CMP gather have been NMO corrected with stacking velocities interpreted from a conventional velocity analysis. Although this CMP position is away from the complex part of the model the moveout for events on the larger-offset traces is nonetheless influenced by the velocity in the complex part of the model. For example, for the trace with 2-km offset, the source is located at surface position 4.475 km, which is over the complex part of the model (Figure 3.1). For the larger-offset traces the gather therefore exhibits residual moveout. Cross-correlations (shown in Figure 3.23) between the reference trace and the NMO-corrected data traces therefore show peaks with good standout at, or close to, the correct time lags (i.e. at zero-lag since no static distortions have been imposed on the data) for offsets up to 1.5 km. For larger offsets, the main peak does not have such prominent standout; indeed sometimes sidelobes have larger amplitude than that of the correct peak, which will cause cycle skipping when the cross-correlations are interpreted in order to give time shifts. Additionally, errors are introduced when the main peak is not positioned correctly due to the residual moveout.

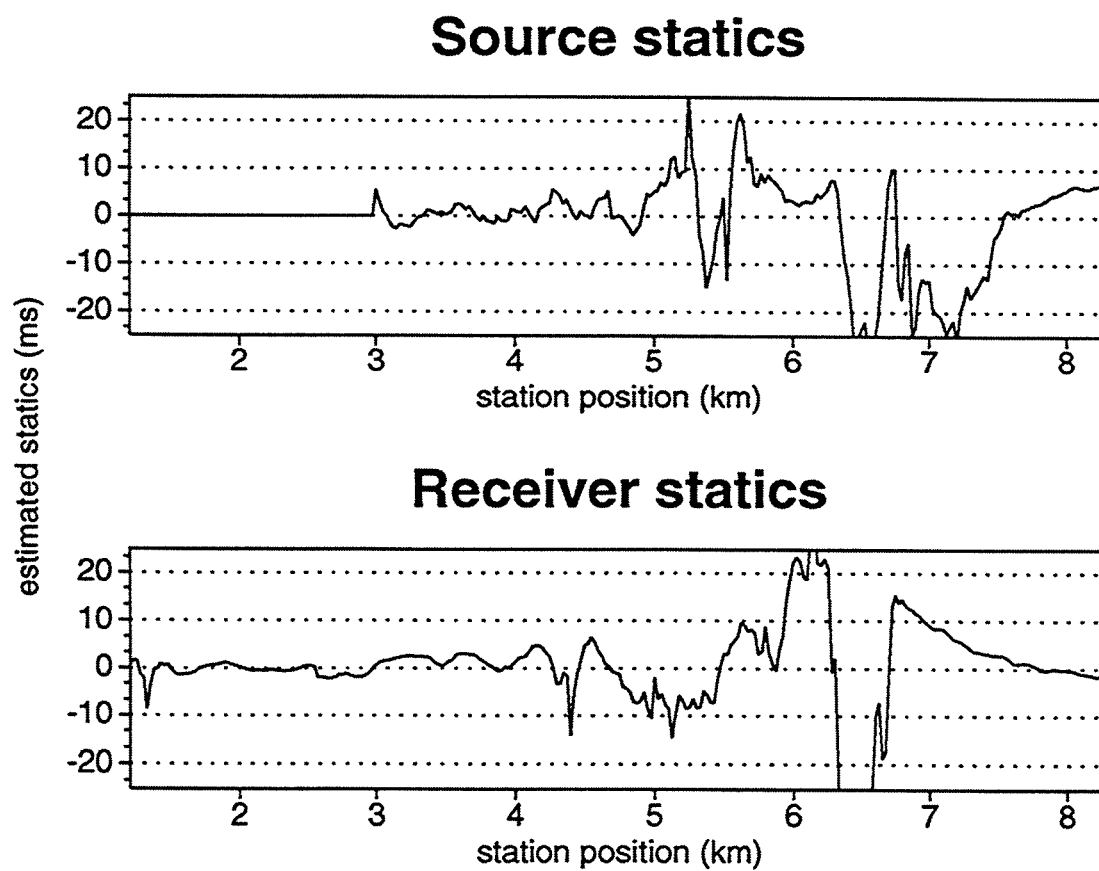


FIG. 3.19. Conventionally estimated source and receiver statics from the deconvolved Marmousi data that have no statics contamination imposed.

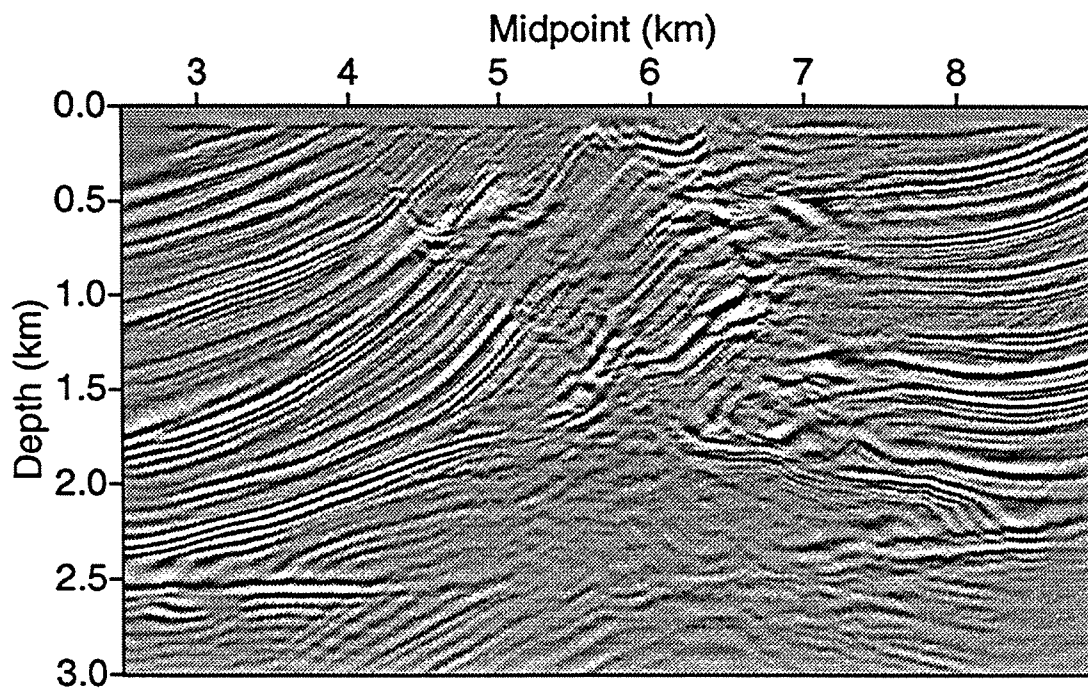


FIG. 3.20. Prestack depth-migrated image of Marmousi data that have been "corrected" with static time shifts that were estimated from the original Marmousi data by a conventional statics-estimation method. The migration velocity is the exact Marmousi velocity shown in Figure 3.1.

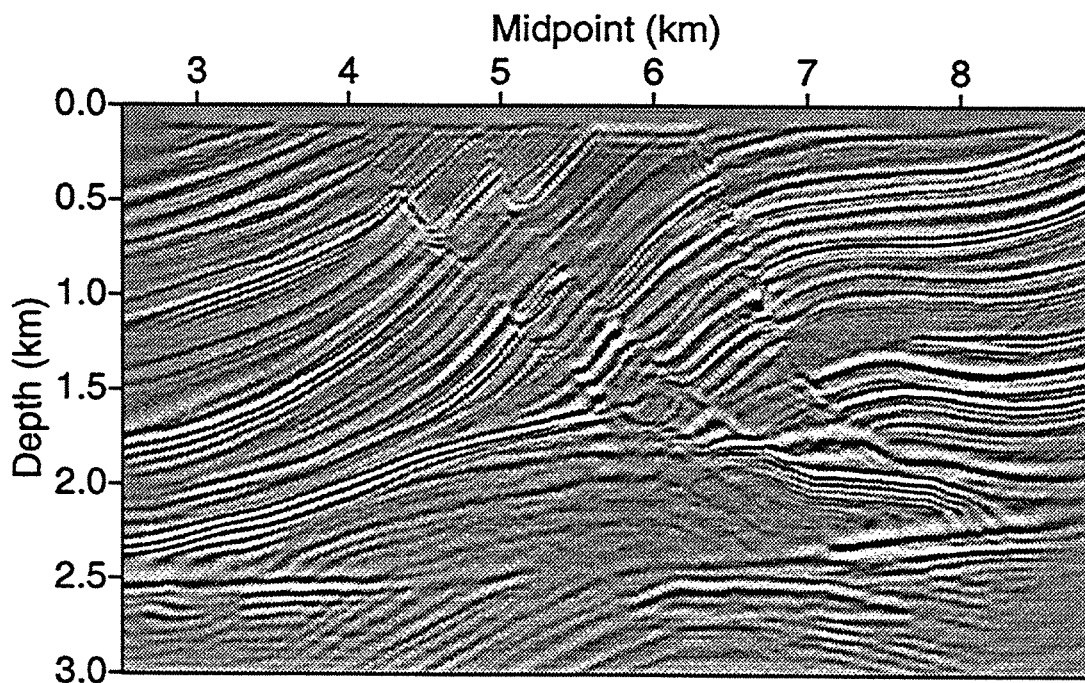


FIG. 3.21. Prestack depth-migrated image of the original Marmousi data. The migration velocity is the exact Marmousi velocity shown in Figure 3.1.

Part of the error introduced by the erroneous moveout correction can be accommodated by the  $m_k X_{ij}^2$  term in equation (2.1). Furthermore, redundancy of the picked time-lags can help to reduce the error. However, the part of the residual moveout that is related to non-hyperbolic moveout or crossing events cannot be ameliorated in a conventional statics approach. Judging from the solution in Figure 3.17, the  $m_k X_{ij}^2$  term and redundancy succeeded in correcting for the moveout error away from the complex part of the model. In the complex part of the model, however, large errors remain.

Figure 3.24 shows NMO-corrected traces and the reference trace, as before, but now from the complex portion of the model (surface location 5.9 km), and Figure 3.25 shows the cross-correlation traces. Now the hyperbolic moveout correction is poor for all offsets. As a result, the cross-correlation functions (Figure 3.25) for even the shortest-offset traces have no distinct peak value near zero lag even though the data have been deconvolved. Useless time shifts would be inferred, and cycle skipping would arise for most of the traces in the gather. Now, the  $m_k X_{ij}^2$  term cannot compensate for the moveout error since the moveout is non-hyperbolic and crossing events exist in this CMP gather. Furthermore, redundancy cannot help the estimation algorithm converge to the correct solution either since the time lags for the smaller-offset traces also contain large errors.

Actually, the NMO correction at these CMP locations is better than at some neighboring locations. Where lateral velocity variation in the overburden is rapid, such as in the Marmousi model, stacking velocity can vary rapidly along a line (Miller, 1974;

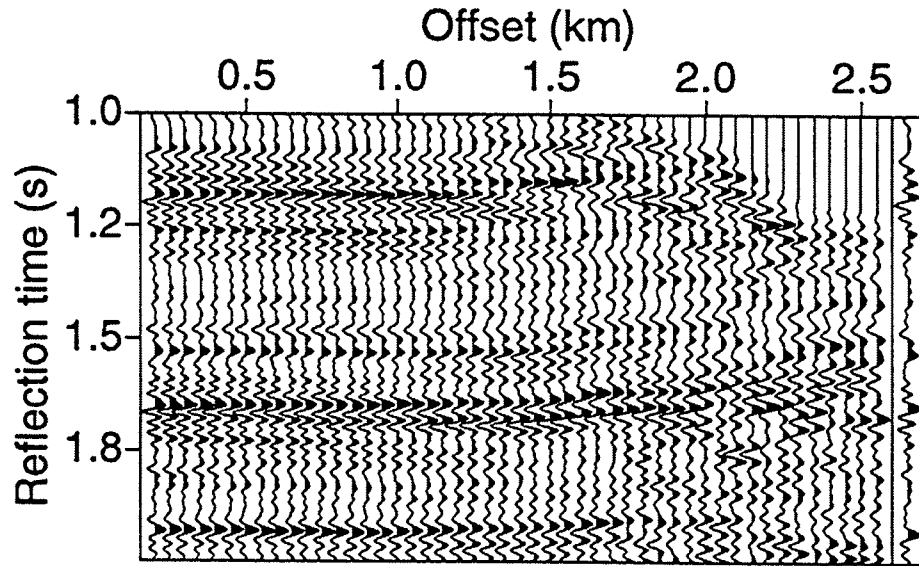


FIG. 3.22. NMO-corrected CMP gather at surface location 3.475 km, from the deconvolved Marmousi data set, and its stacked trace (the reference trace) at the far right. The stacked trace has been gained relative to the others.

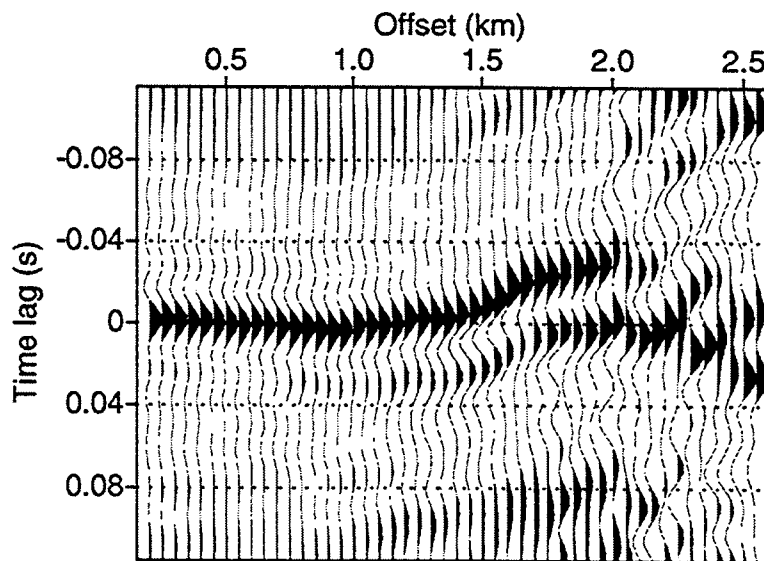


FIG. 3.23. Cross-correlations for the NMO-corrected CMP gather at surface location 3.475 km, from the deconvolved Marmousi data with no imposed statics shifts.

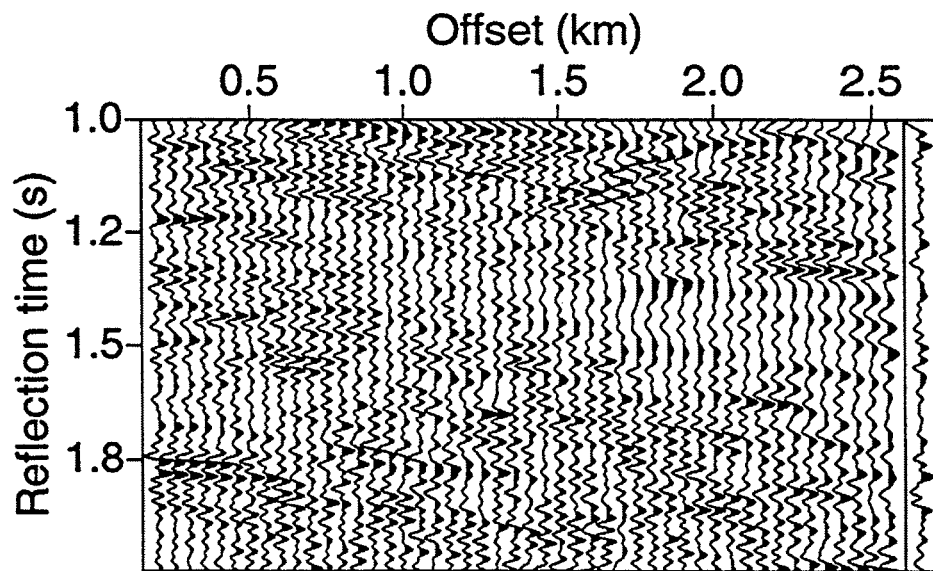


FIG. 3.24. NMO-corrected CMP gather at surface location 5.9 km, from the deconvolved Marmousi data set, and its stacked (and gained) trace, the reference trace, at the far right.

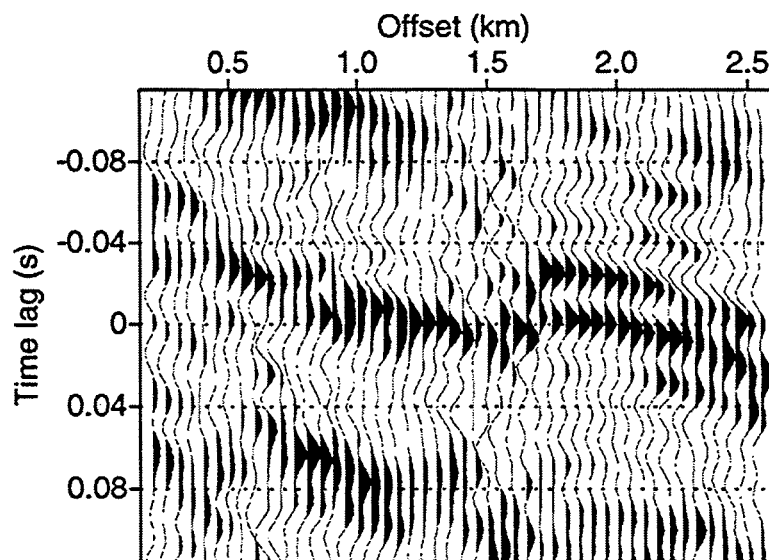


FIG. 3.25. Cross-correlations for the NMO-corrected CMP gather at surface location 5.9 km, from the deconvolved Marmousi data.



Larner et al., 1983). The location of the CMP gather shown in Figure 3.22 is only one of the 28 locations along the line at which the stacking velocity was computed. The stacking velocity obtained for this CMP gather therefore may not be representative of the best NMO-correction velocity at nearby CMP locations even when the proper moveout correction is approximately hyperbolic. Without considerable effort at estimating NMO velocities at closely spaced locations (whether or not departures from hyperbolic moveout are large), we can expect large errors in stacking velocity across such a section.

### 3.3 Application of a conventional statics-estimation method to Marmousi data contaminated by both static shifts and noise

Noise of many types, random or coherent (such as multiple energy, out-of-plane reflections, ground roll, mode conversions, refractions) may contaminate the seismic data. The synthetic Marmousi data, however, do not contain significant noise. Some multiple energy is present as described by Berkhout et al. (1990), but its amplitude is not large. Here, I add further complication to the statics-contaminated Marmousi data by superimposing random bandlimited noise. Figure 3.26 shows the short-offset traces of the original, deconvolved Marmousi data contaminated with random noise in addition to the same static time shifts imposed above. The noise is bandlimited to the same general frequency band as that of the signal, and, as before, the root-mean-square amplitude of the noise is  $1/2$  the peak signal amplitude, multiplied by .707 (Again, for such a noise level, we say that the signal-to-noise ratio is  $SNR=2$ ). In addition to the added noise, these data suffer from all the problems mentioned above: static time distortions, conflicting dip, and complex moveout. We might expect that velocity analysis in statics-contaminated data from a complex subsurface with such SNR will produce stacking velocities with gross errors, causing the residual moveout to be even larger than in the previous cases.

Conventional statics-estimation procedure fails to estimate accurate statics, for this case, even for the sources and receivers away from the complex part of the model. Figure 3.27 shows the large errors in the estimated source and receiver statics for this noisy data set. Compare these errors with those obtained in the noiseless case shown in Figure 3.17. The errors now have increased significantly for the sources and receivers away from the complex part of the model. This increase is caused partly by the noise that deteriorates the quality of the data and the reference traces, and partly by an increased error in the stacking velocities that were obtained from velocity analysis. These erroneous stacking velocities cause large residual moveout, even in the simple part of the model.

Figure 3.28 shows a window of the NMO-corrected CMP gather, at surface location 3.475 km, for the noise- and statics-contaminated Marmousi data. Even if we could identify a reflection, it would be difficult to estimate the correct stacking velocity that aligns reflections in the gather. Noise and statics time shifts both add to deteriorate of the coherency panels and complicate attempts to aligning reflections in the CMP gather. To a certain extent, the human eye can “filter” out the contaminations caused by the noise and static time shifts (in Figure 3.28 we can see “flattened” reflections around 1.65 s and 1.95 s), but this can be done only with a great margin of error. Remember that

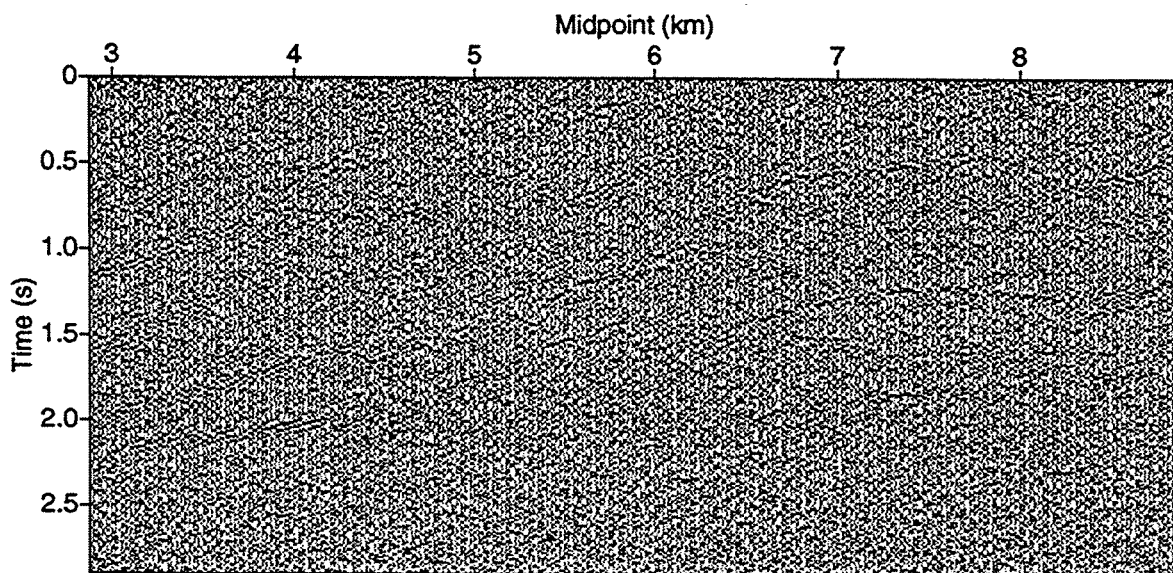


FIG. 3.26. Shortest-offset time section from the Marmousi data contaminated by the imposed source and receiver statics and bandlimited random noise. (Compare with the uncontaminated section in Figure 3.2)

this CMP position is away from the complex part of the model. In the complex part of the model where moveout is complicated this analysis will be even more difficult because there, complicated moveout will add to the problems caused by noise and static time distortions.

Statics estimation for the noisy data, but with NMO correction done with good stacking velocity, can help infer how much of the errors shown in Figure 3.27 can be attributed to the larger residual moveout. Let us therefore use stacking velocities obtained from the velocity analysis for the original, non-statics-contaminated Marmousi data in another test with these noisy data.

Figure 3.29 shows the error in the computed source and receiver statics when the noise-contaminated data are NMO-corrected with the stacking velocities obtained from the original data.

Compare these errors with those shown in Figure 3.27. In the simple part of the model the use of the better stacking velocities yields improved statics estimates. However, for many source and receiver positions the error remains large, indicating that accurate stacking velocities are only part of the problem. Comparing the errors in Figure 3.29 with those in Figure 3.17, where no noise was imposed on the data, we can conclude that the errors away from the complex part of the model are primarily due to the deterioration of the data and the reference traces caused by the noise. In the complex part of the model, between 4.5 km and 6.5 km, the errors shown in Figure 3.29 are comparable to the errors shown in Figure 3.17. Apparently, the statics estimates with already large errors in the complex area do not suffer as much from the added noise as do the reasonably good

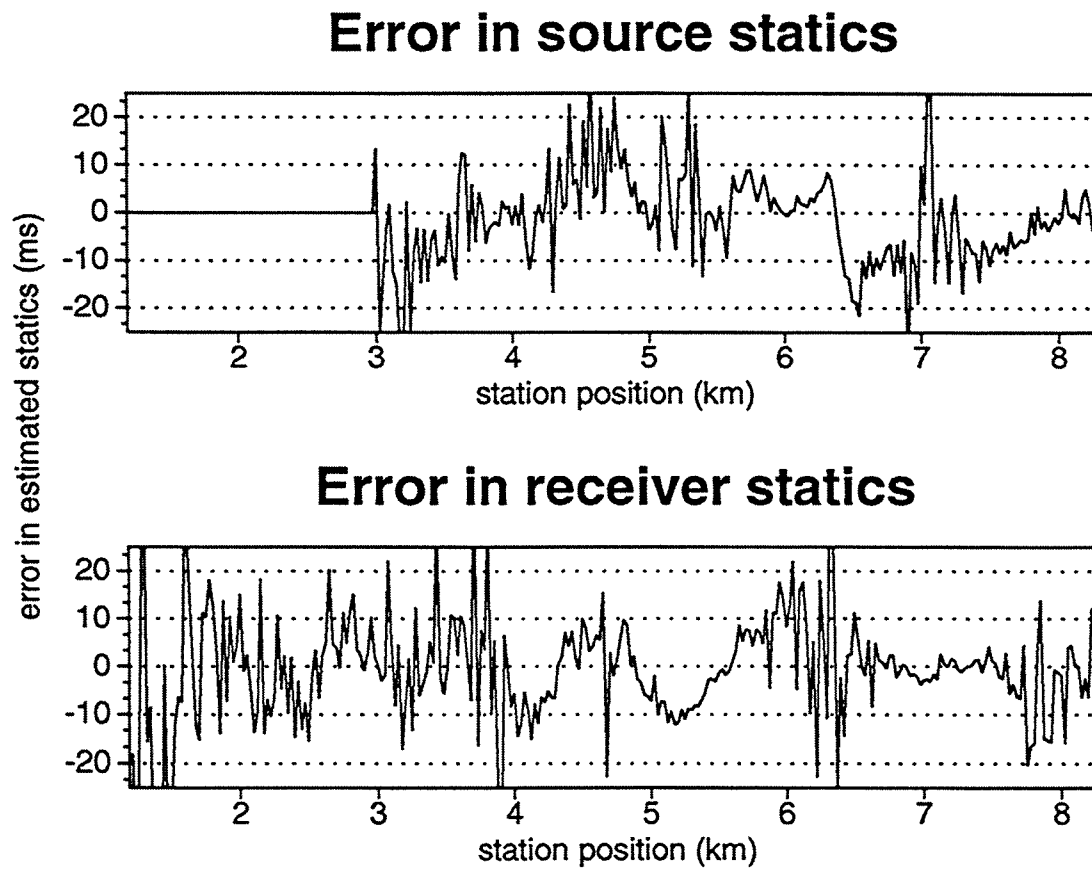


FIG. 3.27. Error in conventionally estimated source and receiver statics in noisy (SNR=2), statics-contaminated Marmousi data.

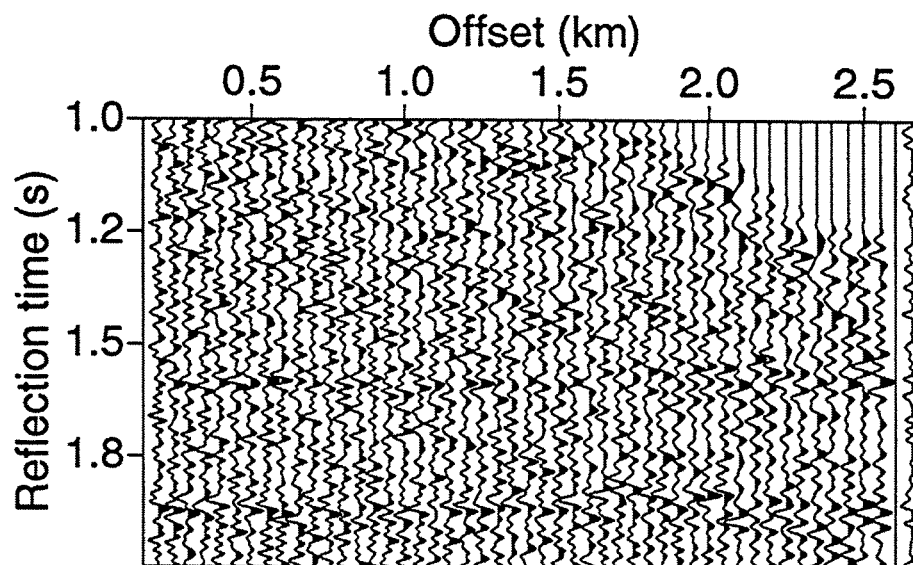


FIG. 3.28. NMO-corrected CMP gather at surface location 3.475 km, from the noise- and statics-contaminated Marmousi data set.

estimates for the simpler part of the model.

In this chapter we have seen that proper treatment of the oscillatory character of the original Marmousi data reduces the error in statics estimation obtained by a conventional method. Furthermore, bandlimited random noise adds to the error in the statics estimation not only because it compromises the quality of velocity analysis, but also because it distorts the reference trace and introduces errors in estimated time shifts. If, in some way, we could obtain reasonable stacking velocities and we could reduce the random noise, the statics estimation might improve somewhat. What would remain in areas of complex structure, however, is the error due to an improper moveout correction. No NMO correction can correct for non-hyperbolic moveout due to rapidly varying velocities, or for the dip-dependence of the moveout. This error in the moveout correction forms an obstacle that cannot be overcome with conventional processing methods. Prestack depth migration *can* correct complicated moveout, so let us investigate benefits that might be gained if it is incorporated into the moveout-correction step in statics-estimation procedures.

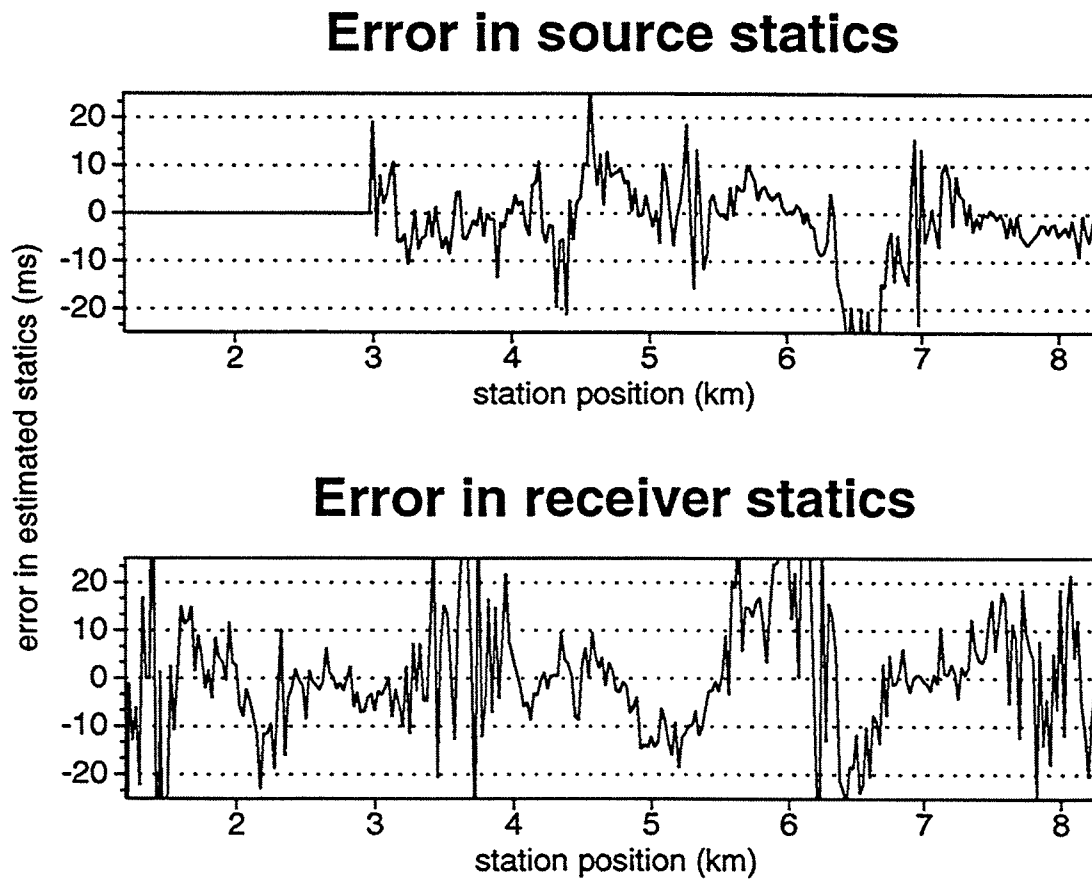


FIG. 3.29. Error in conventionally estimated source and receiver statics in noisy (SNR=2) data, NMO-corrected with stacking velocities obtained from velocity analysis applied to the original (noiseless) Marmousi data.

## Chapter 4

### PRESTACK DEPTH MIGRATION IN THE STATICS-ESTIMATION PROCESS

Of the several problems that complicate conventional statics estimation, I have highlighted the non-hyperbolic moveout, the multi-valued nature of the moveout velocity where events cross, and rapid lateral variation of stacking velocity, all of which arise in areas where the subsurface is structurally complex. All these problems are related to shortcomings in the NMO-correction step of conventional statics-estimation procedures. What is needed is an alternative to the NMO correction. One such an alternative is to apply, in addition to NMO correction, a dip-moveout (DMO) correction to the data. While it can correct for multi-valued moveout velocity, however, DMO will not correct for non-hyperbolic moveout. Prestack depth migration, when done with the correct velocity model, accomplishes proper moveout correction for data from complex structure. Here, following J.P. Diet (personal communication, 1993) and Tjan et al. (1994), I propose to introduce prestack depth migration into the statics-estimation process, as a substitute for the NMO correction.

Let us suppose that, aside from other structural complexity, the subsurface is two-dimensional (that is, the subsurface has a common-strike direction, and the survey line is in the dip direction). We also suppose that our prestack migration algorithm is accurate. If we knew the subsurface velocity structure perfectly (this requirement will be dropped below), then prestack depth migration would yield traces that, except for static time shifts in the data, have reflections aligned on the generated CRP gathers. CRP stacking would then yield stacked traces that, with the exception of the high-cut filtering action caused by averaging traces that have static shifts, would faithfully represent the traces in the CRP gather. Then, as simulated in Figure 2.2, we could expect the cross-correlation process to yield good time shifts for use in the conventional solution of a counterpart to equation (2.1). Thus, we might suggest doing prestack depth migration, CRP stacking to obtain a reference trace, cross-correlating to obtain time shifts, and finally using those time shifts (actually depth shifts, but we can convert them to effective shifts in vertical time) in a conventional iterative approach to solve for the source and receiver static corrections.

There is a problem with this approach, however. Since prestack migration involves a summation of large numbers of traces (over the length of the migration aperture), the near-surface-induced time shifts on all those traces input to the migration process are mixed together in each migrated data trace. Clearly, it is meaningless to attempt, through the cross-correlation process, to derive time shifts for the individual migrated data traces relative to the CRP-stacked traces. In fact, in all likelihood, even if the original data contained substantial time shifts, the migration process would wash out the

trace-to-trace timing variations in the migrated data traces.

To obtain time shifts for the original data traces, as is needed in order to estimate source and receiver statics, those original traces must be cross-correlated with the reference traces. This could not work in the described process, however, because the reference traces have been migrated, whereas the original data traces have not. To resolve this problem, we introduce yet another process, which is equal in cost to the prestack depth migration. We apply a multi-offset modeling (i.e., inverse prestack depth migration), using the CRP-stacked traces as input, to generate the final reference traces. This process yields one reference trace for each data trace on the seismic line.

Note that since the data and reference traces are now back in the unmigrated domain, all the non-hyperbolic moveout remains in the data. What the prestack migration, CRP stacking, and multi-offset modeling has accomplished, however, is a removal of moveout as an issue. Since each data trace and its associated reference trace both have the same moveout and the same crossing events, the only significant sources of time shift are the statics-related time shifts and noise. In addition, there would be an inconsequential contribution from the net result of the sum of all the time shifts that contributed to the CRP stack of the migrated traces.

As a final step in this procedure the statics corrections can be performed under the familiar assumption that they are surface-consistent. Any of the conventional approaches described in Chapter 2 can be used to estimate the static time shifts. In the correlation method, for example, one would use the remodeled trace as the reference trace instead of the stack of a NMO-corrected CMP gather, as is done conventionally. The trace-to-trace time shifts obtained from peaks in the cross-correlation functions would then be input to the standard system of linear equations [equation (2.1)]. Stacking-power methods would maximize the power of the stack of the cross-correlations instead maximizing the power of the stack of the NMO-corrected data as is done conventionally.

Although, the migration-based process is costly as compared with conventional methods and success relies on having an accurate velocity model, for data from a complex subsurface, this approach nevertheless offers a chance to improve the statics solution beyond that possible with conventional methods. So, let us proceed with tests of this migration-based statics-estimation procedure on the Marmousi data.

#### 4.1 Statics estimation with the migration-based method using the exact velocity and the original Marmousi data.

First, let us test the migration-based statics-estimation method in the ideal situation, where the data do not suffer from noise or statics time distortions, and let us use the exact Marmousi velocity model shown in Figure 3.1. Recall that a similar experiment with a conventional statics-estimation method produced statics estimates where none existed (Figure 3.19).

Prestack depth migration with the exact velocity perfectly aligns the events in the CRP gathers, which are then stacked into the image of the subsurface shown in Figure 3.21. Naturally, this migration result is outstanding because of the good data quality

and the use of the exact velocity model. Next, the reflectivity function in this migrated image, with its contained wavelet information, is input to multi-offset modeling. The reflectivity function acts as a distribution of sources along reflectors; no wavelet is assumed. The wavefield generated by these sources is propagated through the background velocity (here, the exact Marmousi velocity model) to the surface, thus achieving a remodeling of all the offsets that were in the original data. For the prestack depth migration, I used a shot-geophone migration in the frequency domain, as described by Denelle et al. (1986). The modeling is based on the same theory and does the opposite of the migration.

Because the correct velocity model is used in both the prestack migration and multi-offset modeling, the derived reference traces do not suffer from errors due to an incorrect moveout correction. Figure 4.1 shows the CMP gather at surface location 3.475 km of the original data, a gather of the remodeled data, and the cross-correlation of the two. As expected, the largest peak in the cross-correlation appears at zero lag, indicating that no errors were introduced during the migration and the modeling.

The CMP gather at surface location 3.475 km has its midpoint location away from the more complex part of the model, although long-offset traces sample the complex portion of the model. Even over the complex portion of the model, e.g., for the gather at surface location 5.9 km (Figure 4.2a), the migration-based method produces excellent reference traces (Figure 4.2b) and the cross-correlations of the traces in the two gathers show good standouts of the main peak at the correct position (zero lag), as seen in Figure 4.2c.

Figure 4.3 shows the estimated statics time shifts in these statics-free data and, as should be, no statics shifts are estimated. Compare this result with the result of the conventional statics estimation in the original Marmousi data (Figure 3.19) where large errors were introduced in the statics solution. Clearly, the prestack migration followed by the multi-offset modeling succeeded in generating good reference traces for these statics-free data traces, whereas the conventional approach generates erroneous reference traces because the NMO correction is not sufficient to correct for crossing and non-hyperbolic events.

## 4.2 Statics estimation with the migration-based method using the exact velocity for statics-contaminated Marmousi data

Now let us go one step further and, once again, add the problem of static time distortions to the data. The imposed source and receiver statics are those shown in Figure 3.3, and the near-offset section of the data is shown in Figure 3.4. Due to the static time shifts imposed on the data, the stack of the migrated data using the exact velocity model, shown in Figure 4.4, now has deteriorated compared to the migrated image of the original Marmousi data (Figure 3.21). Events in the migrated section are not as well focussed or continuous, and the stacked noise contaminates the section. Primarily, however, the events in this migrated section are still positioned correctly because the exact velocity model was used. Because use of the exact velocity model in the prestack migration aligns events in CRP gathers well, the high-cut filtering action of stacking is



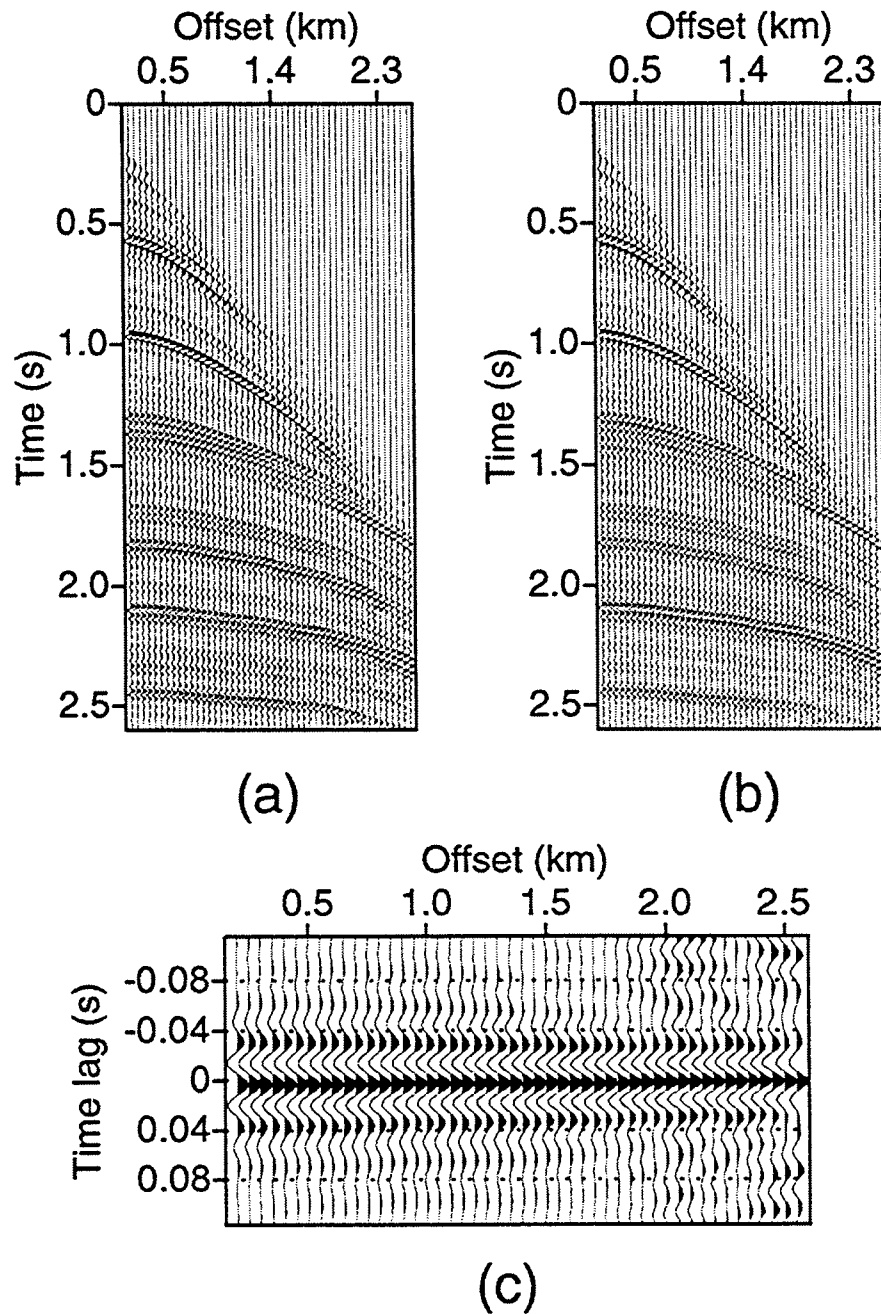


FIG. 4.1. CMP gather at surface location 3.475 km away from the complex part of the model (a) and its associated migrated and remodeled reference gather (b). Both migration and modeling are done with the exact velocity model. (c) Cross-correlation of the traces in the two gathers.

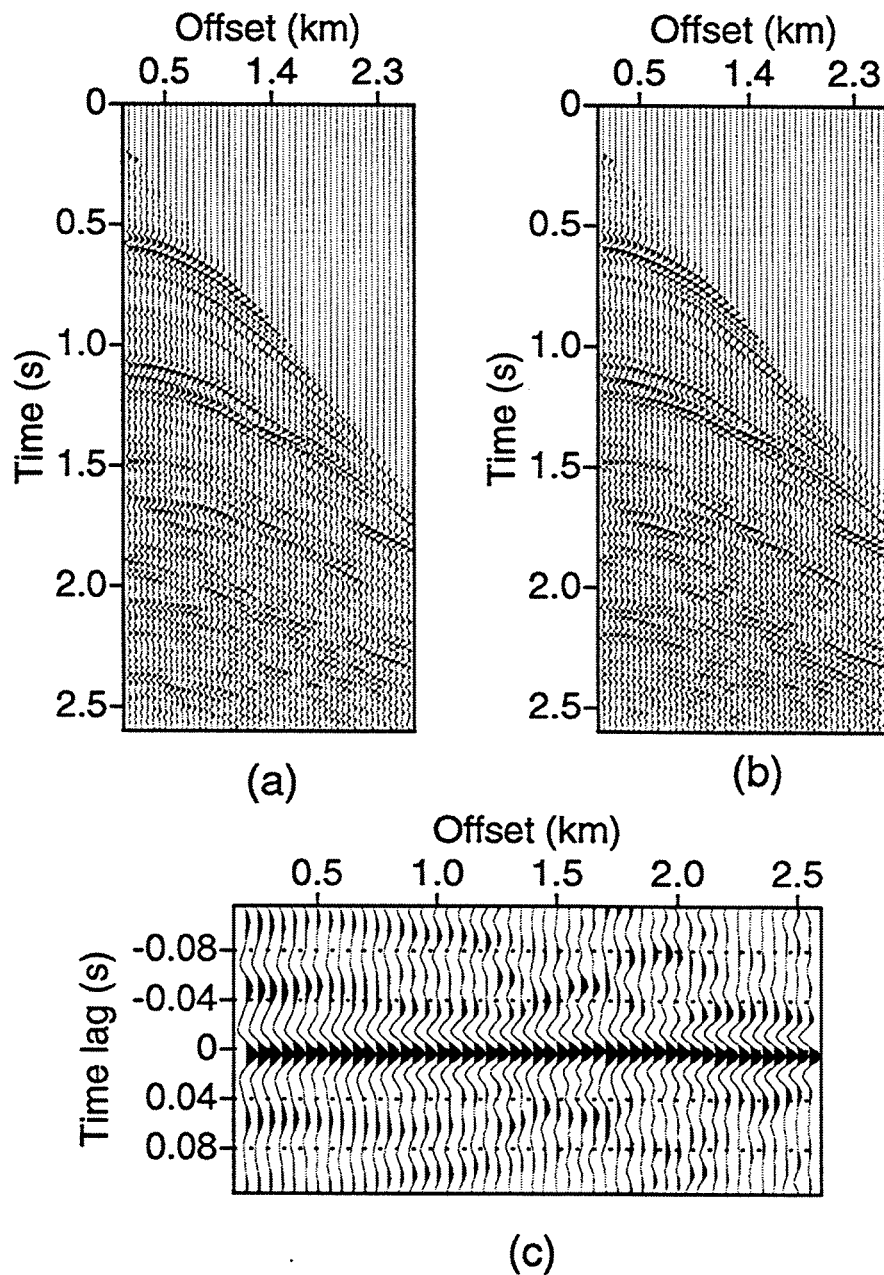


FIG. 4.2. CMP gather at surface location 5.9 km, over the complex part of the model (a) and its associated migrated and remodeled reference gather (b). Both migration and modeling are done with the exact velocity model. (c) Cross-correlation of the traces in the two gathers.

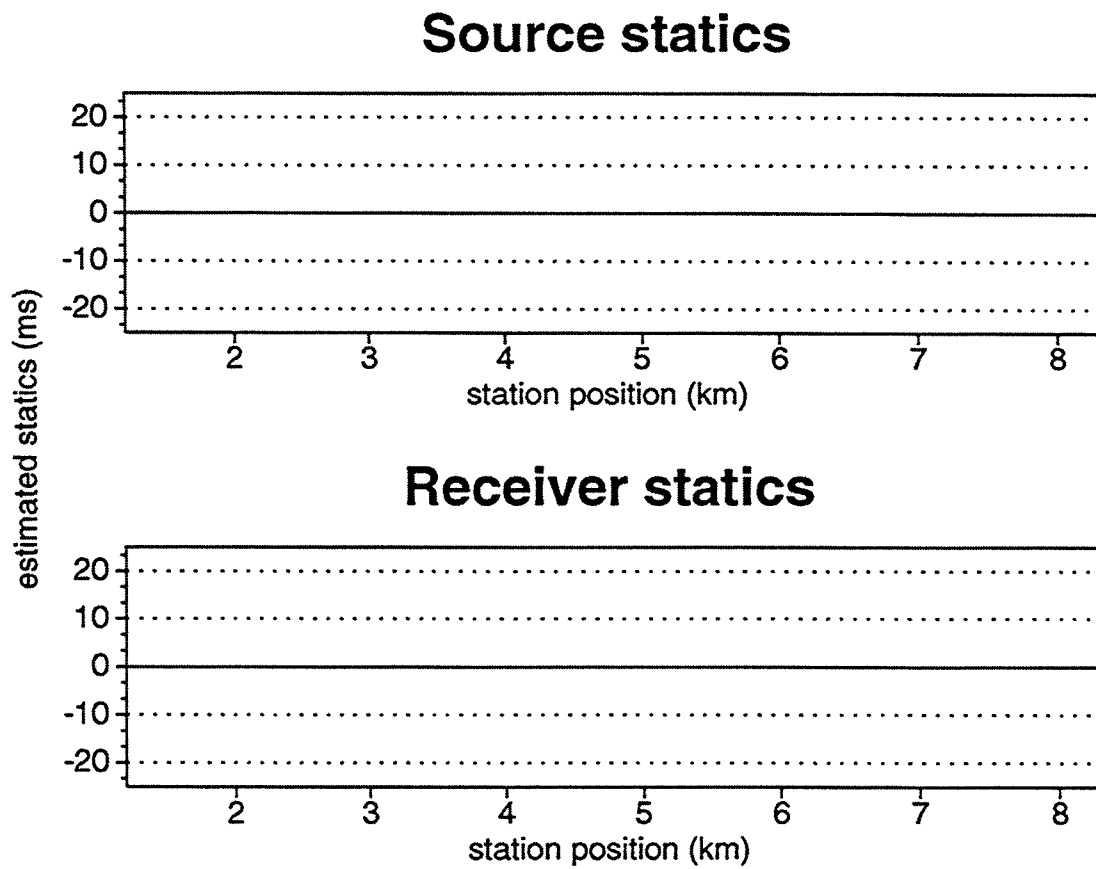


FIG. 4.3. Source and receiver statics corrections estimated in the original Marmousi data, which have no additive static time distortions. The migration-based method was used with the exact velocity model.

attributable to the imposed static time shifts. Remodeling from this migrated image with the exact velocity model puts the reflections back to their original position in the data, with the correct moveout, except for small distortions due to the added statics. The remodeled traces therefore should serve well as reference traces for the original data traces.

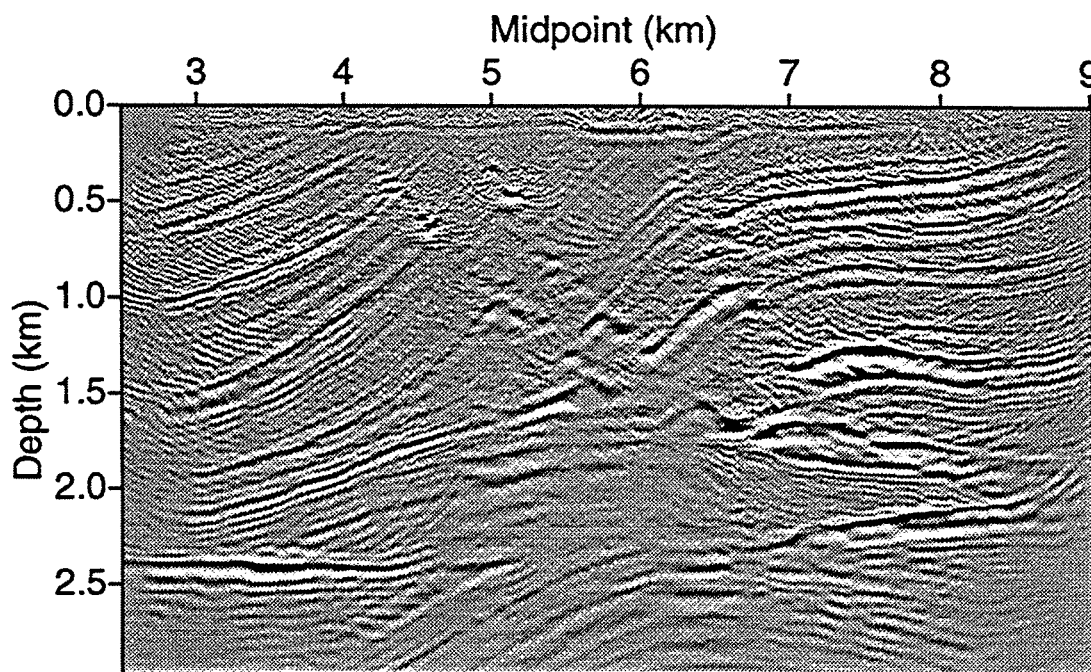


FIG. 4.4. Prestack depth-migrated image of the statics-contaminated Marmousi data. The exact velocity model was used for the migration.

Figure 4.5 shows the CMP gather of the original data at surface location 3.475 km (a), the remodeled gather (b) and the cross-correlation of the two (c). Likewise, Figure 4.6 shows the corresponding gathers for the CMP gather at 5.9 km, near the middle of the model. Both cross-correlations (Figure 4.6c and 4.5c) again show peaks with good standout, at time shifts predicted by the sum of the imposed source and receiver statics time shifts. These predicted time shifts are those that were indicated by the time lags of the main peak in the cross-correlation functions in Figure 3.11 for the gather at 3.475 km, and in Figure 3.15 for the gather at 5.9 km.

The main peaks in the cross-correlations in Figure 4.5c and Figure 4.6c have reasonably good standout for most offsets. However, as with the conventional method, the cross-correlations suffer from an oscillatory character because these data were not deconvolved. As was demonstrated above, use of deconvolution can suppress oscillations in the data and improve the standout of the main peak in the cross-correlations. Here, where we are using the exact velocity, the oscillatory character does not pose a problem. The

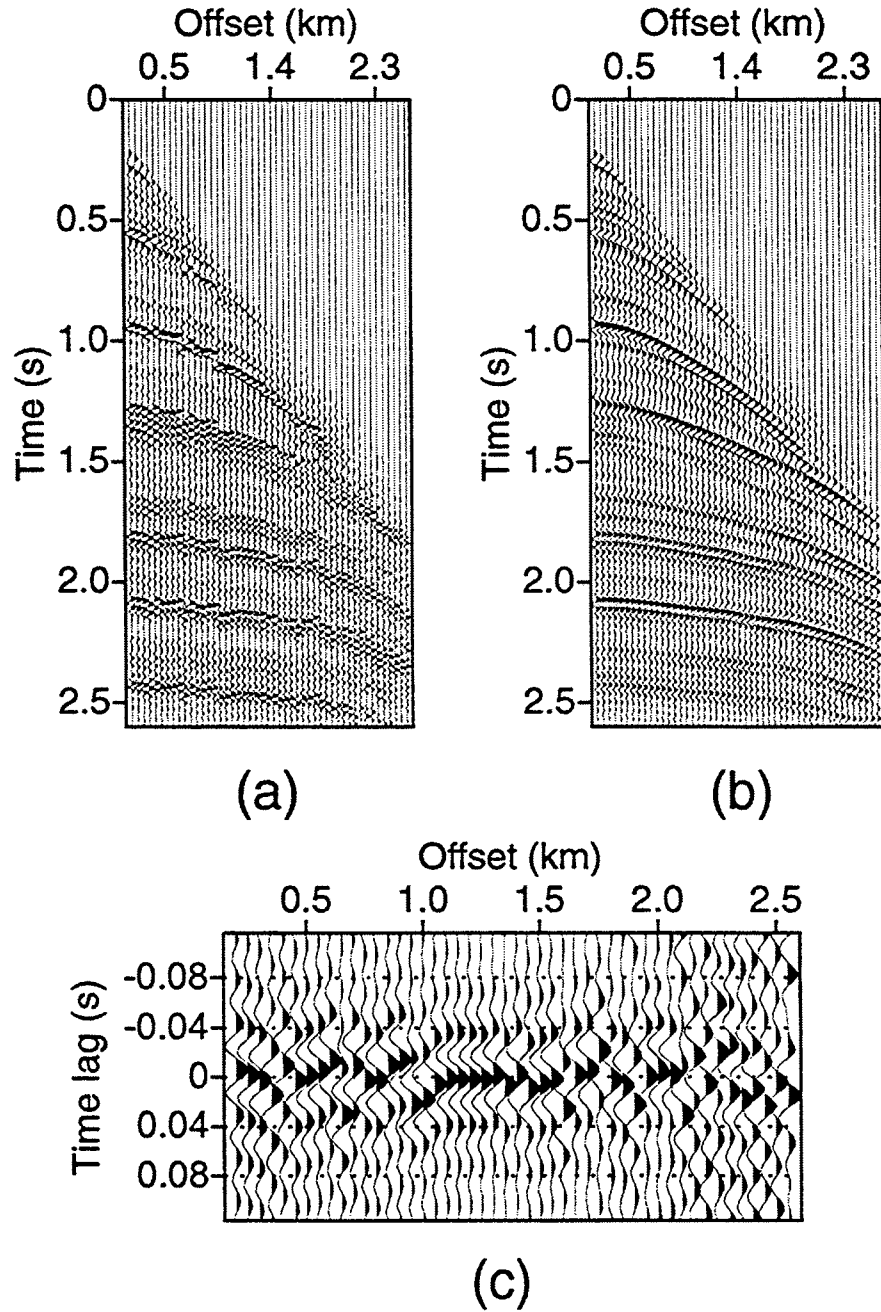


FIG. 4.5. CMP gather from the statics-contaminated data at surface location 3.475 km (a) and its associated migrated and remodeled reference gather (b). Migration and modeling are done with the exact velocity model. (c) Cross-correlation of the traces in the two gathers.

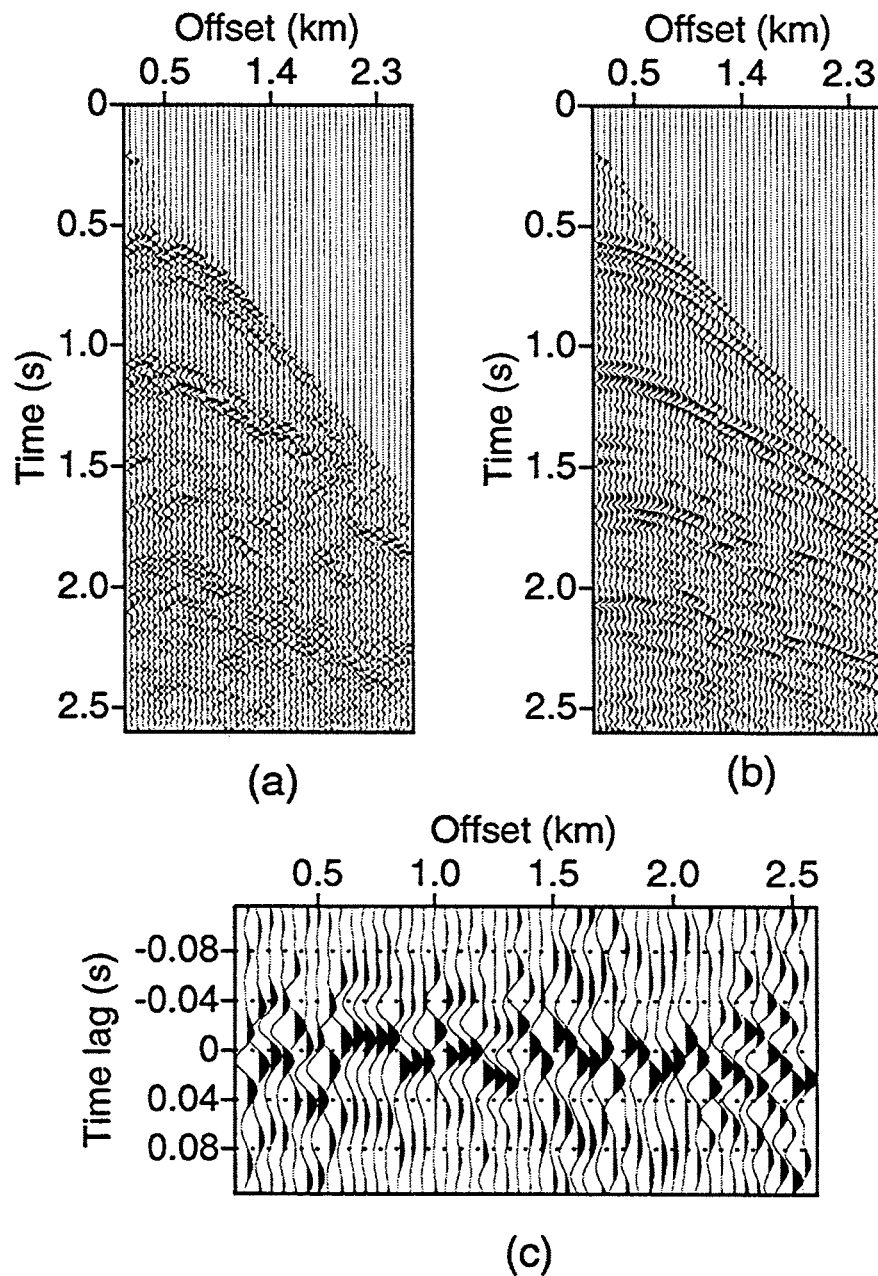


FIG. 4.6. CMP gather from the statics-contaminated data at surface location 5.9 km (a) and its associated migrated and remodeled reference gather (b). Migration and modeling are done with the exact velocity model. (c) Cross-correlation of the traces in the two gathers.

oscillations, however, will cause erroneous statics solutions in less perfect situations, e.g., when data are noisy or the velocity model used is incorrect. Therefore, for all subsequent tests the data have been deconvolved with the same operator applied in the tests with the conventional method.

The time shifts obtained by picking the times of the dominant correlation peaks are shown in Figure 4.7 for the CMP gather at 3.475 km, and in Figure 4.8 for the one at 5.9 km. Clearly, the errors are much smaller than those obtained by the conventional method (Figure 3.12 and Figure 3.16) (the correct time lag is zero for all traces). Specifically the cross-correlations do not suffer from residual moveout as they did for the conventional case, and the errors remain small for the larger offsets.

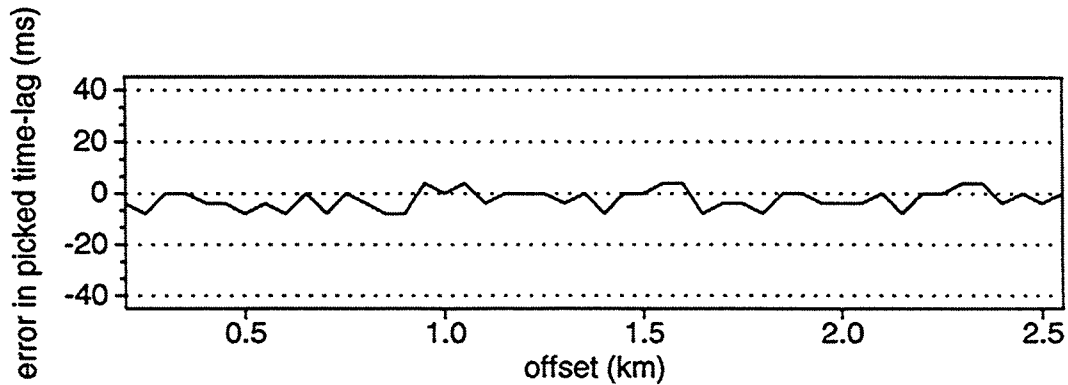


FIG. 4.7. Error introduced by picking peaks in correlations for the CMP gather at 3.475 km after prestack migration, stacking, and multi-offset modeling with the exact velocity model.

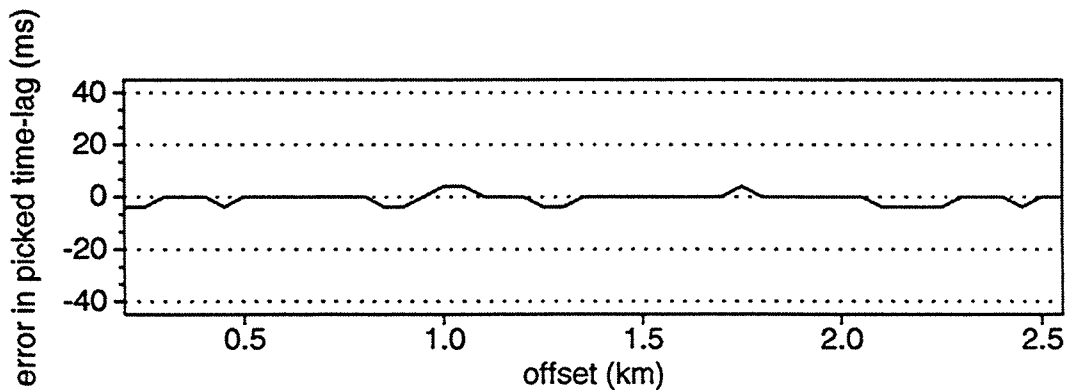
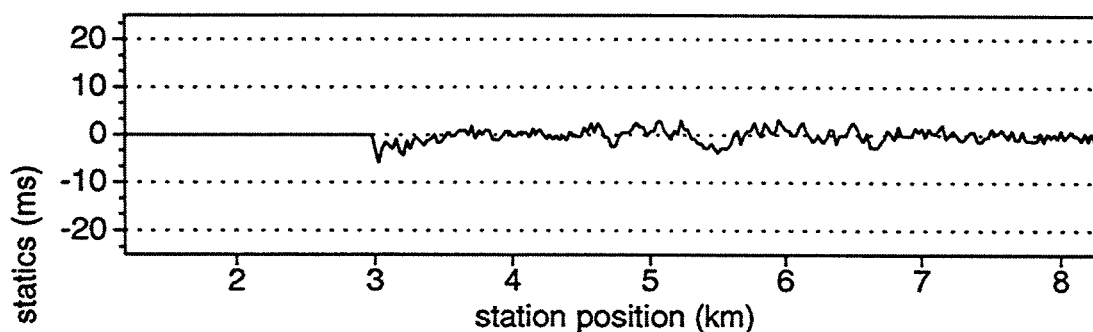


FIG. 4.8. Error introduced by picking peaks in correlations for the CMP gather at 5.9 km after prestack migration, stacking, and multi-offset modeling with the exact velocity model.

Figure 4.9 shows the difference (i.e., error) between the imposed and migration-based source and receiver statics solution for the statics-contaminated Marmousi data. Throughout the section the estimated static corrections are much better here than were those obtained by the conventional method (Figure 3.17). The receiver-statics errors are smaller than 2 ms, which is within half a sample interval, and the shot-statics errors are slightly bigger, but still smaller than a sample interval.

### Error in source statics



### Error in receiver statics

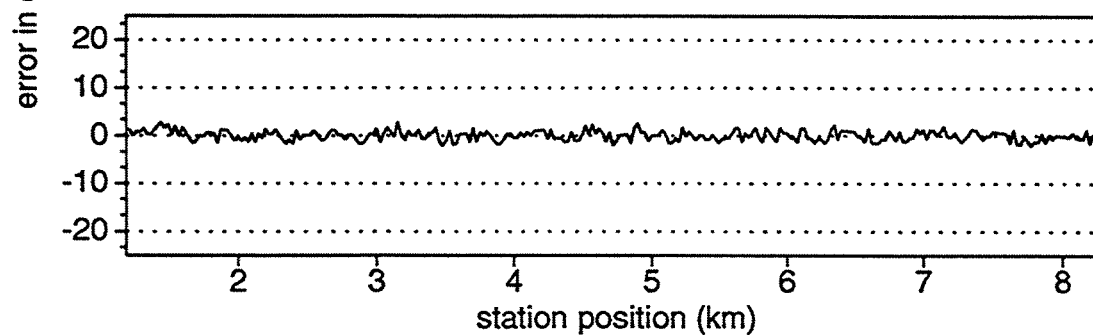


FIG. 4.9. Difference between the imposed random static time shifts and the migration-based estimated source and receiver corrections in the statics-contaminated Marmousi data. The correct velocity was used in both the prestack migration and multi-offset modeling.

The errors have been reduced this much at a high price in computation: we have generated the reference traces by performing prestack depth migration and a multi-offset modeling. Moreover, we have used the *exact* velocity model, as opposed to NMO correction with stacking velocities from a conventional velocity analysis. Nevertheless, this test shows that under ideal conditions (i.e., the exact velocity model is known, the data have no noise, and the near-surface-induced time anomalies are surface-consistent and have no long-wavelength component), for data from complex structure the migration-based



statics estimation method can produce excellent statics estimates, whereas conventional methods suffer from the limitations of the NMO correction and are guaranteed to produce an erroneous solution. Even if we would be able to obtain excellent stacking velocities, success with a conventional method is limited to data with moveout that is single-valued and approximately hyperbolic.

For practical purposes, the migration-modeling method becomes interesting only when it performs well under such less-than-perfect conditions. In practice, we never know the exact velocity model, and the data are contaminated with bandlimited noise, as well as with static time shifts. In the next sections, I test the migration-based method under less-than-perfect conditions.

#### 4.3 Statics estimation by the migration-based method with the exact velocity for Marmousi data contaminated with both statics and random noise

In practice, the migration-based statics-estimation method applied to statics- and noise-contaminated data will suffer from the same two problems as do conventional statics-estimation methods: velocity analysis is equally difficult, and noise will compromise the quality of the data and the reference traces. As before, let us assume for the moment that we know the exact velocity model so we can investigate how noise alone deteriorates the statics estimates in the migration-based method. Figure 3.26 showed the small-offset traces of noise- and statics-contaminated data used in tests with the conventional statics-estimation method. Let us use the same data in a test with the migration-based method using the exact velocity model shown in Figure 3.1.

Figure 4.10 is the prestack migrated image obtained from these data. The image has deteriorated compared to the image of the noise-free data (Figure 4.4), but the high-amplitude events still focus reasonably well. Noise is still present in the data, but the SNR, particularly at the dominant lower frequencies, has been improved significantly by the stacking. This noise reduction makes it possible to again obtain acceptable reference traces, as is shown in Figure 4.11b. This is the reference gather for the statics- and noise-contaminated data shown in Figure 4.11a. Correlation between the data traces and the reference traces yields cross-correlation functions (Figure 4.11c) with deteriorated standout of the main peak compared to the cross-correlation functions in Figure 4.5c. Nevertheless, the main peak in most cross-correlation functions is positioned at or close to the correct position, as a comparison between Figure 4.11c and Figure 3.11 shows.

Figure 4.12 shows the error in the estimated statics in these statics-contaminated, noisy data. Notably the error has not increased much in comparison with the error in the noiseless case (Figure 4.9), except for slightly larger errors in the receiver statics at the side of the model, where the fold is low and edge effects of the migration distort the data. Disregarding these larger errors at the side, the largest errors are of the order of a sample interval (4 ms). Certainly the significant increase of the error in conventional statics estimation for noisy data (Figure 3.29) compared with the conventional estimation for noise-free case (Figure 3.17) does not occur here. Again, the improvement of the statics

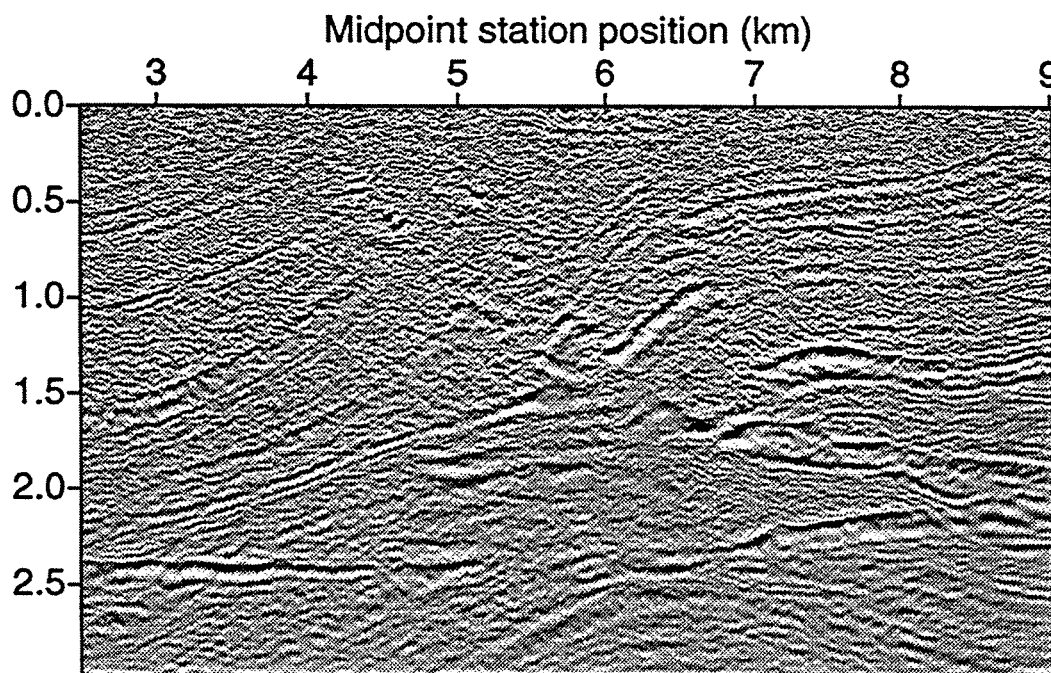


FIG. 4.10. Prestack depth-migrated image of statics- and noise-contaminated Marmousi data (SNR=2). The exact velocity model was used for the migration.

solution with the migration-based method is due to the proper treatment of the moveout in the data (we did not have to estimate a moveout correction here, as we did for the conventional result in Figure 3.29). Of the three problems that complicate the data, prestack migration and modeling with the exact velocity model eliminates the problem of residual moveout so we are left only with the noise and statics time distortions in the data. Unfortunately, for field seismic data we do not know the exact velocity model, and so for the migration-based method we will have to deal with the compounding of three problems — noise, static time distortions, and residual moveout.

#### 4.4 Migration-based statics estimation with an erroneous velocity model

In the previous sections I showed, with examples of statics-contaminated data from the Marmousi model, that a statics-estimation method based on prestack migration and multi-offset modeling yields accurate estimates of surface-consistent static time shifts in data from complex subsurface structures, provided that the exact velocity model is used in both the migration and modeling.

In the early stages of the processing we do not know the velocity model accurately. Consequently we inevitably choose an initial velocity model that contains velocity errors, often large ones. These velocity errors translate into large moveout errors, which will cause errors in the statics solution. Therefore, in the migration-based statics-estimation

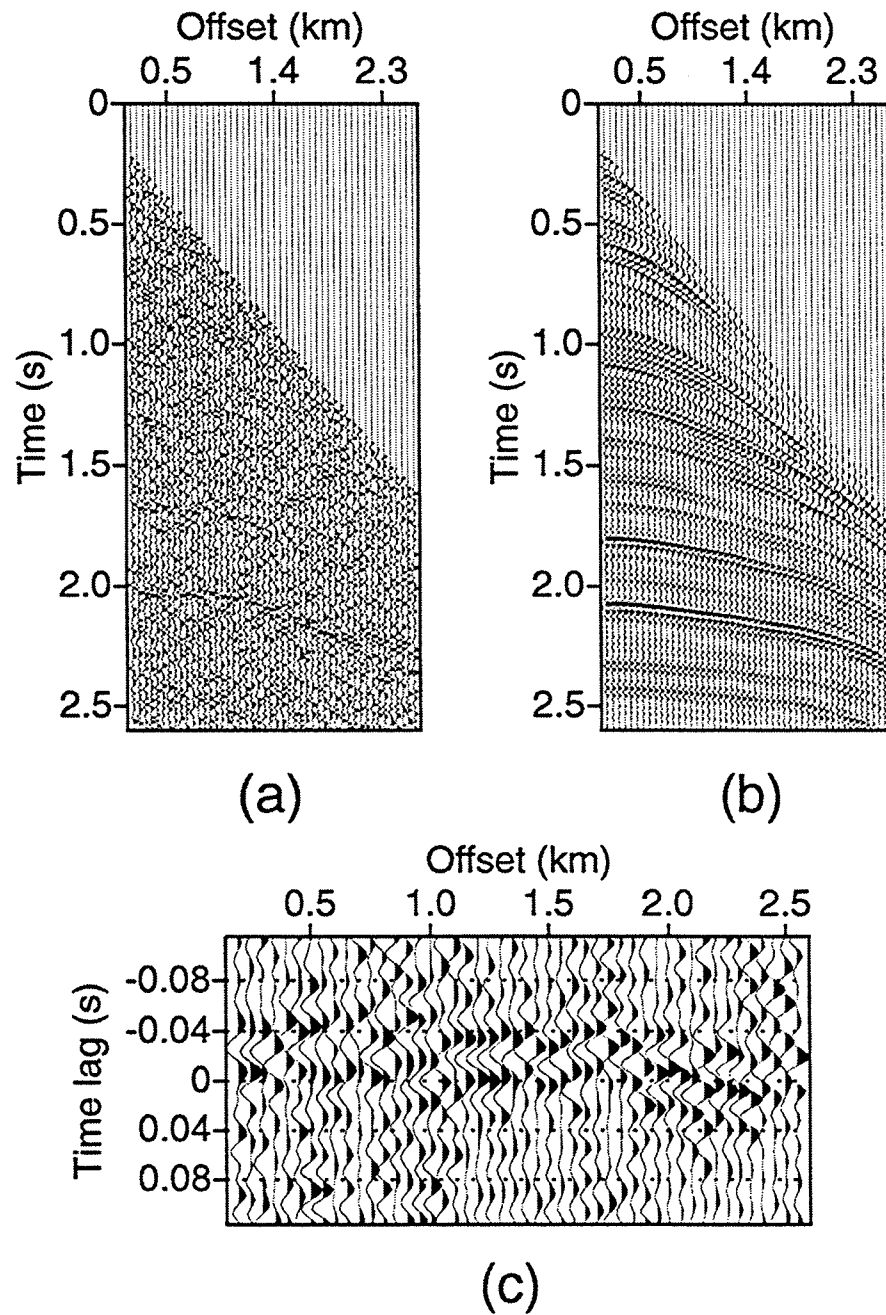


FIG. 4.11. CMP gather from the statics- and noise-contaminated data (SNR=2) at surface location 3.475 km (a) and its associated migrated and remodeled reference gather (b). Migration and modeling are done with the exact velocity model. (c) Cross-correlation of the traces in the two gathers.

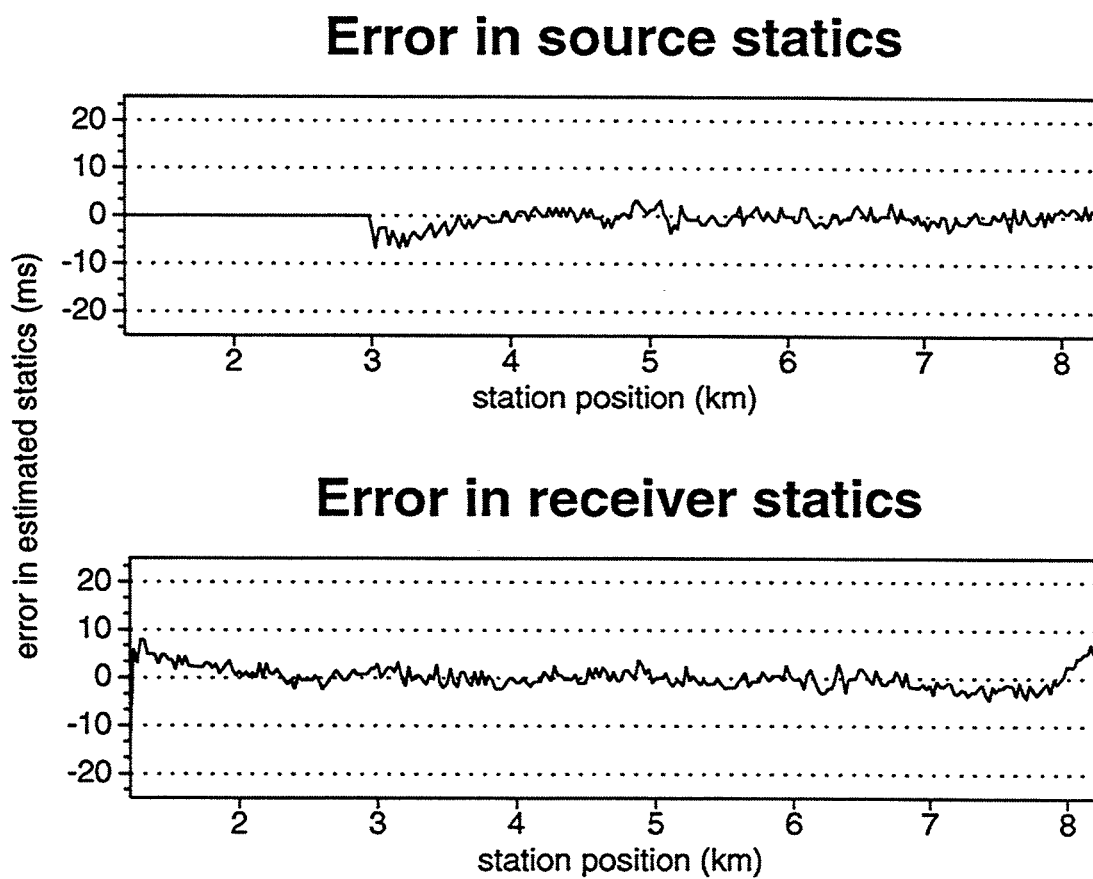


FIG. 4.12. Difference between the imposed random static time shifts and the migration-based estimated source and receiver corrections in statics- and noise-contaminated Marmousi data. The correct velocity was used in both the migration and modeling.

method, a first iteration of the statics solution will certainly be inaccurate.

In general, we obtain an initial model for the interval (i.e., migration) velocities from stacking velocities obtained from a conventional velocity analysis. Unfortunately, conventional velocity analysis for data that are severely contaminated with near-surface time distortions is not trivial. Often, however, we do not need to rely solely on the seismic data for a guess of the subsurface velocities. *A priori* information such as well-log data can give an idea of the velocities in the subsurface. With the Marmousi data set, also, data from two “wells” —at midpoint locations 1504 and 9004 m of the model (see Figure 3.1)— were provided. From these well data Audebert (1991) obtained parameters for a simple, constant-gradient velocity model,

$$v(z) = 1623 + 0.7z \text{ m/s.} \quad (4.1)$$

I will use this simple velocity function as the initial velocity estimate for the statics-estimation process

#### 4.4.1 Marmousi data uncontaminated by statics problems

Let us use this velocity model in a migration-based statics estimation, again applied to the original, non-statics-contaminated Marmousi data that have been deconvolved. Ideally the statics corrections would be zero since the data are free of imposed static time shifts. Figure 4.13 shows the prestack depth-migrated image of these data. It shows reasonably well-focussed reflectors toward the sides of the model, where the constant-gradient velocity model used is close to the correct one. In the complex part of the model, however, poor focussing and mis-positioned reflectors result from errors in the velocity model. Also, this section shows large distortions of imaged structure relative to the result in Figure 4.14, obtained with the correct velocity model. Multi-offset modeling with the same velocity model will inevitably result in erroneous reference traces and therefore in errors in the statics solution. As a result, Figure 4.15 shows estimated statics where none exist in the data. One reason is that since the near-surface is not well modeled, the structural complexity yields dynamic corrections that show up as statics problems. Another reason is that the simple constant-gradient velocity model introduces moveout errors in the reference traces. Yet the erroneous migration-based statics estimates are considerably smaller than those obtained in a similar test with a conventional statics-estimation method based on NMO correction (Figure 3.19). Although prestack migration with this simple velocity model cannot correct non-hyperbolic moveout, it may be able to partly account for the multi-valued moveout whereas NMO-correction cannot. Furthermore, this simple velocity is well behaved and smooth, whereas stacking velocities obtained from conventional velocity analysis for data from complex subsurface structures such as the Marmousi model can be very erratic. They may contain unrealistic velocity inversions or unrealistic lateral velocity jumps which may add to the inaccuracy of the stacking velocity.

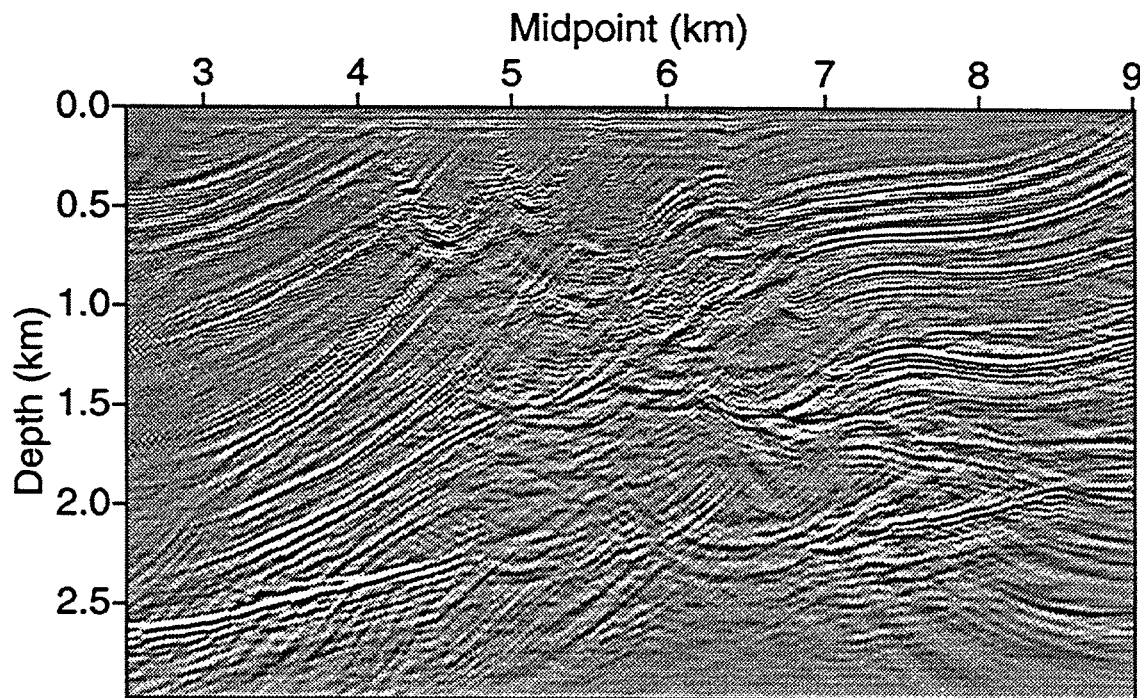


FIG. 4.13. Prestack depth-migrated image of the original, deconvolved Marmousi data. The migration velocity has a constant gradient in depth.

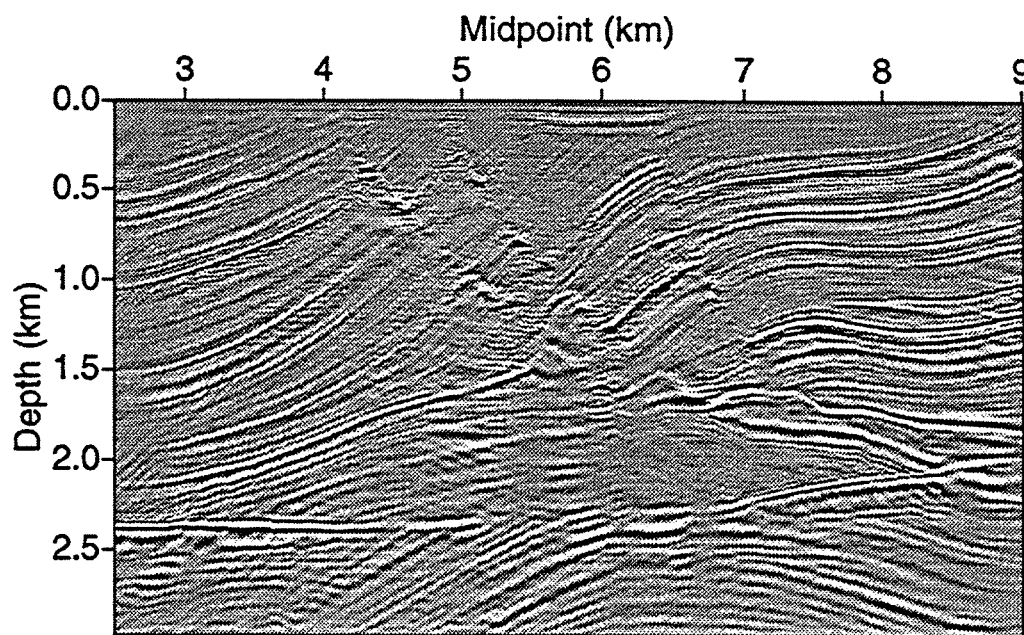


FIG. 4.14. Prestack depth-migrated image of the original, deconvolved Marmousi data. The migration velocity is the exact velocity model shown in Figure 3.1.

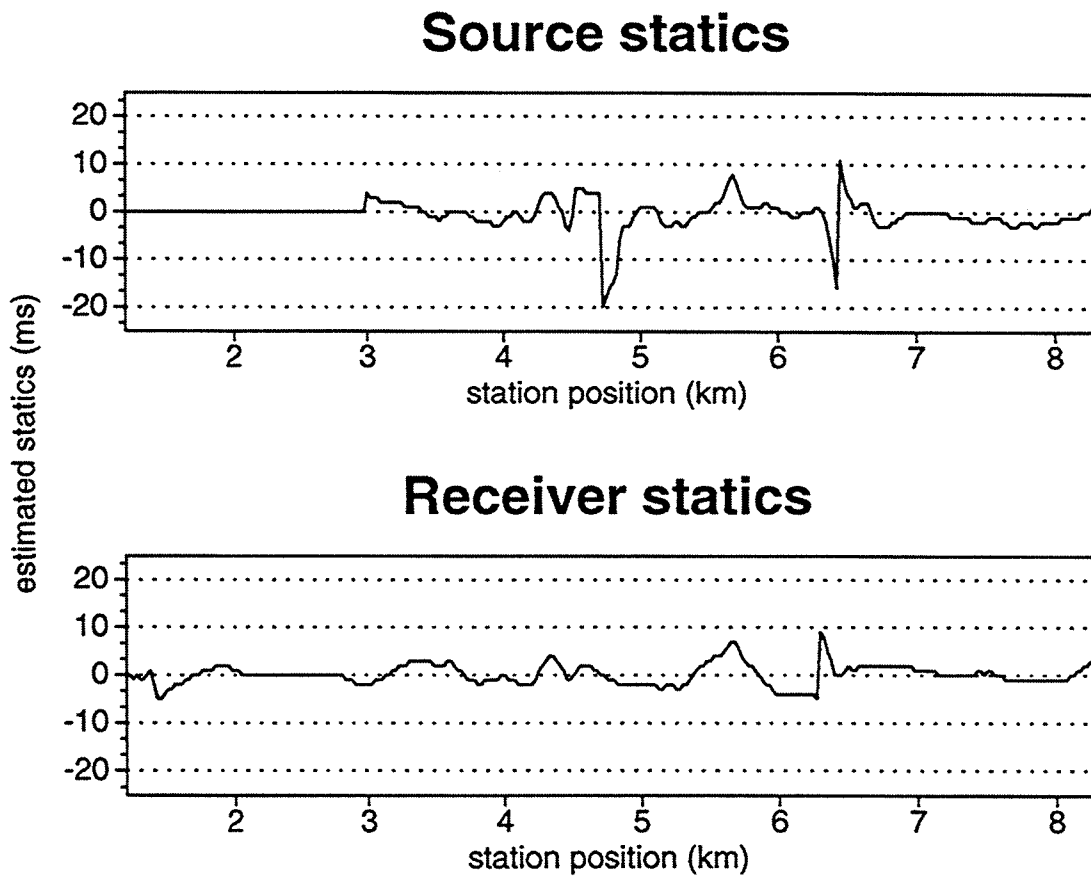


FIG. 4.15. Source and receiver statics corrections estimated from the original Marmousi data, which actually have no additive statics. The migration-based method was used with a constant-gradient velocity model. Ideally, the derived statics corrections would be zero for this test.

#### 4.4.2 Statics-contaminated Marmousi data

Now let us return to the statics-contaminated Marmousi data (Figure 3.4). Figure 4.16 shows the migrated stack of these statics-contaminated data, migrated with the constant-gradient velocity. Now the migrated image suffers from a compounding of the problems of an erroneous migration velocity and the imposed statics. Note especially the loss of high-frequency content compared with the migration result for the original Marmousi data (Figure 4.13). This high-cut filtering action is typical when misaligned reflections are averaged. Despite shortcomings of this image, remodeling of the data from this image, using the constant-gradient velocity, produces reference traces that can be used for statics estimation.

Figure 4.17 shows the error in the source and receiver static corrections when we use these reference traces in the statics-estimation procedure. Compare these errors with those when a conventional statics-estimation method (i.e., one based on NMO correction) is used (Figure 3.17). Even though the initial velocity model for the migration and modeling is simple, the estimated statics corrections are considerably more accurate than those estimated with a conventional method. Prestack depth migration alleviates the problems due to crossing events even though the velocity model is incorrect. Prestack depth migration with this constant-gradient velocity model, however, does not treat non-hyperbolic moveout correctly and thus introduces errors in the complex part of the model between 4.5 and 6.7 km, where not only crossing events but also non-hyperbolic moveout complicate the data. Around station position 6.3 km, a particularly large anomalous error exists in the statics error. This feature is at the location where a large fault in the model cuts the free surface (Figure 3.1). In this region, reflections terminate against the fault, and, since the velocity model is not correct, cycle skipping is likely.

#### 4.4.3 Statics- and noise-contaminated Marmousi data

In the tests shown above, the data are noise-free. I emphasized the problems that conventional method have when the data suffer from the compounding of problems due to static time distortion, noise, and complex subsurface structure. Let us now treat data that suffer from all these problems with the migration-based approach. Figure 3.26 showed the near-offset traces of the Marmousi data contaminated by noise (SNR=2) as well as with statics problems. Let us use these data as input to the migration-based method, using as before the constant-gradient velocity model.

Figure 4.18 is the migrated image obtained from these data. The image is deteriorated compared with the image of the noise-free data (Figure 4.16), but the high-amplitude (but highly-bandlimited) events still focus reasonably well. Noise is still present in the data, but the SNR, particularly at the dominant lower frequencies, has been improved significantly by the stacking. This noise reduction makes it possible to again obtain acceptable reference traces, despite the high-cut nature of the stacked migration.

Figure 4.19 shows the error in the estimated statics in these statics-contaminated, noisy data. Notably, the error has not increased much in comparison with the error obtained in the noiseless case (Figure 4.17). Apparently, the migration-based method



was able to generate reference traces of sufficient quality that the problems due to the noise are minimized.

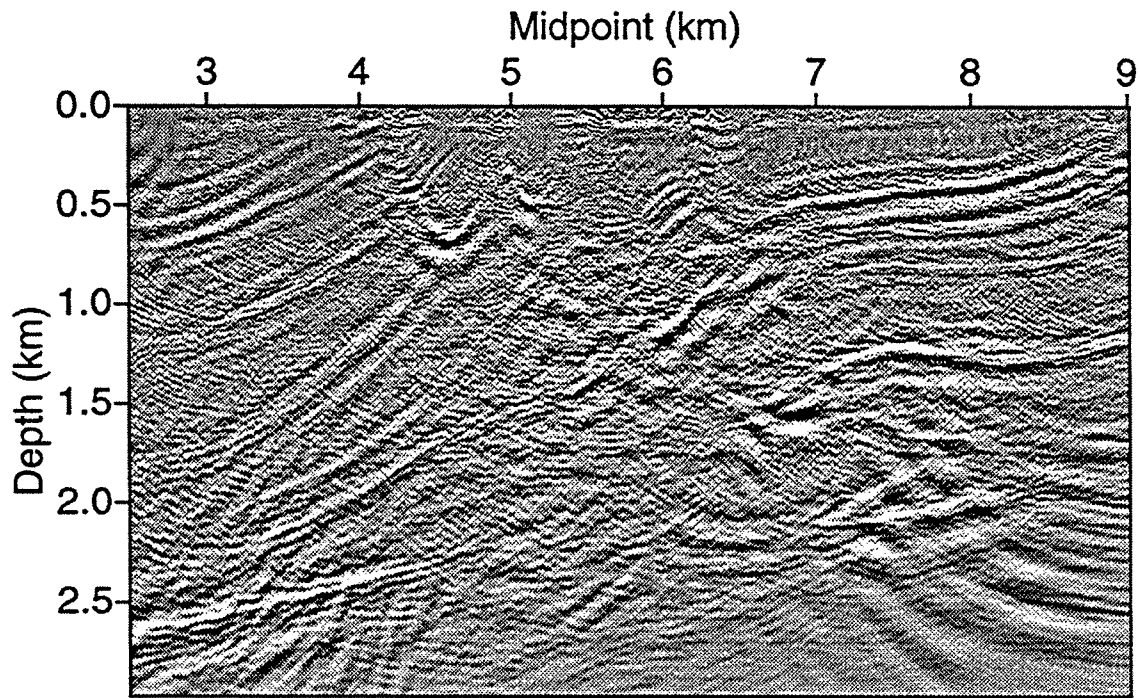


FIG. 4.16. Prestack depth-migrated image of statics-contaminated Marmousi data. The migration velocity has a constant gradient in depth.

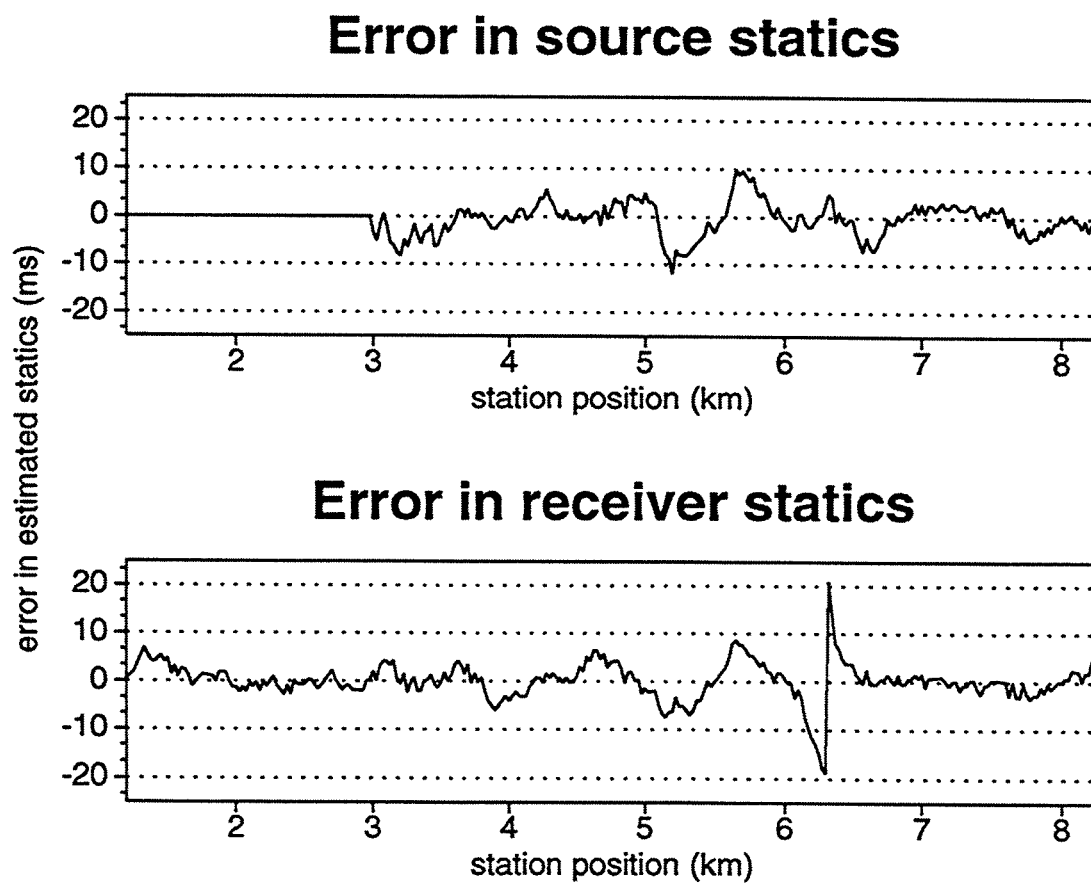


FIG. 4.17. Difference between the imposed random static time shifts and the migration-based estimated source and receiver corrections. The prestack depth migration and multi-offset modeling were done with the constant-gradient velocity model.

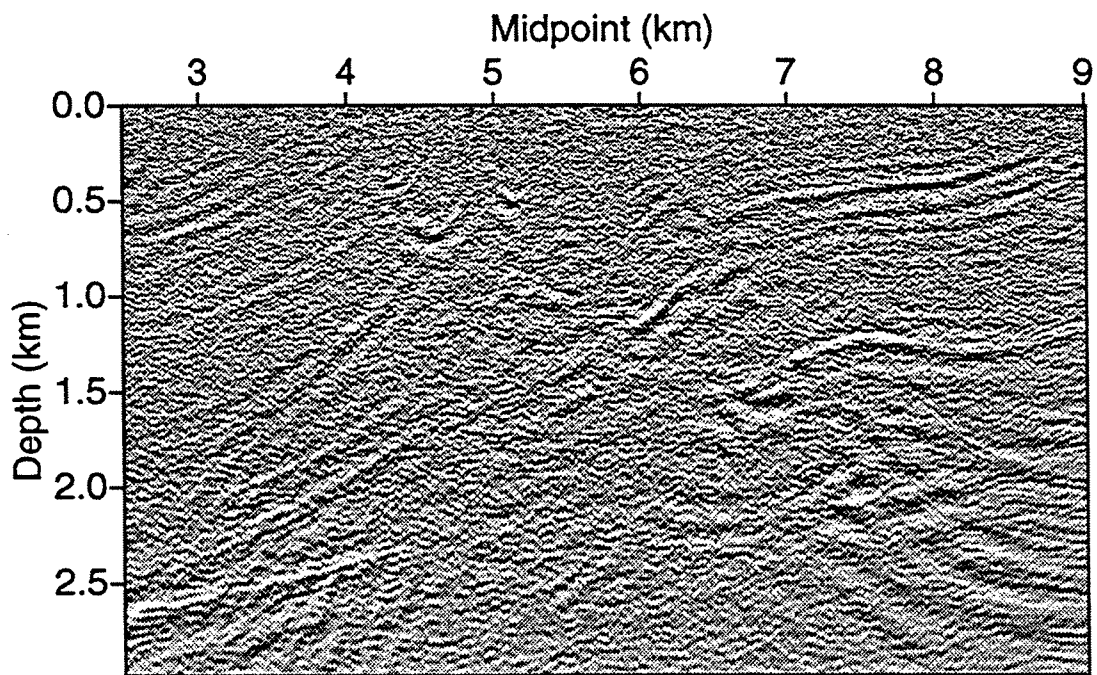


FIG. 4.18. Prestack-migrated image of the noise- and statics-contaminated data. The migration was done with the constant-gradient velocity model.

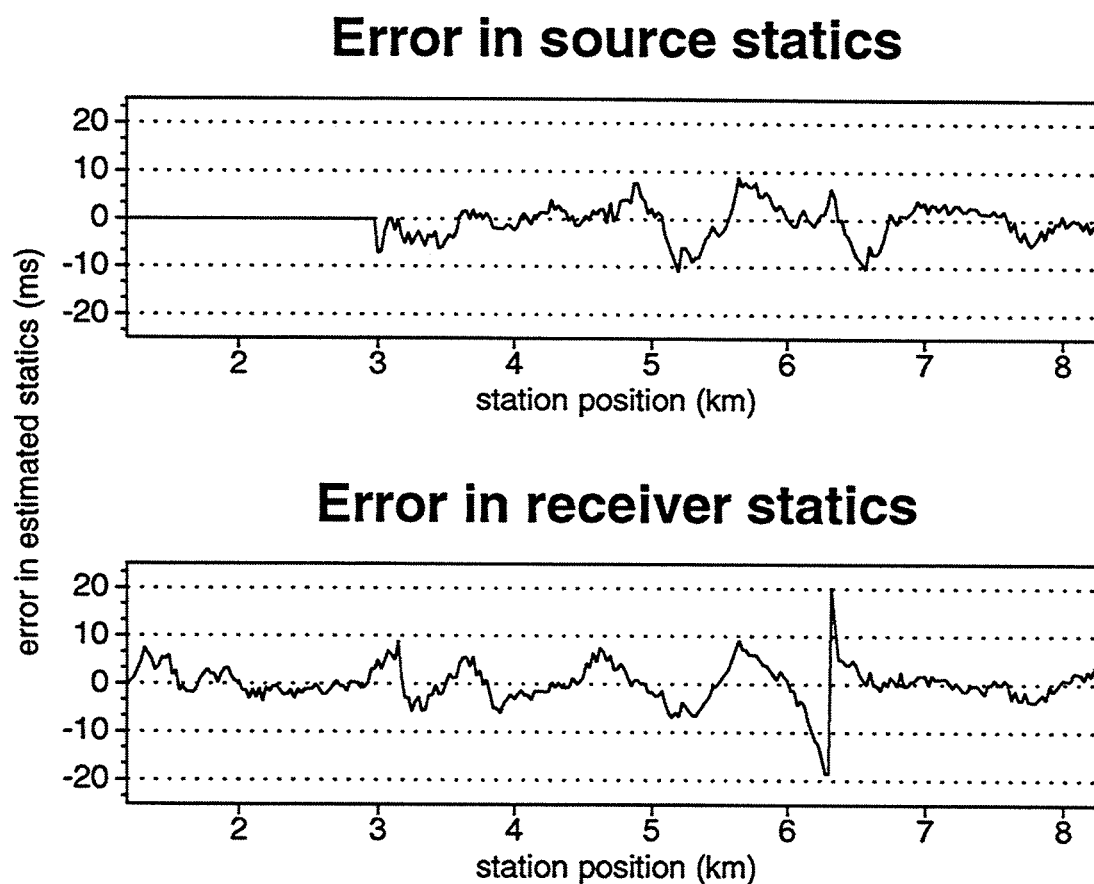


FIG. 4.19. Difference between the applied random static time shifts and the migration-based estimated source and receiver corrections in statics- and noise-contaminated data. The constant-gradient velocity model was used in both the migration and modeling.



## Chapter 5

### SIMULTANEOUS VELOCITY AND STATICS ESTIMATION

Although migration-based statics estimation with the constant-gradient velocity model has reduced the statics contamination significantly, the errors are still too large for accurate imaging in the complex part of the model. The initial velocity model is simply not good enough. Clearly we need to pursue two simultaneous goals here — improvements of both the statics and velocity estimation. The approach we will use is to alternate between velocity and statics estimation.

Conventionally, statics estimation is iterated to obtain a more accurate solution for the source and receiver statics. This is done in combination with conventional velocity analysis. As a first iteration, statics are estimated using stacking velocities obtained from conventional velocity analysis. Then the data are corrected with the estimated statics and a second velocity analysis is done, followed by a second statics estimation, etc., until an accurate statics solution is obtained. Figure 5.1 shows the part of the statics problem that remains unsolved after a second iteration of conventional statics estimation (the errors remaining after the first iteration were shown in Figure 3.17). For this second iteration, updated stacking velocities were obtained from conventional velocity analysis in the statics-contaminated Marmousi data that had been corrected with the statics estimates from this first iteration. After this second pass of conventional statics estimation the short-wavelength errors that were left after the first pass (Figure 3.17) are generally resolved; however, longer-wavelength errors remain. Most of the high-amplitude longer-wavelength components have a wavelength that is smaller than the cable length (2.575 km) and would likely have been resolved by the conventional statics-estimation method if the NMO corrections had been acceptable.

For areas with subsurface structure as complex as that in the Marmousi model, iterative use of prestack depth migration, in conjunction with some process such as depth-focussing analysis (Faye and Jeannot, 1986; Diet and Audebert, 1990) or the perturbation method described by Liu and Bleistein (1994) have been successful in obtaining accurate velocity models after a few iterations — in the absence of statics problems. Here, I follow the method described by Stork (1992) to do the velocity analysis. He uses reflection tomography in the post-migration domain to update the velocity model by flattening events in CRP gathers. I alternate between this form of velocity analysis with the migration-based statics approach just as is done in conventional velocity analysis and statics estimation in conventional processing.

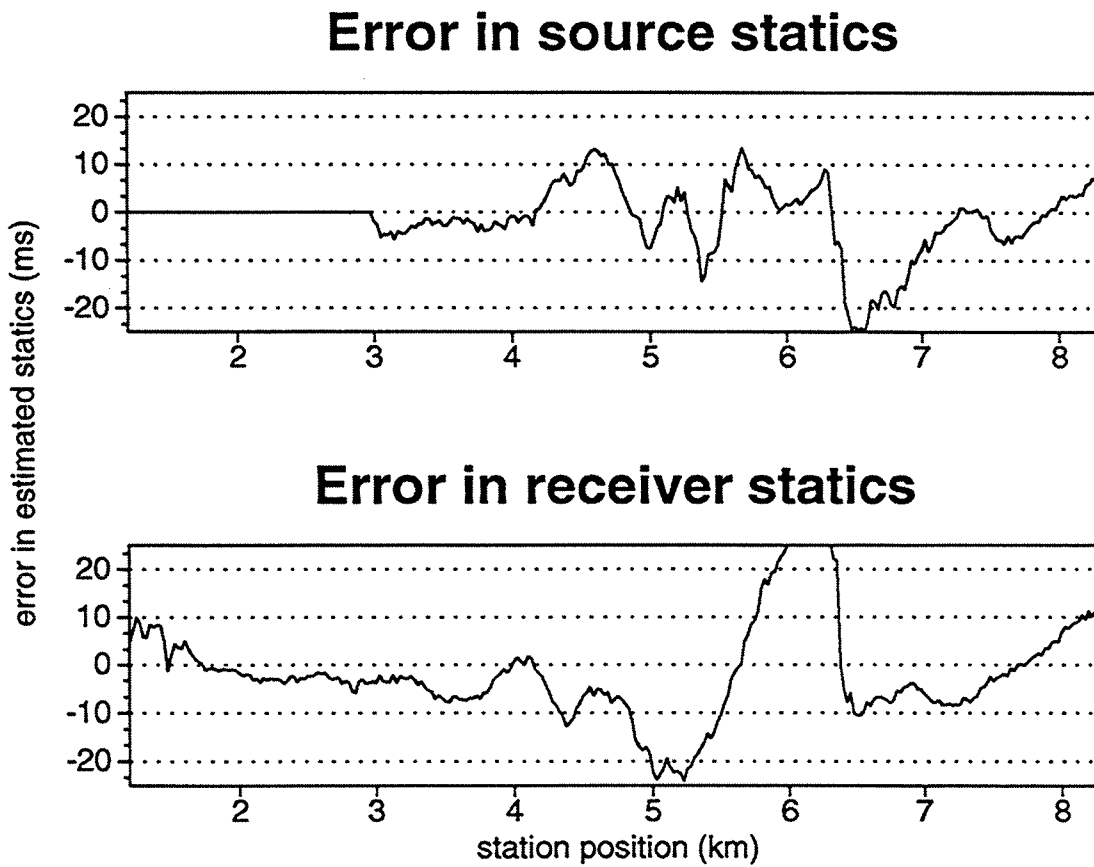


FIG. 5.1. Difference between the imposed random static time shifts and the conventionally estimated source and receiver corrections for the statics-contaminated, deconvolved Marmousi data after two iterations. The second iteration was done with updated stacking velocities.

## 5.1 Iterative sequence

One can envision any of several iterative approaches that combine migration velocity analysis with migration-based statics estimation in a bootstrapping effort to improve both. Here, I implement the following straightforward iterative process, in which prestack migration is exercised repeatedly for the dual purpose of converging on an acceptable statics solution as well as on an acceptable velocity structure.

1. Given an initial guess for the velocity model (e.g., from conventional velocity analysis or well-log data), prestack depth migrate the data and exercise the prestack-migration-based, statics-estimation procedure mentioned above. Specifically, stack the migrated data and perform multi-offset modeling to obtain the reference traces for use in conventional surface-consistent statics estimation.
2. Using the data corrected with the above-derived statics estimates, perform prestack depth migration with the initial velocity model. With these migrated data, follow the approach of Stork (1992) to obtain an updated velocity model.
3. Return to step 1, but now use the updated velocity model in the prestack depth migration of data and in the multi-offset modeling. Repeat steps 1 through 3, as necessary.

Within this iterative sequence, I consider two different options. These options pertain to the return to step 1 with the updated velocity model. In option *cum*, the statics estimates are cumulative. The updated velocity model is used in prestack migration of data that have had the statics corrections from the previous iteration applied. In this variation, the reference traces generated by multi-offset modeling are cross-correlated with the data, again after having had statics corrections previously applied. The statics estimates computed during the iteration are added to previously accumulated statics corrections. In the second option, option *fresh*, full statics estimates are freshly computed during the iteration. The original statics-contaminated data are used in building the reference traces (i.e., in the migration, stacking and multi-offset modeling) and are correlated with those reference traces.

I find that each of these options has its advantages and disadvantages for the iterative processing. To achieve some desired purpose, the two variations can be used interchangeably from one iteration to the next. The results, below, suggest a desired strategy for the choice of options.

Unquestionably, multiple iterations of prestack migration and modeling is costly. A prestack depth migration is performed for each step of velocity estimation and a second prestack depth migration is performed for each step of statics estimation. Additionally, for the statics estimation, multi-offset modeling, which is as costly as prestack migration, is required. In a less costly alternative approach, one might use the same prestack-migrated data for both velocity analysis and statics estimation at each iteration. Such an approach would add only a multi-offset modeling for statics estimation to the prestack migration already done for the velocity analysis. Here, I follow the more costly the approach listed above.



While the use of prestack migration and multi-offset modeling is unquestionably more computationally intensive than simple NMO correction in conventional statics estimation, we should keep in mind that, in areas of complex subsurface structure, iterative use of prestack migration is generally deemed essential in order to obtain acceptable velocity estimates for prestack depth migration, in the absence of statics problems. The dominant cost in such iterative effort at velocity determination is not the computational cost of doing depth migration, but rather the interactive effort required to develop a velocity model.

Large statics distortions in data make analysis of complex moveout particularly difficult. Let us therefore use only coarse velocity information as input to the statics-estimation procedure in the first step in this approach. Hopefully, even with a coarse first estimate, we can reduce the moveout problems to a level that allows a first effort at statics estimation that is good enough to allow more refined velocity analysis in a subsequent step. For this first iteration of statics estimation, we could choose either a conventional method or the migration-based method. In the previous section, however, we saw that the migration-based method produces better statics estimates than does a conventional method even with an imperfect initial velocity model. Moreover, Figures 3.19 and 4.15 showed that in data from areas with complex subsurface structure but with little or no near-surface time distortions, conventional methods may introduce errors that are much larger than those introduced by the migration-based method. Therefore, we will use the migration-based approach from the outset.

## 5.2 Implementation on the Marmousi data

Let us return to the Marmousi data that have just static time shifts imposed on them, and follow the above processing sequence. The first step was done in the previous section, with the constant-gradient velocity model as the initial velocity model, and Figure 4.17 showed the error in the statics solution.

After correction of the statics-contaminated Marmousi data with the statics corrections estimated in the first iteration, I apply Stork's migration velocity analysis method in an attempt to improve the velocity model (step 2). The resulting velocity model (let us call it the "first-update velocity model"), shown in Figure 5.2, is then used in the second iteration of the migration-based statics estimation (step 1, second iteration). This first-update velocity model reflects some of the structural shape embodied in the Marmousi depth model (Figure 3.1).

Figure 5.3 shows the image of the corrected Marmousi data, prestack migrated with the updated velocity model of Figure 5.2. Note the large increase in frequency bandwidth compared with the migration shown in Figure 4.16. Because a large portion of the statics contaminations has been resolved in the first iteration of statics estimation and because the velocity model is improved over the initial  $v(z)$  model, the high-cut filtering action of stacking misaligned events has been reduced significantly. The improved bandwidth in Figure 5.3 offers the prospect that the next iteration of the statics-estimation procedure will have the benefit of improved reference traces. At the same time, the poor focussing of

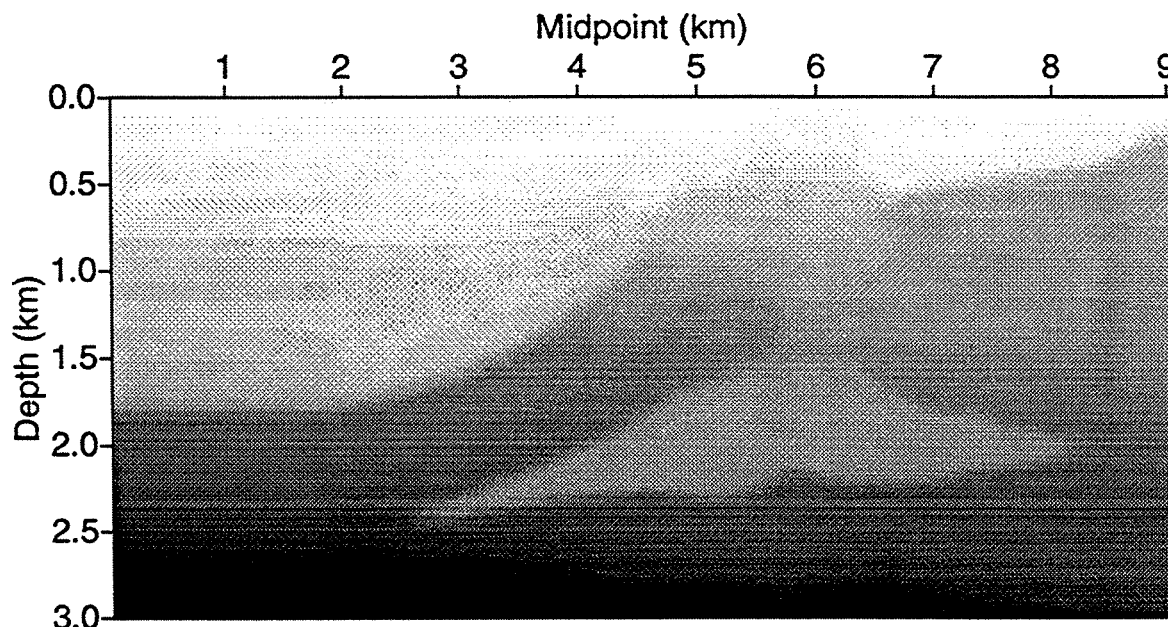


FIG. 5.2. Velocity model after one iteration of migration-velocity analysis (i.e., first-update velocity model). Darker shading indicates higher velocity.

many reflectors in Figure 5.3 indicates that this first-update velocity model still contains large errors.

Figure 5.4 shows the difference between the cumulative source and receiver statics estimated from the first two iterations of statics estimation and the imposed statics (option *cum* was used here). Likely because of the better moveout correction with the improved velocity model (and, consequently, the better reference traces), the statics errors in Figure 5.4 have reduced somewhat across the entire section (compare with Figure 4.17). The large errors in the more complex part of the model (specifically the anomalously large errors at station position 6.3 km), however, remain. Apparently the second statics-estimation iteration, with the more accurate velocity model, could not recover from the cycle skip introduced in the first iteration. Perhaps it would be better to compute statics corrections afresh from the uncorrected data (i.e., follow option *fresh* with the updated velocity model).

As a test of this possibility, let us interrupt our process for a moment and use a velocity model that is believed to be good in the second iteration of the migration-based statics-estimation procedure. Performing his velocity-analysis approach on the original Marmousi data, Liu (1995) has obtained a velocity model (Figure 5.5) that produces an excellent image of the subsurface. Let us, therefore, try Liu's high-quality velocity model for the second iteration of our processing sequence. Figure 5.6 shows the prestack-migrated Marmousi data, corrected with the statics solution of the first statics-estimation iteration (in which the constant-gradient velocity model was used) but mi-

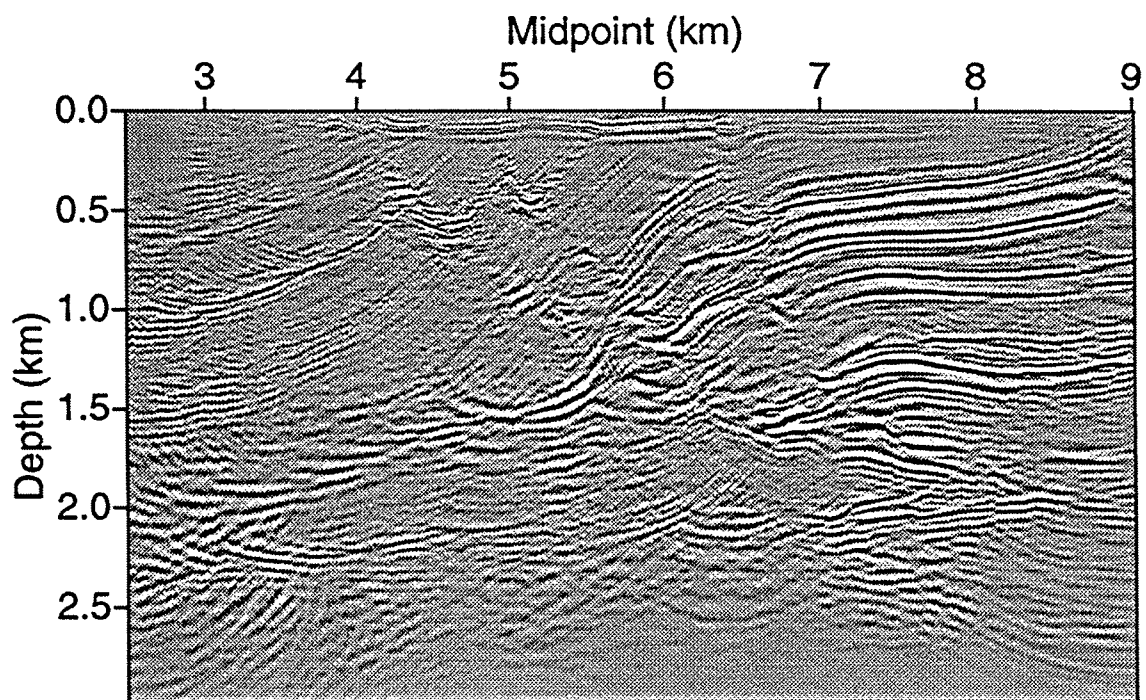


FIG. 5.3. Prestack depth-migrated image of the Marmousi data corrected with statics corrections obtained in the first iteration of statics estimation. The migration-velocity model is shown in Figure 5.2.

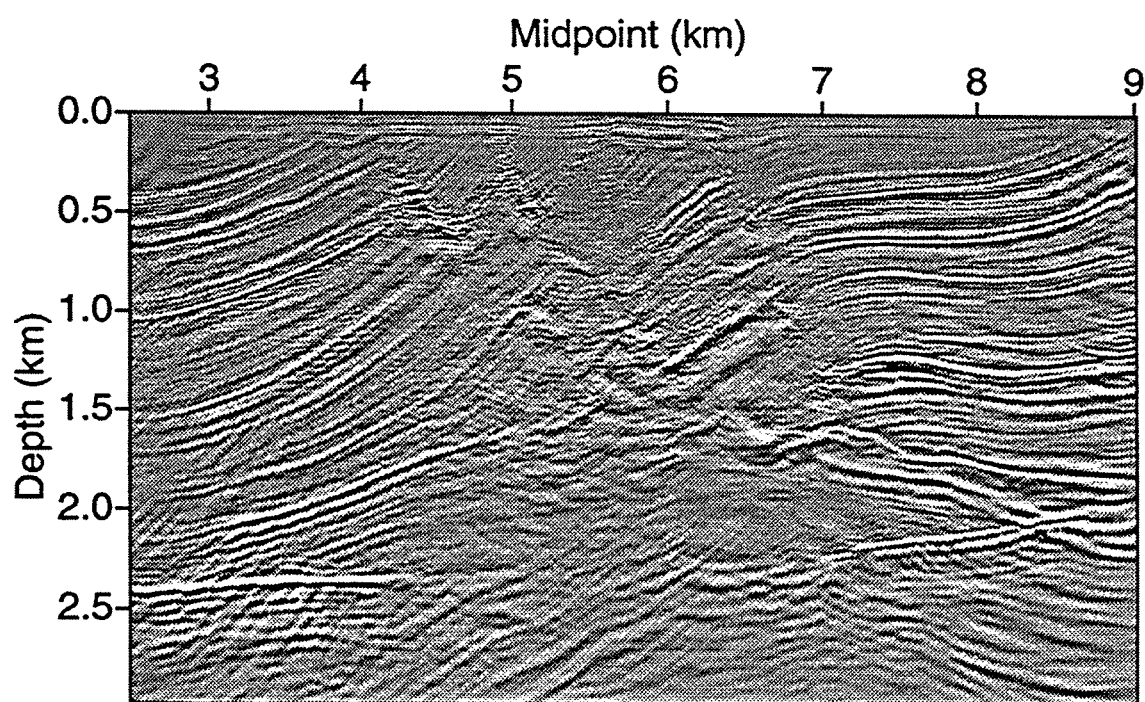


FIG. 5.6. Migrated image of the statics-contaminated Marmousi data with statics corrections obtained from one iteration of the migration-based approach. Liu's velocity model, shown in Figure 5.5, was used for this migration.

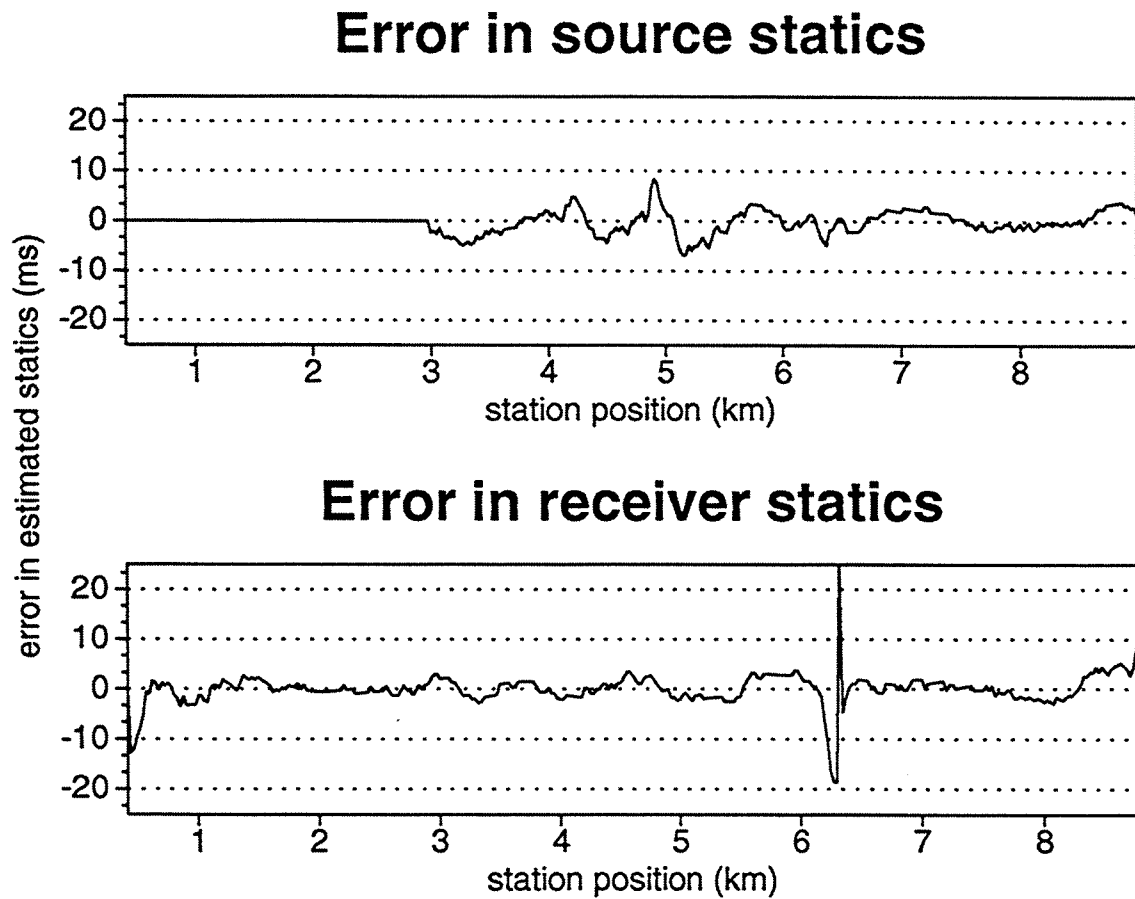


FIG. 5.7. Difference between the imposed random static time shifts and the cumulative migration-based estimated source and receiver corrections after two iterations. Here Liu's velocity model was used in option *cum* during the second iteration of the processing sequence.

however, that the general statics solution has larger errors than those in Figure 5.6. Apparently, although use of the improved velocity model in option *fresh* helps to overcome the cycle-skip problem, option *cum* has merit in generally improving portions of the solution that are not plagued by cycle-skipping. I will return to this point below.

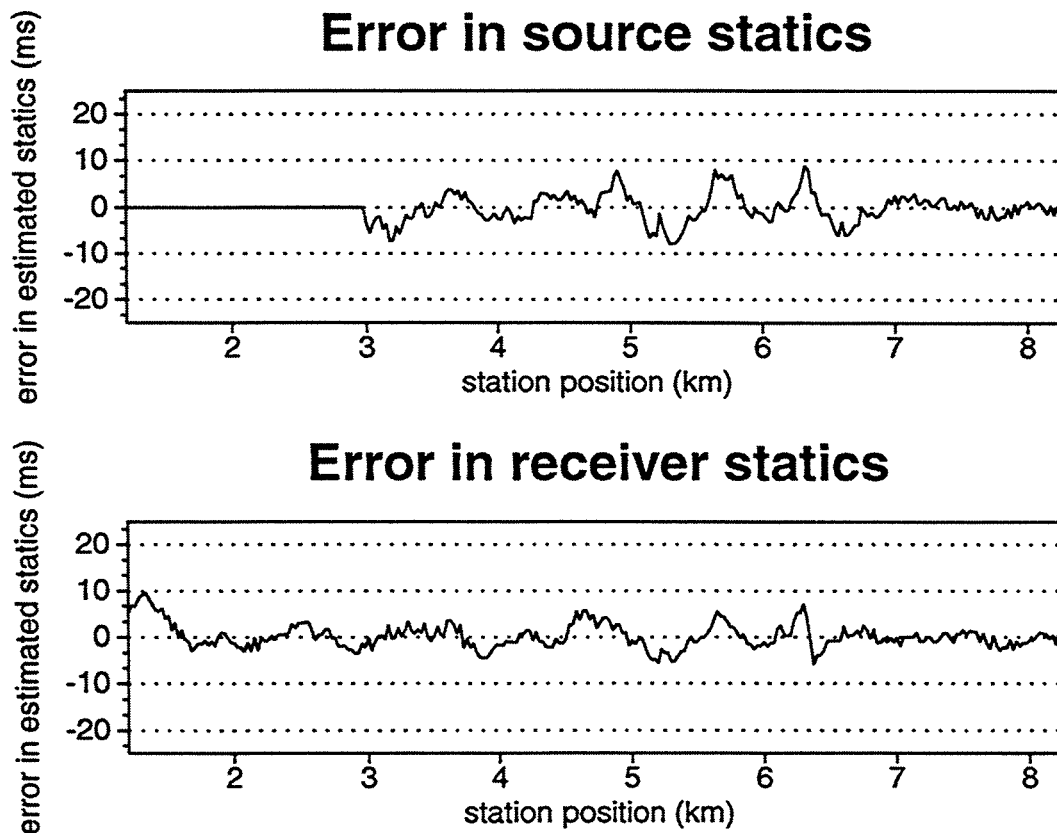


FIG. 5.8. Difference between the imposed random static time shifts and the migration-based estimated source and receiver corrections. Here Liu's velocity model was used in option *fresh* during the second iteration of the processing sequence.

Based on the result with Liu's velocity model, let us return to our iterative solution of the Marmousi data. Instead of following option *cum* as we did in generating Figure 5.4, let us exercise option *fresh* in the second iteration. That is, let us return to our statics and velocity iterations, but use the original, statics-contaminated data for a statics-estimation iteration with the first-update velocity model shown in Figure 5.2. Figure 5.9 shows the migration of the original, statics-contaminated data with this first-update velocity model. Again, note the high-cut filtering action attributable to the statics contamination, but now the reflectors are more accurately positioned compared with the migration based on the constant-gradient velocity (Figure 4.16) — but less accurately than in the migration with Liu's velocity model.

Figure 5.10 shows the error for a statics estimation with the first-update velocity

model, obtained after a first iteration (Figure 5.2), but now done on the original statics-contaminated data. The peak at the fault is still present but has reduced considerably, as have errors elsewhere, compared with the statics estimates from the constant-gradient velocity model (Figure 4.17).

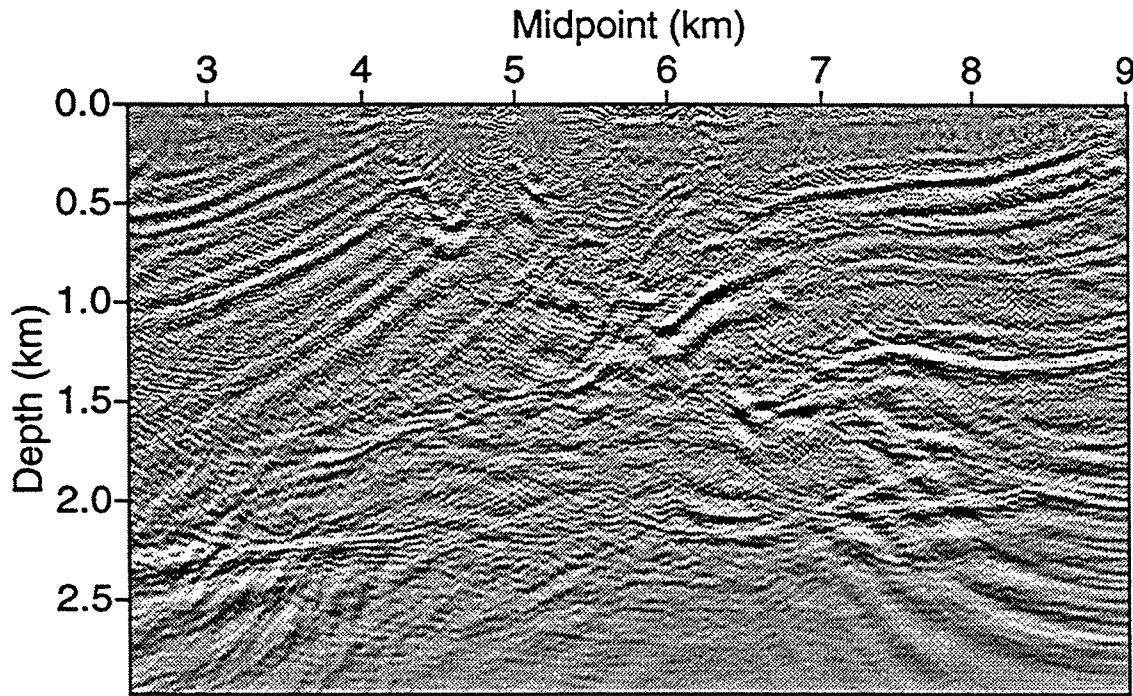


FIG. 5.9. Stack of prestack migration of the original, statics-contaminated data. The migration was done with the first-update velocity model (Figure 5.2).

Finally, let us add one more iteration of the three-step velocity and statics estimation sequence. An updated velocity model (Figure 5.11) is obtained from a migration velocity analysis on data corrected with the newly estimated statics shifts (option *cum*). This second-update velocity model is used in the next iteration of statics estimation. Figure 5.12 shows the stack of statics-corrected Marmousi data, prestack migrated with the second-update velocity model, shown in Figure 5.11. Correction was done with the estimated statics of Figure 5.10. Note the reduced high-cut filtering action compared with that in the image after the first iteration, shown in Figure 5.9.

Figure 5.13 shows the error in the cumulative estimated statics corrections after (1) an initial iteration of statics estimation based on the constant-gradient velocity model, (2) an iteration of statics estimation (option *fresh*) with the first-update velocity model (Figure 5.2), and (3) a final iteration of statics estimation (option *cum*), with the second-update velocity model (Figure 5.11).

Now the errors in the statics solution have reduced to an acceptable level, i.e., errors do not exceed 1-1/2 samples (the sampling interval here is 4 ms). We have arrived at this

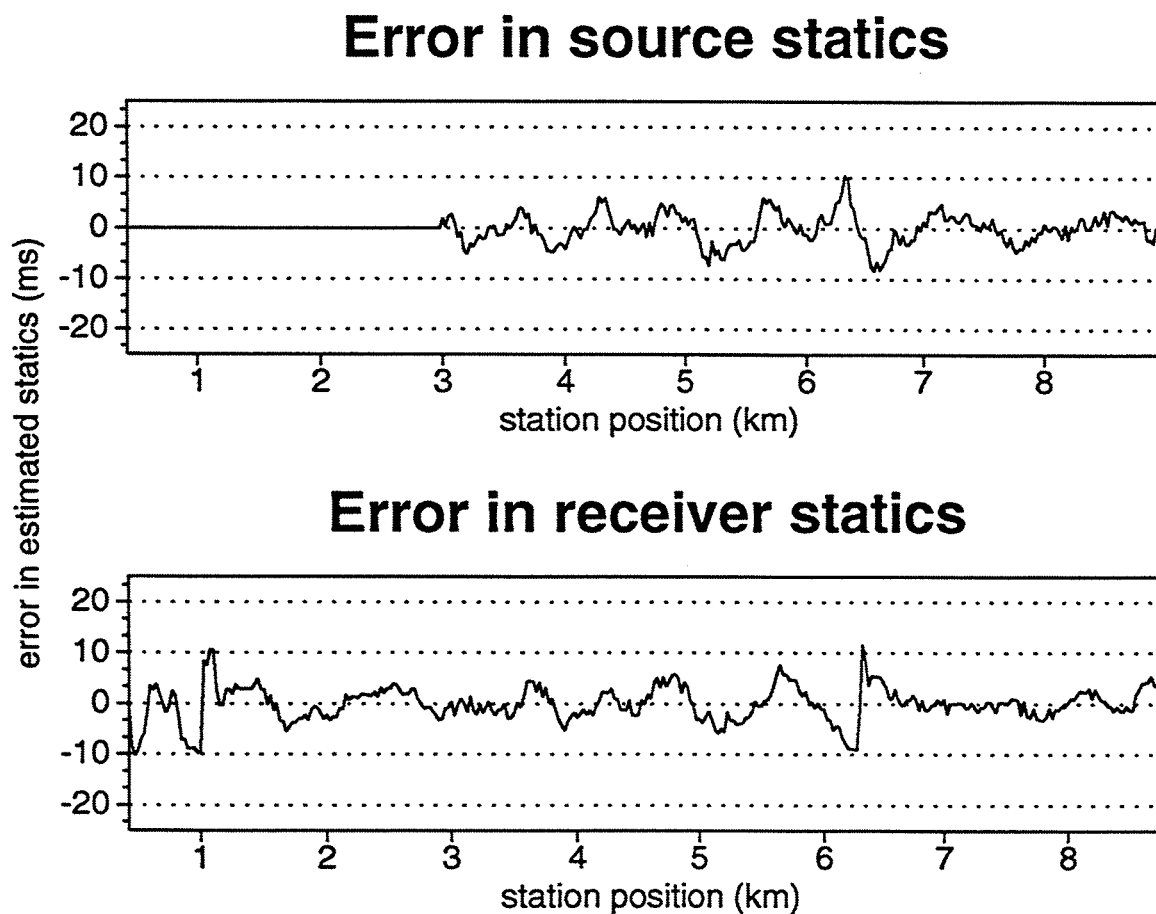


FIG. 5.10. Difference between the imposed random static time shifts and the migration-based estimated source and receiver corrections after statics-estimation (option *fresh*) with the first-update velocity model, shown in Figure 5.2.



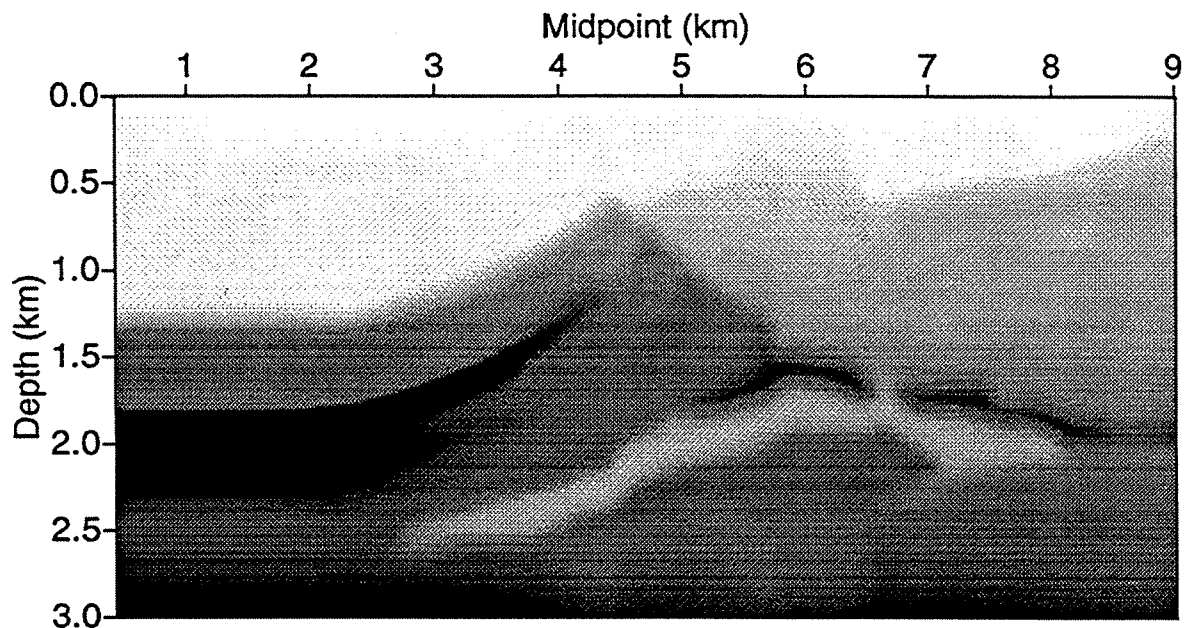


FIG. 5.11. Velocity model after two iterations of migration-velocity analysis (i.e., second-update velocity model).

result after just three iterations of statics estimation, alternated with two iterations of migration velocity analysis. The estimated statics corrections may now be good enough that further iterations to improve the imaging of the subsurface can now be directed solely at improving the velocity model, as is conventionally done in the absence of statics problems.

We have obtained the quite good statics solution suggested in Figure 5.13 through the choice of option *fresh* in the second iteration and option *cum* in the third one. This sequence of option choices was aimed at first overcoming the cycle skipping and then refining the statics solution over less troublesome portions of the data. In general, I recommend estimating fresh statics after each velocity update, because we do not know if large errors such as the one at 6.3 km in Figure 4.17 have been introduced in previous iterations of statics estimation. Once we are satisfied with the obtained statics solution, we can finish with a cumulative statics estimation to further reduce the short-wavelength errors.

Let us review the progress toward a statics solution in this sequence of tests with the Marmoussi data. Figures 5.14 and 5.15 collect results for receiver-statics solutions at various stages of the sequence. The statics errors (i.e., unresolved statics problem in the data) after application of a conventional method based on NMO correction (Figure 5.14a) are large, approaching the size of the statics problem that was imposed on the Marmoussi data. One iteration of the migration-based statics approach (Figure 5.14b), in which a simple linear  $v(z)$  model was used for the prestack migration and modeling, was sufficient

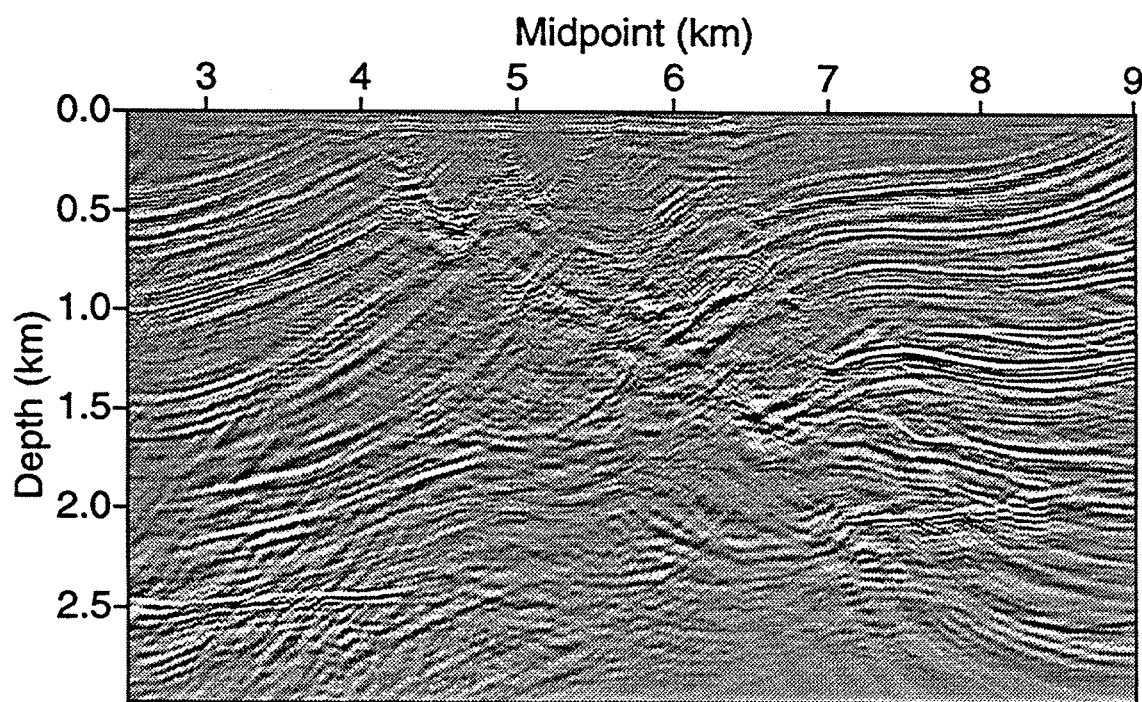


FIG. 5.12. Stack of prestack migration of the statics-corrected data. The migration was done with the second-update velocity model of Figure 5.11 applied to data corrected with statics estimates obtained from the second iteration of the processing sequence.

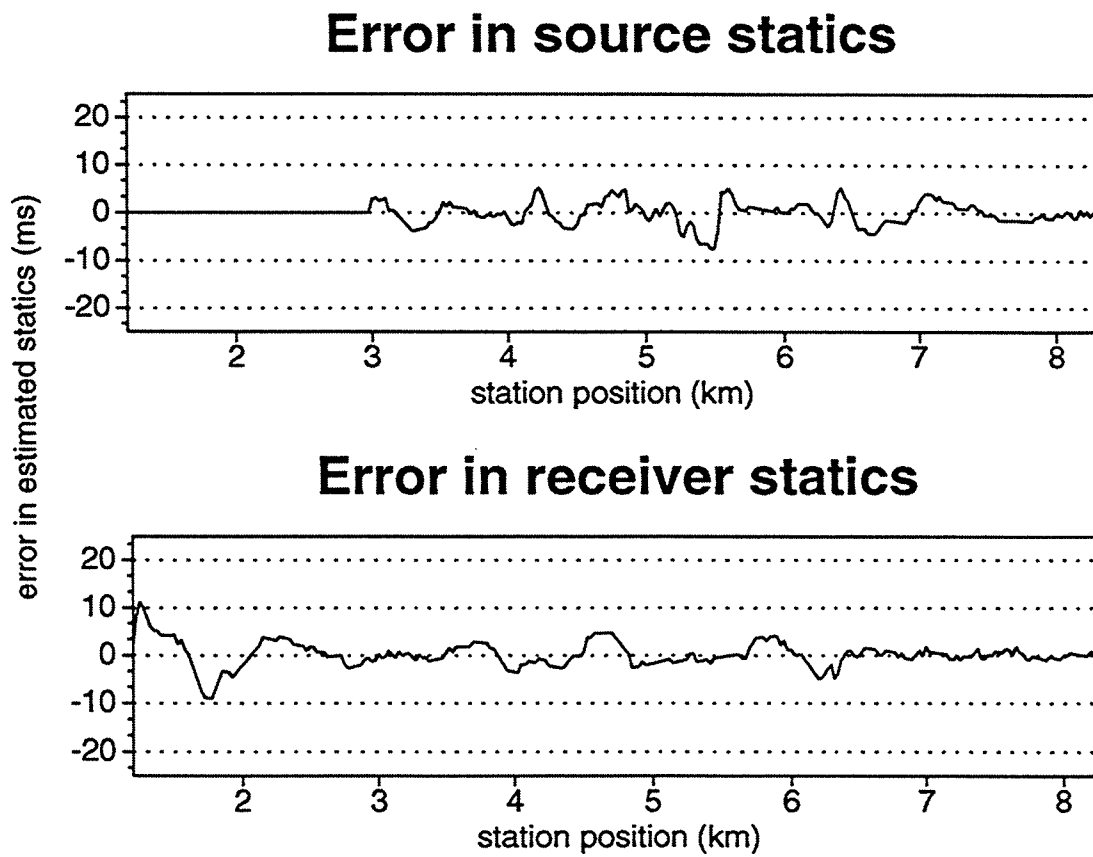


FIG. 5.13. Difference between the imposed random static time shifts and the cumulative migration-based estimated source and receiver corrections after three iterations.

to reduce the statics errors substantially, although the solution was poorest over the most complex portion of the Marmousi model. In particular, cycle-skips near 6.3 km left a large statics anomaly in that region. A second iteration of a conventional method applied to data that were corrected with statics estimated conventionally in the first iteration, using updated stacking velocities, leaves large-amplitude longer-wavelength errors (Figure 5.14c). The short-wavelength variations, in contrast, have been resolved well. Note that the errors after two iteration of conventional estimation are larger than those after just one iteration of migration-based estimation with the simple, constant-gradient, velocity model, most likely due to the ability of the migration-based approach to largely resolve the problem of a multi-valued stacking velocity.

Figure 5.15a shows the residual statics errors after a second iteration of statics estimation using the upgraded velocity model (the first-update velocity model) and option *cum*. While this iteration yields an improved solution over most of the line, it is unable to overcome the cycle-skip problem, near 6.3 km, that arose in the previous iteration.

An alternative second iteration of statics estimation again used the first-upgrade velocity model, but this time with option *fresh*. This option was chosen (with success, as seen in Figure 5.15b) for the purpose of suppressing the cycle-skip problem near 6.3 km. Use of option *fresh* at this stage, however, yielded a poorer statics solution over other portions of the data than was achieved with option *cum* (Figure 5.15a). A third iteration, this time with the second-update velocity model and option *cum* (Figure 5.15c) gives further improvement in the statics solution over the entire model.

If further iterations of the sequence are deemed desirable (the effort may not be justified here), option *cum* will be the preferred choice since the residual statics errors in Figure 5.15c appear to be free of large errors such as those that result from cycle-skipping. In comparing the residual-statics problems remaining after the various iterations, as seen in Figure 5.14 and Figure 5.15, we see that, with the exception of the problems near 6.3 km, the solution in Figure 5.15a (after just two iterations) is quite good. The alternative solution in Figure 5.15b, followed by the third iteration to yield the result in Figure 5.15c, primarily improves just the problems over the complex portion of the model.

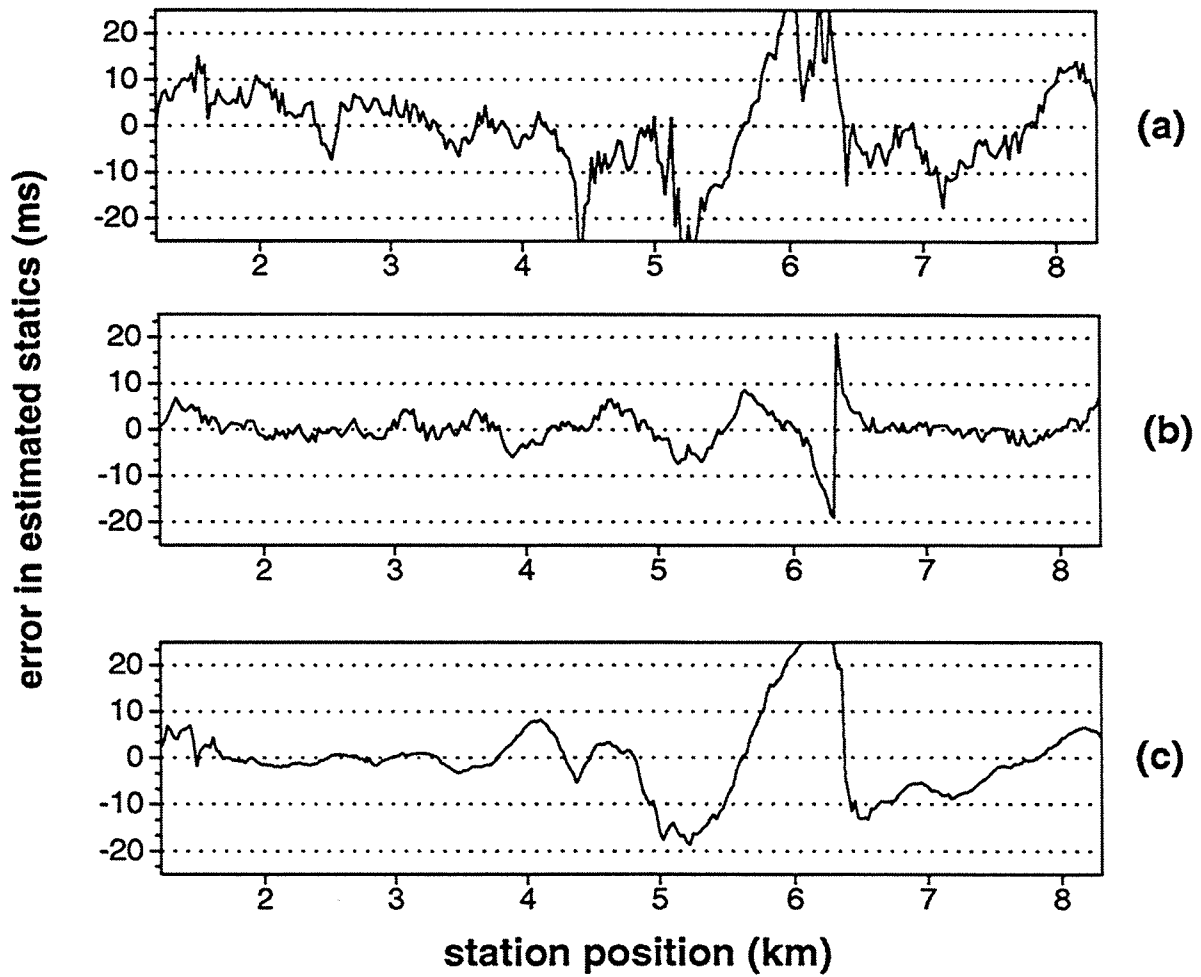


FIG. 5.14. Collected residual receiver statics errors, from previous figures, after various stages of iterative conventional statics estimation or migration-based statics estimation. The sets of residual statics errors are described in the text.

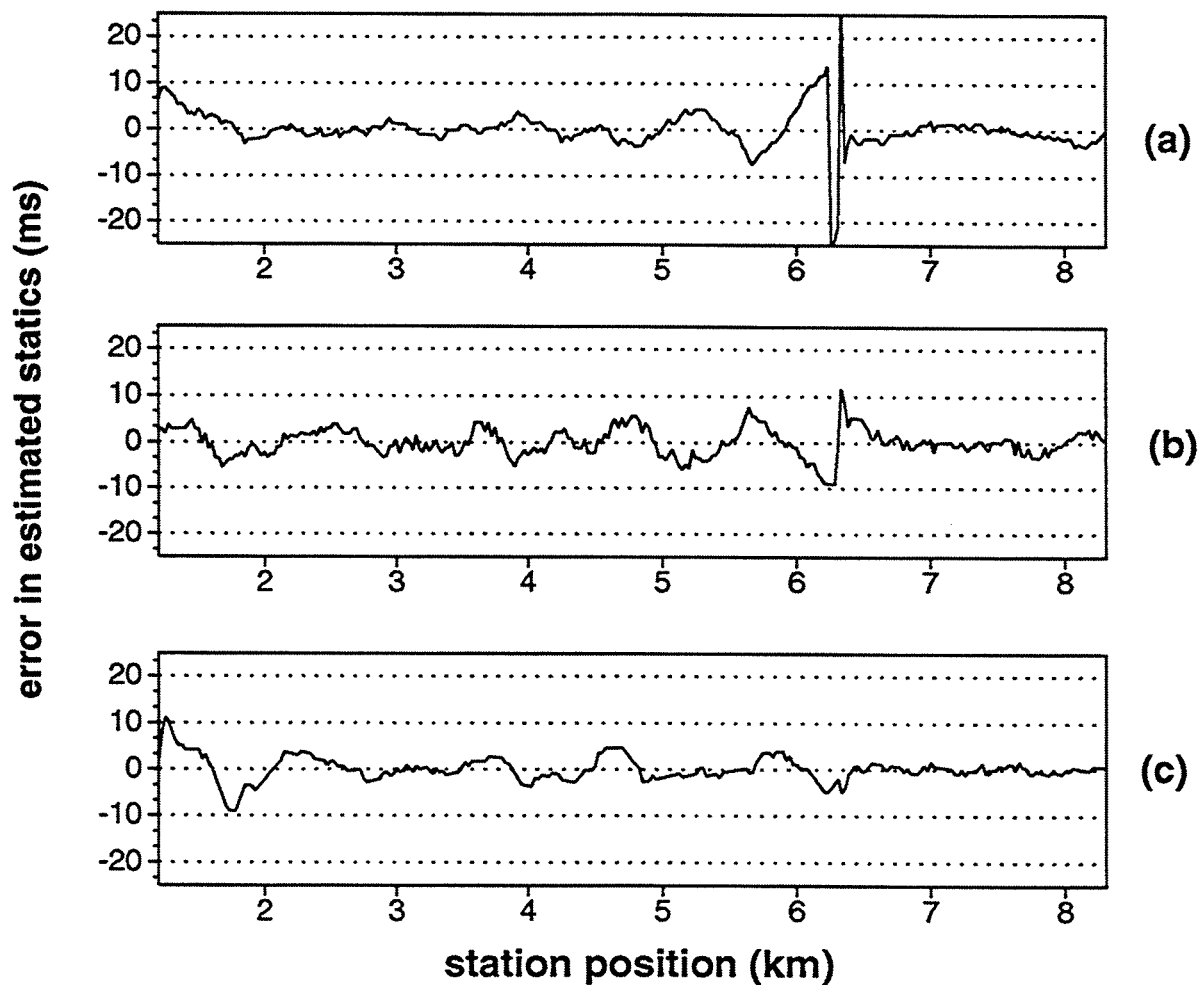


FIG. 5.15. Collected residual receiver statics errors, from previous figures, after various stages of iterative migration-based statics estimation. The sets of residual statics errors are described in the text.



## Chapter 6

### CONCLUSION AND RECOMMENDATIONS

Through the simulations in the first chapter, we have seen that whereas noise and imperfect NMO corrections compromise the quality of statics solution that we can expect, and large statics problems compromise the quality of the stack, it is the simultaneous occurrence of all these complicating factors that introduces the largest problems for statics-estimation efforts. In the absence of complex structure, large static problems and noise are often well treated (even where the assumption of surface-consistency is suspect). Likewise, the CMP stack is superb for suppression of many types of noise when the data do not suffer from poor NMO correction or from large statics problems. Also, velocity analysis works well where statics problems are absent and the subsurface structure is not complex. But combine these troublesome issues into a single data set, and none of them are adequately treated. Here, for example, we have seen that the conventional statics approach failed when it was applied to the Marmousi data contaminated by imposed surface-consistent statics.

The migration-based statics approach yields excellent statics estimates for statics-contaminated data from complex subsurface structure — the Marmousi data— when the exact velocity is known. When the velocity model is not known and the migration based approach is applied with a coarse initial  $v(z)$  velocity model, the statics estimates contain errors. However, these errors are considerably smaller than those obtained by a conventional approach based on NMO-velocity analysis. Additive noise also may not pose as severe a problem for the migration-based method as it does for a conventional approach. The errors in conventionally estimated statics increase significantly when noise is added, while those for the migration-based approach increase only slightly, even when a constant-gradient initial velocity model is used. Moveout correction is better in the migration-based approach since migration also can correct events with dip-dependent and multi-valued moveout as opposed to just NMO-correction in the conventional methods. Additionally, deriving stacking velocities in noise- and statics-contaminated data from complex subsurface structures, as was done for the conventional statics estimation, is an unstable process and a source of errors. The better treatment of the moveout sufficiently suppresses the problems due to the noise imposed here. Clearly, the problems imposed by the added random noise in the tests with the noisy data are not severe enough to unsettle the migration-based method. I have not, however, tested statics-estimation methods on data that also suffer from the many types of coherent noise (e.g., multiple energy, out-of-plane reflections, ground roll, etc.).

For both the conventional and the migration-based method, the oscillatory character of the Marmousi model data posed a problem, even in parts of the data where the moveout is normal. The oscillations yield large side-lobes in the cross-correlation functions thus



increasing the chance for cycle skipping. Spiking deconvolution of the data improved the stand-out of the main peaks in the cross-correlations significantly.

The treatment of statics- and noise-contaminated data from structurally complex areas presents a chicken-and-egg problem: statics correction, velocity estimation, suppression of noise, and imaging are all intertwined. In conventional processing, the answer has been to iterate the various processes: get a first estimate of the stacking velocity; attempt statics estimation and correction; with the obtained statics solution, attempt to improve the estimate of stacking velocity; and so on. Given the mixture of problems in complex areas, we must also be prepared to iterate several times with the migration-based statics-estimation procedure. Such an effort would entail considerable cost, but even in the absence of statics problems we presently iterate between velocity estimation and migration in complex areas. As implemented here, the added cost for the statics estimation effort compared with that of iterative velocity analysis is an additional prestack depth migration and a multi-offset modeling for each iteration. These computer-intensive steps, however, likely introduce only modest additional cost and effort relative to the intensive interactive interpretation required for the velocity modeling.

It is encouraging that a good statics solution can be obtained well before the velocity problem has been resolved. This was shown in the tests with the Marmousi data, which yielded a good statics solution after three iterations. Once satisfied with the obtained statics solution, we can direct all attention to iterative improvement of the velocity model alone. Then, after having converged on an acceptable velocity model, we can revisit the migration-based method for one final effort at statics estimation.

Prestack depth migration is being used increasingly in practice as the performance of high-speed computers continues to improve. Application of prestack depth migration and the effort required to obtain good estimates of velocity has been limited to data that do not have measurable statics problems (e.g., marine data). Such tasks may have been judged too costly to be implemented as part of the effort to solve statics problems. Indeed, compared with a conventional statics-estimation method the migration-based method is costly, especially when applied iteratively. However, there is room for improvement and the migration-based approach could be made more cost effective.

I described one iterative approach, but one might think of different, less costly, iterative approaches. For example, a combined use of the migrated data for both the velocity and statics estimation would leave only an extra multi-offset modeling for the statics effort during each cycle of iterations. A disadvantage of this specific sequence may be that, whereas we have seen the merit of estimating fresh statics for most iterations, velocity analysis is most stable when applied to data that have benefited from previous iterative steps at statics correction. Especially when the statics contaminations have longer-wavelength variations (shorter than a cable length, but long enough to be misinterpreted as moveout), it is difficult to know whether to attribute moveout to statics or to velocity.

In the tests with the Marmousi data I migrated and remodeled the entire data set in each iteration. However, static time shifts are estimated in correlation windows of the data centered on strong reflectors. It would therefore be more economical, in the

simultaneous statics- and velocity-estimation efforts, to migrate and remodel only part of the data and resolve statics and velocity down to the correlation window. After a satisfactory statics solution is obtained, we can then iterate to resolve the velocity for the entire section.

Here, I made the large step of going from NMO correction to prestack depth migration. However, less costly alternatives than the migration-based approach should be considered. For data that do not suffer from significant non-hyperbolic moveout, but that do contain dip-dependent and multi-valued moveout it may suffice to apply a DMO correction in addition to the NMO correction. In this procedure, instead of the multi-offset modeling, inverse DMO and inverse NMO would be used producing the reference traces.

The migration-based statics estimation with the constant-gradient velocity model for the Marmousi data showed that such an approach can improve the statics solution significantly compared to the conventional NMO-based statics solution. It suggests that time migration may be a good first step in the statics-estimation effort. Time migration with the constant-gradient velocity model treats the problems due to multi-valued moveout better than do conventional NMO-based approaches, even though it cannot address the problems due to non-hyperbolic moveout. Perhaps the well-behaved nature of the constant-gradient velocity model, as opposed to the often erratic lateral variations in stacking velocities (particularly where subsurface structure is complex), also contributed to the improved accuracy of the solutions.

Refraction-based statics estimation would circumvent many of the problems involved with statics estimation in data of complex subsurface structure. Common practice, however, is to apply refraction-based statics estimation prior to a final effort at reflection-based residual-statics estimation. Although the refraction-based statics solution may be accurate, a reflection-based estimation based on simple NMO correction may re-contaminate this good solution, as tests with the original Marmousi data with no statics imposed on them showed. Use of refraction-based statics estimation alone may sometimes be an acceptable alternative to the costly migration-based statics-estimation procedure. However, when dealing with complex subsurface structures, these structures often reach up to the surface (as is the case with the Marmousi model). In such cases, some of the essential requirements for refraction-based methods — presence of refraction energy and somewhat planar refractors — may be violated.

The examples shown here were all done with the Marmousi synthetic data set, with surface-consistent static time distortions imposed on the traces. Although we have shown that the migration-based method can work well for such data, even when the initial velocity model is far from correct, field seismic data are not so ideal. Noise, both random and coherent, may contaminate the data, and time distortions may be neither surface-consistent nor static, and will certainly contain variations along the surface with wavelengths longer than the cable length. Therefore, further tests need to be done to assess the migration-based method under more realistic conditions. One first step towards field data would be to impose more realistic (e.g., non-surface-consistent) near-surface-induced time distortions on the data, for example by adding a low-velocity layer, at

shallow depths, to the Marmousi model. A full effort at refraction-statics estimation, followed by the migration-based approach should be performed.

Ultimately, the migration-based statics estimation method (perhaps extended to 3D) needs to be tested on field data. Of course, conventional methods would suffer from the same additional problems present in more realistic data. The expectation is that the degradation that reality imposes on the migration-based approach is less severe than that imposed on the conventional approach by virtue of the opportunity to reduce moveout problems from the combination of so many compounded problems.

## REFERENCES

- Audebert, F., 1991, Marmousi: a bench-mark for (S-G) prestack depth migration: Poster at the SEG workshop: "Recent advances in 2D prestack imaging": 61st Ann. Internat. Mtg., Soc. Expl. Geophys.
- Berkhout, A. J., Cox, H., Verschuur, E., and Wapenaar, C. P. A., 1990, The DELPHI approach to macro model estimation: Proceedings of the workshop on Practical Aspects of Seismic Data Inversion; held at the 52nd EAEG Meeting, Copenhagen, 1990.
- Denelle, J. P., Dézard, Y., and Raoult, J. J., 1986, 2-D Prestack Depth Migration in the (S-G- $\omega$ ) Domain: 56th Ann. Internat. Mtg., Soc. Expl. Geophys., Expanded Abstracts, 327-330.
- Diet, J. P. and Audebert, F., 1990, A focus on focussing: 52nd Ann. Internat. Mtg., EAEG, Expanded Abstracts, 327-330.
- Faye, J. P., and Jeannot, J. P., 1986, Prestack migration velocities from depth focussing analysis: 56th Ann. Internat. Mtg., Soc. Expl. Geophys., Expanded Abstracts, 438-440.
- Hileman, J., Embree, P., and Pflueger, J., 1968, Automated statics corrections: Geophys. Prosp., **16**, 326-358.
- Larner, K. L., Gibson, B., and Chambers, R., 1983, Imaging beneath complex structure: in Seismic Expression of Structural Styles, 1, ed. by A. W. Bally: AAPG, Tulsa, 26-39.
- Lawton, D., 1989, Computation of refraction static corrections using first-break travel-time differences: Geophysics, **54**, 1289-1296.
- Liu, Z., and Bleistein, N., 1994, Velocity analysis by perturbation: 64th Ann. Internat. Mtg., Soc. Expl. Geophys., Expanded Abstracts, p. 1191-1194.
- Liu, Z., 1995, Migration velocity analysis: Ph.D. thesis, Colorado School of Mines.
- Marsden, D., 1993a, Statics corrections — a review, part I: The Leading Edge, **12**, 43-49.
- , 1993b, Statics corrections — a review, part II: The Leading Edge, **12**, 115-120.
- , 1993c, Statics corrections — a review, part III: The Leading Edge, **12**, 210-216.
- Miller, M., 1974, Stacking of reflections from complex structures: Geophysics, **39**, 427-440.

- Ronen, J., and Claerbout, J., 1985, Surface-consistent residual statics estimation by stack-power maximization: *Geophysics*, **50**, 1267-1279.
- Rothman, D., 1985, Nonlinear inversion, statistical mechanics, and residual statics estimation: *Geophysics*, **50**, 2784-2796.
- Rothman, D., 1986, Automated estimation of large residual statics corrections: *Geophysics*, **51**, 332-346.
- Stork, C., 1992, Reflection tomography in the postmigrated domain: *Geophysics*, **39**, 680-692.
- Stork, C., and Kusuma, T., 1992, Hybrid genetic autostatics: New approach for large-amplitude statics with noisy data: 62nd Ann. Internat. Mtg., Soc. Expl. Geophys., Expanded Abstracts, 1127-1131.
- Taner, M. T., and Koehler, F., 1969, Velocity spectra — digital computer derivation and applications of velocity functions: *Geophysics*, **39**, 859-881.
- Taner, M.T., Koehler, F., and Alhilali, K, 1974, Estimation and correction of near-surface time anomalies: *Geophysics*, **41**, 441-463.
- Tjan, T., Audebert, F., and Larner, K. L., 1994, Prestack migration for residual statics estimation in complex media: 64th Ann. Internat. Mtg., Soc. Expl. Geophys., Expanded Abstracts, 1513-1516
- Versteeg, R., and Grau, G., 1991, The Marmousi experience: Proceedings of the workshop on Practical Aspects of Seismic Data Inversion: held at the 52nd EAEG Meeting, Copenhagen, 1990.  
Proceedings of the workshop on Practical Aspects of Seismic Data
- Wiggins, R., Larner, K. L., and Wisecup, D., 1976, Residual statics analysis as a general linear inverse problem: *Geophysics*, **41**, 922-938.

